University of Alberta

Investigation of the Prader-Willi syndrome protein MAGEL2 in the regulation of Forkhead box transcription factor FOXO1

by

Julia Devos

A thesis submitted to the Faculty of Graduate Studies and Research
in partial fulfillment of the requirements for the degree of

Master of Science

in

Medical Sciences – Medical Genetics

Spring 2013
Edmonton, Alberta

Abstract

Prader-Willi syndrome (PWS), a genetic disorder resulting from the loss of expression of multiple genes including *MAGEL2*, is characterized by hyperphagia and childhood-onset obesity. These symptoms point to dysfunction in the regulation of energy homeostasis. *Magel2* is highly expressed in the hypothalamus, the body's main regulator of energy balance. As the Forkhead box transcription factor FOXO1 functions in the hypothalamus to regulate food intake and body weight, I hypothesized that MAGEL2 may be involved in energy homeostasis by regulating FOXO1. Although no interaction was detected between these two proteins, I determined that MAGEL2 alters FOXO1 subcellular localization in a manner dependent upon post-translational modifications of FOXO1. Expression of MAGEL2 increases cytoplasmic localization of acetylated and phosphorylated FOXO1 and increases nuclear localization of deaceteylated FOXO1 in immunofluorescence experiments. The loss of *MAGEL2* expression in PWS may impair proper FOXO1 regulation, reducing the ability of the hypothalamus to maintain energy homeostasis.

Acknowledgements

God has blessed me richly by surrounding me with an amazing network of people who have so graciously helped and supported me during my time as a graduate student at the University of Alberta as well as throughout my entire academic life. The undertaking and completion of the research detailed in this thesis, as well as the thesis itself, would not have been possible without them. With that said, I would like to specifically acknowledge the following people:

Thank you, Dr. Rachel Wevrick, for taking me on as a student in your lab, for guiding me through the process of earning my Master's degree and for always being open and available to talk to whenever I needed. It was a privilege to be your student.

Thank you to past and present members of the Wevrick lab: Jocelyn Bischof, Dr. Rebecca Mercer, Xiao Li, Dr. Qasim Rasi, Sara Weselake and Dr. Jason Bush. I greatly appreciate how you were always willing to lend an ear, to give advice and to help me in whatever way possible. It was a pleasure to work alongside you.

Thank you to Dr. Fred Berry, Dr. Heather McDermid and Dr. Andrea Haqq, for agreeing to be members of my committee and for all of your thought-provoking questions, helpful comments and invaluable suggestions concerning my research and thesis.

Thank you to Dr. Heather Prior of The King's University College for your continued support and encouragement throughout my undergraduate and graduate education.

Thank you to my Mom and Dad, Linda and Henry Devos, for your persistent and whole-hearted belief in me, for your constant love and encouragement and for the generous support you have provided me my whole life. Thanks also to my Mother- and Father-in-law, Monica and Werner Harder, for your love and encouragement.

Thanks to 'the Goose,' my dog Mozart, for being so cute, for bringing me such joy and for your earnest and enthusiastic devotion. I miss you.

And lastly, to my wonderful husband and very best friend Daniel Harder, thank you for being the amazing person that you are, for your limitless love and for all the different ways, both big and small, that you have encouraged and supported me along the way!

Table of Contents

List of Figures

List of Abbreviations

List of Figures

List of Abbreviations

ACC	Acetyl-CoA carboxylase
AgRP	Agouti-related protein
AMPK	5'-AMP activated protein kinase
ARC	Arcuate nucleus
ATG7	E1-like protein autophagy-related 7
ATP	Adenosine triphosphate
BDNF	Brain-derived neurotrophic factor
BIM	Bcl-2 interacting mediator of cell death
BMB	Boehringer Mannheim Blocking reagent
BP	Breakpoint
BSA	Bovine serum albumin
cAMP	Cyclic adenosine monophosphate
CART	Cocaine- and amphetamine- regulated transcript
CBP	CREB-binding protein
CDK2	Cyclin-dependent kinase 2
CK1	Casein kinase 1
CNS	Central nervous system
Co-IP	Co-immunoprecipitation
CREB	cAMP response element-binding
CRM1	Chromosomal region maintenance protein 1
CYFIP	Cytoplasmic FRMP interacting protein
DMEM	Dulbecco's modified Eagle medium
DMN	Dorsomedial nucleus
DYRK1A	Dual-specificity tyrosine-phosphorylated and regulated kinase 1A
ELR	Erythropoietin:leptin receptor
EMSA	Electrophoretic mobility shift assay
Epo	Erythropoietin
ERK	Extracellular-signal-regulated kinase
FASL	Fas ligand
FBS	Fetal bovine serum

FHL2	Four and a half LIM 2
FKHR	Forkhead in rhabdomyosarcoma
FLIP	Fluorescence loss in photobleaching
FOX	Forkhead box
FRAP	Fluorescence recovery after photobleaching
FRE	FOXO-recognized element
FRMP	Fragile X mental retardation protein
G6PC	Glucose-6-phosphatase
GABA	Gamma-aminobutyric acid
GCP5	Gamma-tubulin complex protein 5
GFP	Green fluorescent protein
GHS	Growth hormone secretagogue
GSK-3	Glycogen synthase kinase-3
GST	Glutathione S-transferase
HRP	Horseradish peroxidase
IC	Imprinting center
IGFBP-1	Insulin-like growth factor binding protein-1
IP	Immunoprecipitation
IPW	Imprinted in Prader-Willi
IR	Insulin receptor
IRS	Insulin receptor substrate
IRS	Insulin response sequence
JAK2	Janus kinase 2
LepR	Leptin receptor
LHA	Lateral hypothalamic area
MAGE	Melanoma-associated antigen gene
MAPK	Mitogen-activated protein kinase
MC3R	Melanocortin 3 receptor
MC4R	Melanocortin 4 receptor
MHD	MAGE homology domain
MKRN3	Makorin ring finger protein 3

MnSOD	Manganese superoxide dismutase
MSH	Melanocyte-stimulating hormone
MST1	Mammalian Ste20-like kinase 1
mTORC	Mammalian target of rapamycin complex
NES	Nuclear export sequence
NIPA	Non-imprinted in Prader-Willi/Angelman region
NLS	Nuclear localization sequence
NPY	Neuropeptide Y
NRAGE	Neurotrophin receptor-interacting MAGE homolog
NTS	Nucleus of the solitary tract
PAX	Paired box
PBS	Phosphate-buffered saline
PBSX	PBS with 0.05% Triton X-100
PCK1	Phosphoenolpyruvate carboxykinase 1
PDK1	3-Phosphoinositide-dependent protein kinase 1
PDX1	Pancreas/duodenum homeobox 1
PEI	Polyethylenimine
PI3K	Phosphatidylinositol 3-kinase
PIP2	Phosphatidylinositol-4,5-biphosphate
PIP3	Phosphatidylinositol-3,4,5-triphosphate
PLCγ1	Phospholipase C γ1
PML	Promyelocytic leukemia-associated protein
POMC	Pro-opiomelanocortin
PPAR	Peroxisome-proliferator-activated receptor
PRMT1	Protein arginine methyltransferase 1
PTP1B	Protein tyrosine phosphatase 1B
PVN	Paraventricular nucleus
PWS	Prader-Willi syndrome
ROS	Reactive oxygen species
RT-PCR	Reverse transcription-polymerase chain reaction
SCN	Suprachiasmatic nucleus

SDS	Sodium dodecyl sulphate
SDS-PAGE	SDS-polyacrylamide gel electrophoresis
SGK	Serum- and glucocorticoid-inducible kinase
SHP2	SH2-containing protein tyrosine phosphatase 2
SNRPN	Small nuclear ribonucleoprotein polypeptide N
SNURF	SNRPN upstream reading frame
SOCS3	Suppressor of cytokine signalling 3
SON	Supraoptic nucleus
STAT	Signal transducer and activator of transcription
TBST	Tris-buffered saline with 0.1% Tween-20
TBSTM	TBST with 5% skim milk powder
TRAIL	Tumour-necrosis-factor-related apoptosis-inducing ligand
TRH	Thyrotropin-releasing hormone
TRPC	Transient receptor potential cation
TSH	Thyroid-stimulating hormone
UPD	Uniparental disomy
VMN	Ventromedial nucleus

Chapter 1: Introduction

1.1 Prader-Willi syndrome

1.1.1 Characteristics of Prader-Willi syndrome

Prader-Willi syndrome (PWS) is a human genetic obesity disorder formally identified in 1956 by Andrea Prader, Alexis Labhart and Heinrich Willi (Prader et al., 1956). It has an incidence of approximately 1:15,000 to 1:25,000 live births (Cataletto et al., 2011; Buiting, 2010). In 1993, Holm et al. published consensus criteria for the clinical diagnosis of PWS. These criteria were revised in 2001 by Gunay-Aygun et al. and again in 2008 by Goldstone et al. after genetic testing became the standard for confirming an initial clinical diagnosis of PWS. Some of the defining characteristics of PWS include neonatal hypotonia (Figure 1A) and failure to thrive in infancy followed by childhood-onset obesity, insatiable hunger and hyperphagia (Figure 1B). In general, a fetus with PWS moves less in the womb and is smaller, both in weight and length, upon birth (Miller et al., 2011). PWS neonates are hypotonic and lethargic, have difficulty feeding and gain weight poorly in early infancy (Miller et al., 2011; Cassidy and Driscoll, 2009). Starting in childhood, if diet is not strictly controlled individuals become obese, due to decreased activity levels, lower metabolic rates, increased insatiable appetite and hyperphagia (Jin, 2011; Cassidy and Driscoll, 2009; van Mil et al., 2000). In addition, people with this disorder become dramatically preoccupied with food which results in multiple unique behaviours associated with food. This includes food seeking behaviours such as foraging, hiding, hoarding and sneaking food, eating unappealing food or food-related substances such as garbage or decaying food as well as manipulating, lying or stealing in order to get food (Cataletto et al., 2011; Cassidy and Driscoll, 2009). Individuals with PWS have developmental delay, growth hormone deficiency, short stature and mild to moderate mental retardation. They also have hypogonadotropic hypogonadism resulting in decreased testosterone or estrogen as well as decreased follicle-stimulating hormone and luteinizing hormone, small genitals, cryptorchidism in males, late or incomplete puberty and reduced fertility (Cataletto et al., 2011; Jin, 2011; Cassidy and Driscoll, 2009). Throughout life, an altered body composition has been noted with this syndrome. Individuals have an

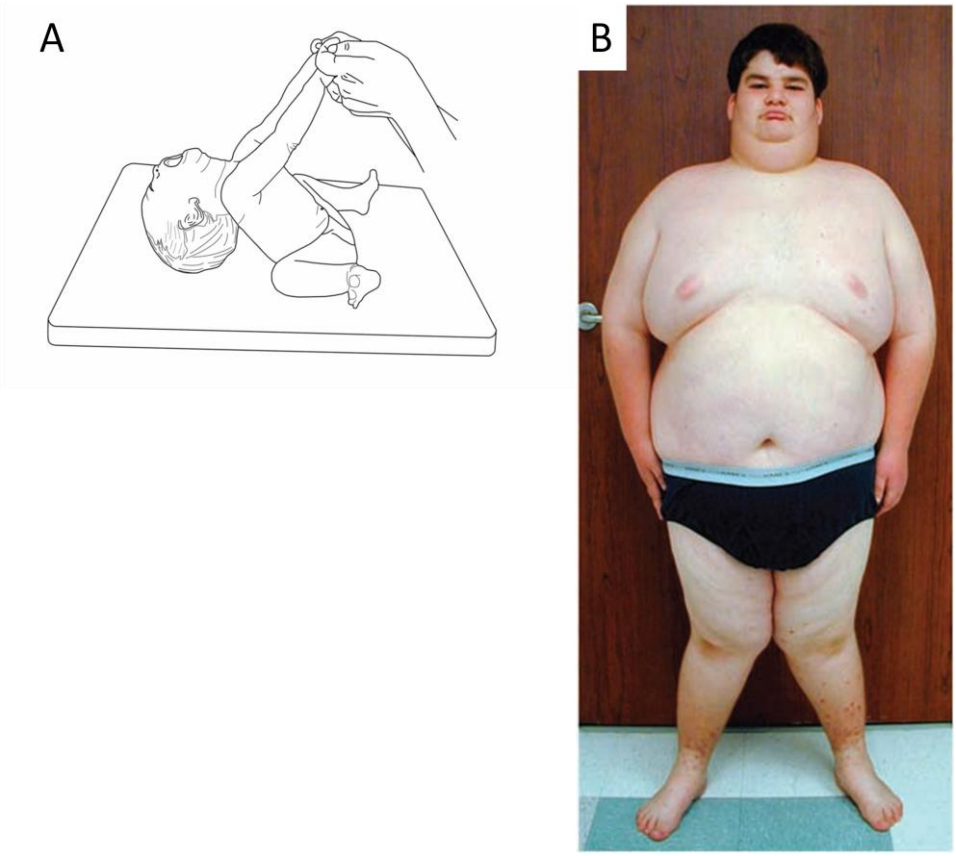

Figure 1. Characteristics of Prader-Willi syndrome (PWS). (A) Illustration of infant with hypotonia typical of PWS. (B) 21-year-old male with PWS exhibiting morbid obesity. Adapted from Jin, 2011 and Cassidy and Driscoll, 2009.

increased percentage of body fat and a decreased percentage of lean mass as compared to both normal weight and obese controls (Brambilla et al., 1997; van Mil et al., 2000). PWS also results in distinctive facial features such as a narrow bifrontal diameter and nasal bridge, almond-shaped palpebral fissures and a downturned mouth with a thin upper lip (Cataletto et al., 2011; Cassidy and Driscoll, 2009). PWS can also cause various sleep abnormalities such as excessive daytime sleepiness, prolonged nocturnal sleep, abnormal circadian rhythm in rapid eye movement sleep, reduced arousal to hypoxia and hypercapnia and obstructive sleep apnea (Weselake and Wevrick, 2012; Nixon and Brouillette, 2002). People with PWS may also have a high pain threshold, thick saliva, short hands and feet, hypopigmentation and scoliosis (Cassidy and Driscoll, 2009). Along with the food-associated behaviours and hyperphagia, other typical behaviours can also be found in these individuals beginning in childhood. This includes temper tantrums, repetitive and compulsive behaviours, stubbornness, skin picking and a fervent insistence on adhering to sameness in the daily routine (Cataletto et al., 2011; Cassidy and Driscoll, 2009; Wigren and Hansen, 2005).

1.1.2 Treatment of Prader-Willi syndrome

There is currently no cure for PWS. Reliable genetic testing has allowed confirmation of PWS to happen early in life. This makes it possible to guide the treatment and care of the disorder at a very young age which is helping to improve the lives of people with PWS overall (Cataletto et al., 2011). Treatment is mostly based on managing the individual, variable symptoms of the disorder with respect to the age of the individual (Cassidy and Driscoll, 2009). For example, infants may need a feeding tube or other assisted feeding methods. Males may require surgery to fix cryptorchidism. There are no drugs to alleviate the enduring hunger and lack of satiation in PWS and so in order to maintain a healthy weight and lifestyle, a strict and consistent diet and exercise plan must be implemented and rigorously adhered to. Education of parents and caregivers is key to maintaining proper nutrition, ensuring regular physical activity as well as managing potential behavioural problems associated with this syndrome. Controlling the

environment and access to food is very important to preventing overeating and obesity in people with PWS.

Growth hormone deficiency is thought to play a significant role in the short stature, increased fat mass and decreased lean mass seen in PWS. Growth hormone therapy has been shown to have many positive effects on PWS individuals of all ages. Growth hormone treatment results in greater adult height, increased lean mass and muscle strength as well as decreased fat mass (Jin, 2011; Carrel et al., 2010; Cassidy and Driscoll, 2009). Mortality in PWS is often related to obesity and involves health issues such as cardiovascular disorders, type 2 diabetes and sleep apnea (Jin, 2011). Death can also be associated with the physical act of eating itself. Due to the acute hyperphagia, individuals may voraciously binge eat which creates a higher risk of choking as well as gastric necrosis or rupture (Cassidy and Driscoll, 2009).

1.1.3 Genetics of Prader-Willi syndrome

PWS is a genetic disorder resulting from the loss of paternal expression of the imprinted genes on chromosome 15q11-q13 (Figure 2). It is the first disorder known in humans to be associated with genetic imprinting (Nicholls et al., 1989). As part of this chromosome 15 region is maternally imprinted, a cluster of genes on the maternal allele are silenced and thus are only expressed from the paternal allele. Consequently, loss of expression from the paternal allele results in an individual being functionally null for these genes, as is the case with PWS. This loss of expression can occur in a few different ways. Approximately 70% of individuals with PWS have a *de novo* deletion of an interstitial, contiguous 5-7Mb region of the paternal allele of chromosome 15 (Jin, 2011; Cassidy and Driscoll, 2009). There are two different types of deletions, representing most deletion cases in PWS. Type I denotes a deletion from breakpoint 1 (BP1) on chromosome 15 to breakpoint 3 (BP3) and an approximately 500 kb smaller type II deletion involves a loss of DNA from breakpoint 2 (BP2) to BP3 (Cataletto et al., 2011). In fewer than 1% of individuals, the deletion is caused by a paternal chromosomal translocation (Goldstone et al., 2008). PWS was also the first

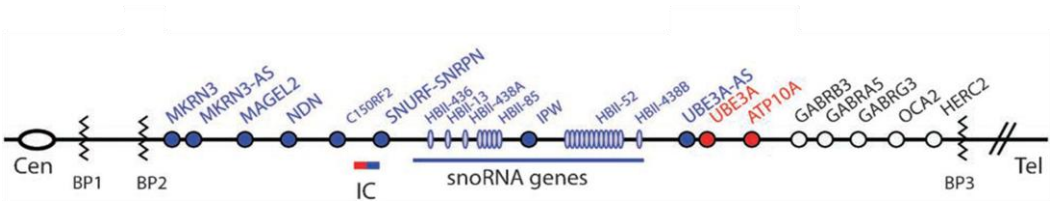

Figure 2. Map of the 15q11-q13 chromosomal region. PWS is caused by a loss of expression of the paternal chromosome 15q11-q13. The blue circles represent maternally imprinted genes and, as such, are only expressed from the paternal allele. Consequently, loss of expression from the paternal allele results in an individual being functionally null for this cluster of genes, as is the case with PWS. This loss of expression can occur in a few different ways, most often it is due to a microdeletion of the paternal 15q11-q13 region between breakpoints (BP) 1 and 3 or 2 and 3. Loss of expression of the paternally imprinted genes, represented by the red circles, results in Angelman syndrome. Non-imprinted genes, which are biparentally expressed, are represented by the white circles. Imprinting is regulated by the imprinting center (IC). Cen – centromere; Tel – telomere. Adapted from Cassidy and Driscoll, 2009.

disorder in humans proven to be caused by a chromosome abnormality called uniparental disomy (UPD) (Nicholls et al., 1989). About 25-30% of affected individuals have maternal uniparental disomy of chromosome 15. This means that, as a result of an error in meiosis, an individual has two copies of the silenced maternal chromosome 15 and no copies of the paternal chromosome 15 (Cassidy and Driscoll, 2009). Lastly, about 2-5% of people with PWS have defects in imprinting of the paternal chromosome 15 (Jin, 2011). In this group, most have an epigenetic defect whereby the paternal chromosome is imprinted and silenced along with the maternal chromosome. About 15% of people with an imprinting defect have a microdeletion in the imprinting center, which is the region responsible for regulating the imprint on chromosome 15 (Buiting, 2010).

1.1.4 Prader-Willi syndrome candidate genes

The 15q11-q13 region, containing both imprinted and non-imprinted genes, can be described as having four parts (Figure 2) (Cassidy and Driscoll, 2009). Starting with the most centromeric region located between the proximal BP1 and BP2, there are four non-imprinted genes which are expressed from both the maternal and paternal alleles, *NIPA1*, *NIPA2*, *CYFIP1* and *GCP5*. Although these genes are biallelically expressed there is evidence that the loss of expression of these genes from one allele, as seen in individuals with type I deletions as compared to type II deletions or UPD, experience increased behavioural and psychological problems and thus contribute to the PWS phenotype (Butler et al., 2004).

Further telomeric to this area is the PWS region in which all of the genes are maternally imprinted and so are only expressed from the paternal allele. This includes *MKRN3*, *MAGEL2*, *NDN*, *C15orf2* and *SNURF-SNRPN* followed by a group of C/D box small nucleolar RNA (snoRNA) genes *SNORD107* (*HBII-436*), *SNORD64* (*HBII-13*), *SNORD108* (*HBII-437*), *SNORD109A* (*HBII-438A*), *SNORD116* (*HBII-85*), *SNORD115* (*HBII-52*) and *SNORD109B* (*HBII-438B*). All of the snoRNA genes exist as single copies except for *SNORD116* (*HBII-85*) and *SNORD115* (*HBII-52*) which are present as clusters of multiple gene copies

(Cavaille et al., 2000). In between SNORD116 and SNORD115 is IPW, a non-protein coding gene called Imprinted in Prader-Willi syndrome (Wevrick and Franke, 1997). The Imprinting Center is also located in this area, immediately proximal to and overlapping with the promoter and first exon of the SNURF-SNRPN gene (Buiting, 2011). The function of makorin ring finger protein 3 (MKRN3) is unknown but it has been suggested that it may have possible functions in protein-protein interactions as well as RNA-binding (Jong et al., 1999). *MAGEL2* and *NDN*, encoding the proteins MAGEL2 and necdin respectively, are members of the melanoma-associated antigen gene (MAGE) family. MAGEL2 has been found to interact with the circadian rhythm proteins BMAL1 and PER2 as well as to repress CLOCK:BMAL1 heterodimer-mediated transcription of *Per2* in a luciferase assay and alter the subcellular localization of CLOCK and BMAL1 in cultured cells (Devos et al., 2011). *MAGEL2* is further described below. Necdin has been found to have roles in cell survival and differentiation. It interacts with multiple proteins including EID-1, p75 neurotrophin receptor, p53, SIRT1 and FOXO1 (Hasegawa et al., 2012; Hasegawa and Yoshikawa, 2008; Bush and Wevrick, 2008; Tcherpakov et al., 2002). The interaction between necdin and FOXO1 is described in more detail below. *C15orf2*, chromosome 15 open reading frame 2, is an intronless gene encoding a protein which associates with the nuclear pore complex (Neumann et al., 2012). Initially, the *SNURF-SNRPN* gene was believed to be a ten exon gene encoding two separate proteins, SNURF (SNRPN upstream reading frame) and SNRPN (small nuclear ribonucleoprotein polypeptide N). Subsequent research found that this gene is actually much more complex and has multiple non-protein coding exons located both 5' and 3' of the original *SNURF-SNRPN* gene which produce many alternatively spliced transcripts including the untranslated IPW. In addition, the snoRNA genes located in this region are encoded in the introns of the *SNURF-SNRPN* gene and are spliced from the *SNURF-SNRPN* transcript (Runte et al., 2001). The snoRNA genes are not directly imprinted and so consequently their expression is dependent on the methylation status of the *SNURF-SNRPN* gene itself. Since *SNURF-SNRPN* is maternally silenced and is

only expressed from the paternal allele, so are all the snoRNA genes. Translocations or uncommon microdeletions resulting in deficiency of the *SNORD116* (*HBII-85*) gene cluster in multiple individuals have been found to result in most of the major PWS characteristics suggesting the importance of this snoRNA gene to the PWS phenotype (de Smith et al., 2009; Sahoo et al., 2008; Schule et al., 2005; Gallagher et al., 2002; Wirth et al., 2001). However, the functional role of SNORD116 in the pathophysiology of PWS remains to be elucidated.

Next is the Angelman syndrome region containing two genes, *UBE3A* and *ATP10A*. *UBE3A*, which encodes an E3 ubiquitin ligase, is non-imprinted except for in the brain where only the maternally inherited allele is expressed. Angelman syndrome is a genetic disorder involving either the loss of maternal expression of the imprinted genes on chromosome 15q11-q13 or *UBE3A* mutations (Buiting, 2010). This syndrome is characterized by developmental delay, disorders in movement, speech impairment as well as distinctive typical behaviours involving frequent laughing or smiling, hand flapping or waving and a happy, excitable demeanor (Williams et al., 2006). As of yet there is no research showing that *ATP10A*, thought to encode an aminophospholipid transporting enzyme, has any involvement in the Angelman syndrome phenotype.

Lastly, the most distal region extends from the end of the Angelman syndrome region to BP3. This area contains non-imprinted genes including the GABA receptor genes *GABRB3*, *GABRA5* and *GABRG3* as well as *OCA2* and *HERC2* (Cassidy and Driscoll, 2009). Mutations in *OCA2* are known to result in oculocutaneous albinism type 2, and hemizygosity for this gene can contribute to hypopigmentation or albinism in people with PWS.

1.2 MAGEL2

1.2.1 MAGE protein family

MAGEL2, encoded by the intronless *MAGEL2* gene, is a member of the MAGE protein family. All members of this family have an approximately 170 amino acid MAGE homology domain (MHD) which consists of two winged-helix

motifs. Via the MHD, MAGE proteins interact with and enhance the function of E3 RING ubiquitin ligases (Doyle et al., 2010). Members of the MAGE family also have roles in cell survival and differentiation, cell cycle progression and apoptosis (Bush and Wevrick, 2008; Barker and Salehi, 2002). Accordingly, neurotrophin receptor-interacting MAGE homolog (NRAGE), MAGE-G1 and necdin have all been found to promote cell cycle arrest as well as interact with the p75 neurotrophin receptor to mediate increased cell death (Salehi et al., 2000; Kuwako et al., 2004). The family is named after the first MAGE protein to be discovered, MAGE-A1, which was found by van der Bruggen et al. in 1991 as a cell surface, cytotoxic T cell-recognizing antigen in a melanoma cell line (Ohman Forslund et al., 2001). There are more than 60 human MAGE genes which have been classified as either type I or type II (Doyle et al., 2010). Type I MAGE genes are all located on the X chromosome and are mostly limited to expression in the testis and in tumours originating from various tissues (Barker and Salehi, 2002; Gillespie and Coleman, 1999). Type II MAGE genes, including *MAGEL2* and *NDN*, are located on chromosomes other than the X chromosome and are expressed in a wide variety of tissues throughout development and adulthood (Doyle et al., 2010; Barker and Salehi, 2002; Boccaccio et al., 1999). A few of the type II MAGE proteins such as necdin as well as most type I proteins consist predominantly of the MHD and very short N and C terminal regions. The rest of the type II MAGE proteins, including MAGEL2, are larger with longer N and/or C terminal regions (Barker and Salehi., 2002).

1.2.2 Magel2 expression pattern

The human *MAGEL2* gene is maternally imprinted and so is only expressed from the paternally inherited allele. Via Northern blot analysis, *MAGEL2* expression has been found in various fetal tissues including the brain, kidney, liver and lung as well as in multiple regions of the adult brain such as the putamen, temporal lobe, frontal lobe, occipital lobe, medulla, cerebral cortex and spinal cord (Lee et al., 2000). Using RT-PCR, expression of *MAGEL2* has also been found in the placenta and again in the fetal and adult brain (Boccaccio et al.,

1999). The murine ortholog, *Magel2*, is located in a conserved syntenic region on chromosome 7 of the mouse and is also only paternally expressed (Boccaccio et al., 1999). Expression of *Magel2* has been found by RT-PCR in the adult brain, the placenta as well as embryonic days 13.5 and 14.5 (E13.5 and E14.5) of the mouse (Boccaccio et al., 1999). *Magel2* expression has also been detected during embryogenesis by Northern blotting at E11, E15 and E17 (Lee et al., 2000). RNA *in situ* hybridization in mouse embryos revealed expression of *Magel2* at E9-E13 with the highest level of expression occurring in the hypothalamus, cerebral cortex and spinal cord (Lee et al., 2000). Further research by Lee et al. in 2003, using RNA *in situ* hybridization with E12.5 embryos, revealed that there is a low level of *Magel2* expression throughout parts of the developing mouse brain such as in the mantle layers, the metencephalon of the hindbrain as well as in the infundibulum which becomes the posterior lobe of the pituitary. However, *Magel2* was also found to be very highly expressed in specific regions of the brain at E12.5 including the ventral thalamus as well as the supraoptic/paraventricular area of the anterior hypothalamus. At E15.5 and E18.5, *Magel2* is highly expressed in the hypothalamus including the dorsal medial suprachiasmatic nucleus (SCN), the supraoptic nucleus (SON) and the preoptic area. Moderate *Magel2* expression is also found in the arcuate nucleus (ARC) and the paraventricular nucleus (PVN) of the hypothalamus (Lee et al., 2003). Using mice with a paternally inherited *lacZ* knock-in allele (described below), expression of *Magel2* was again detected in the brain during embryogenesis, specifically in the neural tube, forebrain, midbrain and hypothalamus. In the adult, most *Magel2* expression was found in the hypothalamus, including the SON, SCN, PVN, ARC and ventromedial nucleus (VMN) (Figure 3) (Kozlov et al., 2007). The expression pattern of *Magel2* throughout embryogenesis and adulthood would suggest that it plays a role in the development of the central nervous system (CNS) as well as in the proper functioning of the brain, the hypothalamus in particular, throughout life.

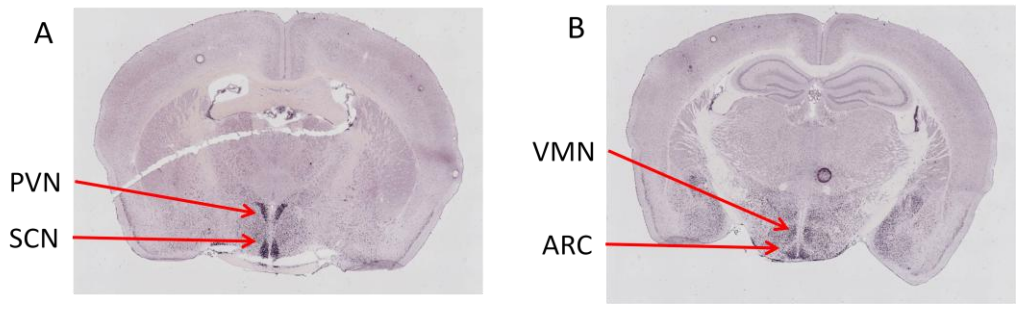

Figure 3. *Magel2* is highly expressed in the hypothalamus. RNA *in situ* hybridization images of two coronal sections of the adult mouse brain. As pointed to by the red arrows, *Magel2* is strongly expressed in (A) the paraventricular nucleus (PVN) and suprachiasmatic nucleus (SCN) as well as in (B) the ventromedial nucleus (VMN) and arcuate nucleus (ARC) of the hypothalamus. The section shown in (A) is anterior to (B). Adapted from the Allen Brain Atlas (Allen Institute for Brain Science).

1.2.3 Magel2-null mice

A mouse strain deficient for *Magel2* was created by using gene-targeting to replace the open reading frame of *Magel2* with a *lacZ* knock-in expression cassette (Bischof et al., 2007; Kozlov et al., 2007). Mice with a paternally inherited *lacZ* knock-in allele are *Magel2*-null since the imprinted maternal allele is silenced. *Magel2*-null mice have a reduced embryonic viability, apparent by E12.5, which results in an approximately 10% underrepresentation of *Magel2*-null pups as compared to wildtype pups (Bischof et al., 2007; Kozlov et al., 2007). Although there is no difference in weight between *Magel2*-null versus wildtype embryos at E18.5 or between pups at postnatal day 1 (P1), *Magel2*-null pups weigh significantly less than wildtype littermates from P7 until weaning which occurs between P21 and P28. Starting at about 4 weeks of age, *Magel2*-null mice begin to gain weight, equalling mean wildtype weight at about 5 to 6 weeks of age and then surpassing wildtype weight resulting in overweight adult *Magel2*-null mice as compared to wildtype littermates (Bischof et al., 2007). Although there is no significant difference in mean weight between wildtype and *Magel2*-null male mice at 16 weeks of age, there are very significant differences in body composition. As a percentage of their total mass, *Magel2*-null mice have decreased lean mass and increased fat mass as compared to wildtype mice. They also have increased plasma leptin levels consistent with their increased fat mass, and increased fasting insulin levels. Despite this increased adiposity, *Magel2*-null mice actually have an approximately 10% reduced total food intake, but they are also significantly less active than wildtype mice (Bischof et al., 2007; Kozlov et al., 2007). *Magel2*-null mice also exhibit defects in circadian rhythm, with an altered pattern of food intake throughout the 12h/12h light/dark cycle and increased subjective daytime activity when in constant darkness (Bischof et al., 2007; Kozlov et al., 2007). In addition, *Magel2*-null mice experience reduced reproductive function. Female mice have longer and delayed puberty, longer and irregular estrous cycles as well as an absence of corpora lutea in the majority of ovaries from older mice at 26 weeks of age. Male mice have decreased testosterone levels and a reduced preference for the odour of females in estrous.

Both showed early reproductive decline, extended length of time required for breeding and infertility by 24 weeks of age (Mercer and Wevrick, 2009). The abnormalities in mice lacking expression of *Magel2* are very comparable to the symptoms observed in PWS. Although *Magel2*-null mice are not hyperphagic or substantially obese like in PWS or other mice models of obesity, they do recapitulate much of the PWS phenotype including decreased post-natal weight gain followed by a switch to significant weight gain, altered body composition with decreased lean mass and increased fat mass, reduced fertility, circadian rhythm defects and decreased activity levels. This strongly suggests that the loss of *MAGEL2* plays a significant role in the pathophysiology of PWS.

1.3 Energy homeostasis

1.3.1 Hypothalamus

The characteristics of PWS, including childhood-onset obesity, hyperphagia, insatiable hunger and decreased activity levels, are strongly suggestive of dysfunctional homeostatic regulation of energy. These characteristics along with other PWS symptoms such as neonatal hypotonia and failure to thrive, sleep abnormalities, growth hormone deficiency, developmental delay and hypogonadotropic hypogonadism are all very indicative of hypothalamic dysfunction. The hypothalamus is the main monitoring and control center for energy balance in the body. It responds to nutrient and hormone levels in order to regulate homeostatic processes including appetite and energy expenditure. Accordingly, the high and almost exclusive expression of *Magel2* in the hypothalamus of the adult mouse brain, along with the close parallels between the PWS phenotype and some of the findings in *Magel2*-null mice including altered body composition and decreased activity levels, leads to the hypothesis that the loss of *Magel2* may directly contribute to the energy imbalance, putatively originating from hypothalamic dysfunction, typical of PWS.

The hypothalamus continually monitors and regulates the overall energy status of the body by integrating information about energy stores and expenditure. It does this by sensing and responding to central and peripheral signals and

subsequently activating the appropriate downstream responses (Boguszweski et al., 2010; Barsh and Schwartz, 2002). The hypothalamus is composed of multiple distinct nuclei, including the ARC, PVN, VMN, dorsomedial nucleus (DMN) and lateral hypothalamic area (LHA), each with roles in energy homeostasis (Suzuki et al., 2012). In the ARC, there are two populations of neurons crucial to mediating the effects of the peripheral energy signals: pro-opiomelanocortin (POMC) neurons and neuropeptide Y (NPY) neurons (Figure 4). Both types of neurons project into many hypothalamic nuclei including the PVN, VMN, DMN and LHA (Suzuki et al., 2012; Mercer et al., 2011; Woods et al., 2008). When POMC neurons are activated, both *POMC* and cocaine- and amphetamine-regulated transcript (*CART*) are expressed. POMC can be cleaved into multiple different peptides, one of which is α-melanocyte-stimulating hormone (α-MSH). Alpha-MSH binds to melanocortin 3 and 4 receptors (MC3R and MC4R) signalling to decrease appetite and food intake and increase energy expenditure, for example, by activating the expression and release of thyrotropin-releasing hormone (TRH) in the PVN (Morris and Rui, 2009; Gao and Horvath, 2008). Activation of melanocortin receptors results in the activation of adenylate cyclase, the enzyme which produces cyclic adenosine monophosphate (cAMP) from adenosine triphosphate (ATP) (Barsh and Schwartz, 2002). The increased intracellular cAMP stimulates increased phosphorylation of the cAMP response element-binding (CREB) transcription factor. Phosphorylated CREB then binds to CREB-binding protein (CBP) and activates expression of *TRH*. TRH subsequently stimulates the production of thyroid-stimulating hormone (TSH) which functions to increase metabolic rate (Harris et al., 2001). CART has also been found to reduce food intake (Aja et al., 2001). Melanocortin receptor activation also stimulates increased expression of brain-derived neurotrophic factor (*BDNF*) in the VMN. Deficiency of either BDNF or its receptor TrkB has been found to result in hyperphagia and obesity (Morris and Rui, 2009). When activated, NPY neurons release both NPY and agouti-related protein (AgRP). NPY mainly binds to NPY receptors on neurons of the PVN where it signals to increase appetite and food intake. AgRP functions to increase appetite indirectly

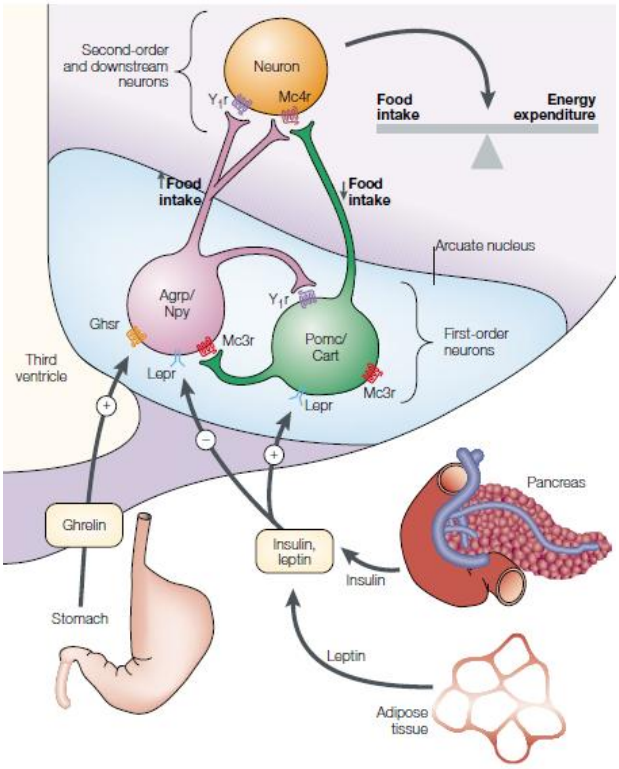

Figure 4. Energy homeostasis is regulated by the hypothalamus. The NPY and POMC neurons located in the arcuate nucleus of the hypothalamus respond to circulating peripheral signals, including ghrelin, leptin and insulin, by activating or repressing downstream neuronal activity in other hypothalamic nuclei. Activation of NPY neurons increases appetite and decreases energy expenditure whereas activation of POMC neurons decreases appetite and increases energy expenditure. Ghsr – growth hormone secretagogue receptor; LepR – leptin receptor; Mc3/4r – melanocortin 3/4 receptor; Y_1r – neuropeptide Y1 receptor. Adapted from Barsh and Schwartz, 2002.

as a competitive antagonist of MC3R and MC4R, which blocks α-MSH binding, preventing its downstream anorexigenic effects (Boguszweski et al., 2010; Morris and Rui, 2009). In addition, activated NPY neurons directly inhibit POMC neuronal activation by releasing γ-aminobutyric acid (GABA), an inhibitory neurotransmitter (Morris and Rui, 2009; Cowley et al., 2001).

The peripheral signals that act upon POMC and NPY neurons include 'satiety signals' such as ghrelin or other gastrointestinal peptides and 'adiposity signals' such as the hormones leptin and insulin (Boguszweski et al., 2010; Valassi et al., 2007). Satiety signals function in short-term energy regulation by influencing the initiation and termination of meals as well as the interval between meals. They may either act directly on the neurons of the ARC or they may signal through the nucleus of the solitary tract (NTS) of the brainstem. Ghrelin, produced mainly by the stomach, is a hormone with strongly orexigenic effects. It signals through the growth hormone secretagogue (GHS) receptor expressed on NPY neurons of the ARC resulting in increased food intake. Ghrelin also signals the release of growth hormone via GHS receptors in the pituitary gland (Barsh and Schwartz, 2002). Other satiety signals function to reduce food intake, such as peptide YY3-36 which is released from the intestine after a meal in proportion to the amount of calories ingested. Peptide YY3-36, an agonist of the putative inhibitory presynaptic receptor NPY Y2 receptor (Y2R), has been found to significantly reduce NPY release from NPY neurons (Batterham et al., 2002; King et al., 1999). Adiposity signals are involved in long-term energy regulation by relaying information about the body's energy stores. Leptin and insulin, released from adipose tissue and the pancreas, respectively, bind to their respective receptors on POMC and NPY neurons in the ARC in order to decrease appetite and increase energy expenditure (Boguszweski et al., 2010; Valassi et al., 2007). Both leptin and insulin hyperpolarize NPY neurons which inhibits the neurons from firing and prevents the release of GABA (Cowley et al., 2001; Spanswick et al., 2000). The lack of GABA release disinhibits POMC neuronal activity. Leptin signalling also directly activates the depolarization of POMC neurons in the hypothalamus which has been proposed to occur via transient receptor

potential cation (TRPC) channel activation by an insulin receptor substrate (IRS)-phosphatidylinositol 3-kinase (PI3K)-phospholipase C γ1 (PLCγ1) pathway (Qiu et al., 2010; Cowley et al., 2001).

1.3.2 Leptin signalling pathway

The leptin signalling pathway is critical to maintaining energy homeostasis. It also has roles in immunity, bone homeostasis and reproduction. Leptin, an endocrine hormone, is expressed from the *obese* (*ob*) gene. Genetic mutations in the *ob* gene, resulting in leptin deficiency, have been found to cause hyperphagia, decreased energy expenditure and extreme morbid obesity in both humans and mice (Morris and Rui., 2009; Gale et al., 2004). The leptin receptor (LepR), a member of the class I cytokine receptor family, is expressed from the *diabetes* (*db*) gene. There are multiple alternatively spliced isoforms of the LepR but only LepRb has the long intracellular domain required for leptin signal transduction. LepR deficiency, resulting from *db* gene mutations, also causes obesity in both humans and mice (Boguszweski et al., 2010). Leptin is produced by adipose tissue at levels which are directly proportional to fat mass. It is released into the bloodstream and transported to the brain where it crosses the blood brain barrier and binds to the long form of the leptin receptor (LepRb) which is expressed highly in the hypothalamus (Sahu et al., 2004). When leptin binds to LepRb many downstream pathways are activated (Figure 5). LepRb dimerizes causing Janus kinase 2 (JAK2), a tyrosine kinase, to autophosphorylate. Activated JAK2 subsequently phosphorylates tyrosine 985, tyrosine 1077 and tyrosine 1138 of the intracellular domain of LepRb. Phosphorylated tyrosine 985 binds with SH2-containing protein tyrosine phosphatase 2 (SHP2) which leads to the phosphorylation and activation of extracellular-signal-regulated kinase/mitogen-activated protein kinase (ERK/MAPK). Activation of ERK is common in many cellular signalling pathways, pairing receptor activation by proteins such as growth hormone, interleukin-6, epidermal growth factor and granulocyte colony-stimulating factor with downstream events including regulation of apoptosis, cell cycle progression and cellular differentiation

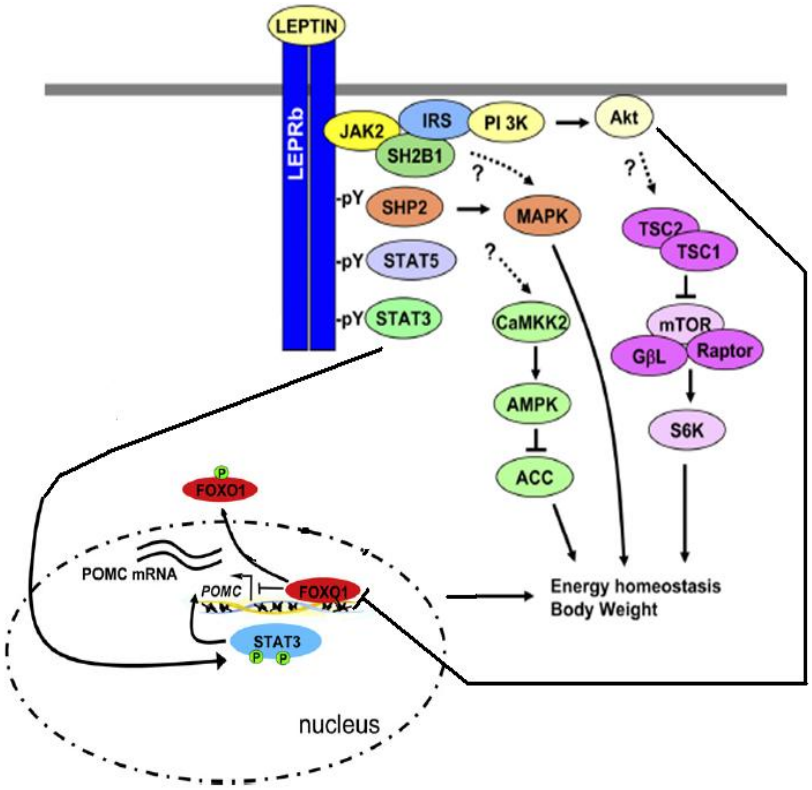

Figure 5. Model of the leptin signalling pathway. Leptin, a hormone produced by adipose tissue, binds to the leptin receptor and activates many downstream pathways. The tyrosine kinase JAK2 autophosphorylates and subsequently phosphorylates tyrosine 985, tyrosine 1077 and tyrosine 1138 of the leptin receptor. Phosphorylation of tyrosine 985 leads to the phosphorylation of ERK. Phosphorylation of tyrosine 1138 activates the phosphorylation of transcription factor STAT3. Phospho-STAT3 translocates to the nucleus and activates the transcription of target genes, such as *POMC*, which are important in mediating the anorexigenic effects of leptin signalling. Phosphorylated JAK2 binds to the adapter protein SH2B1, which binds concurrently to insulin receptor substrate (IRS) leading to phosphorylation of IRS and activation of phosphatidylinositol 3-kinase (PI3K). PI3K activation leads to phosphorylation of the kinase AKT at the plasma membrane. Phosphorylated AKT translocates to the nucleus where it phosphorylates the Forkhead box protein FOXO1. Phosphorylated FOXO1 is excluded from the nucleus and thus is no longer able to repress transcription of *POMC* or activate transcription of genes involved in increasing appetite. Leptin signalling also results in the dephosphorylation and inactivation of AMPK. Adapted from Morris and Rui, 2009 and Belgardt et al., 2008.

(McCubrey et al., 2007; Bjorbaek et al., 2001). Inhibition of ERK in the hypothalamus of rats has been found to block the anorexigenic effects of leptin (Rahmouni et al., 2009). Signal transducer and activator of transcription 3 (STAT3) binds with phosphorylated tyrosine 1138 via a consensus binding motif and is subsequently phosphorylated by JAK2. Phosphorylated STAT3 translocates to the nucleus and directly activates the transcription of target genes, such as *POMC* and *TRH*, which, as previously discussed, are important in mediating the anorexigenic effects of leptin signalling. STAT3 has also been found to inhibit the transcription of the orexigenic *AgRP* (Kitamura et al., 2006). Phosphorylation of tyrosine 1077 leads to the phosphorylation and activation of STAT5. Deficiency of either STAT3 or STAT5 is known to result in hyperphagia and obesity (Morris and Rui, 2009). Phosphorylated JAK2 binds to the adapter protein SH2B1, which binds concurrently to IRS leading to phosphorylation of IRS and activation of PI3K. Activated PI3K phosphorylates phosphatidylinositol-4,5-biphosphate (PIP2) producing phosphatidylinositol-3,4,5-triphosphate (PIP3). PIP3 then binds to the serine/threonine kinase AKT and 3-phosphoinositide-dependent protein kinase-1 (PDK1) at the plasma membrane where AKT is phosphorylated by PDK-1 as well as the serine/threonine kinase mammalian target of rapamycin complex 2 (mTORC2). AKT is involved in many cellular processes. This includes cell survival, growth, proliferation, angiogenesis, metabolism and migration via signalling of multiple downstream pathways such as mTOR complex 1 (mTORC1) activation (Manning and Cantley, 2007). Phosphorylated AKT translocates to the nucleus where it phosphorylates the Forkhead box protein FOXO1. Phosphorylated FOXO1 is excluded from the nucleus which inhibits its ability to activate transcription of genes involved in increasing appetite such as *NPY* and *AgRP* or to repress transcription of genes involved in suppressing appetite such as *POMC*. FOXO1 is further discussed below. Inhibition of the PI3K pathway has been shown to block the anorexigenic effects of leptin in rats (Zhao et al., 2002; Niswender et al., 2001). Leptin signalling also results in the dephosphorylation and inhibition of 5'-AMP activated protein kinase (AMPK). AMPK, which is active when phosphorylated,

inhibits acetyl-CoA carboxylase (ACC) via phosphorylation of serine 79. ACC is an important enzyme in fatty acid biosynthesis as it catalyzes the reaction which produces malonyl-CoA from the carboxylation of acetyl-CoA. Dephosphorylation of AMPK via leptin signalling inhibits AMPK from phosphorylating ACC thus promoting fatty acid biosynthesis (Gao et al., 2007). Constitutively active AMPK as well as ACC inhibition have both been found to reduce the effect of leptin on decreasing food intake and body weight in rodents (Gao et al., 2007; Minokoshi et al., 2004). Leptin signalling also activates the expression of suppressor of cytokine signalling 3 (*SOCS3*) via STAT3. SOCS3 inhibits leptin signalling by binding to and inactivating JAK2 and tyrosine 985 of LepRb. Negative feedback is also provided by protein tyrosine phosphatase 1B (PTP1B) which dephosphorylates JAK2 (Morris and Rui, 2009; Sahu et al., 2004).

1.3.3 Insulin signalling pathway

Insulin is an anabolic hormone produced and released by the beta cells of the pancreas, primarily in response to the increased concentration of glucose present in the blood after food intake (Eslam et al., 2011). It is released into the bloodstream at levels which are proportional to fat mass. Insulin has many important roles in the body. It activates cell growth as well as differentiation and functions as a potent regulator of plasma glucose concentration. Insulin stimulates the uptake of glucose by activating glucose transporter GLUT4 translocation. GLUT4 is transported from intracellular vesicles to the cell membrane where it facilitates the uptake of glucose into the cell, mainly in skeletal muscle and adipose tissue (Saltiel and Kahn, 2001). Insulin also inhibits the production of glucose in the liver. Insulin stimulates the synthesis and storage of lipids, glycogen and proteins as well as inhibits their degradation. Circulating insulin binds to the insulin receptor (IR) which is expressed in most body tissues including liver, muscle and fat (Brüning et al., 2000). Plasma insulin is also transported to the brain where it crosses the blood brain barrier and binds to highly expressed insulin receptors in the ARC of the hypothalamus (Figure 6) (Boguszewski et al., 2010). IR is a tyrosine kinase receptor composed of two

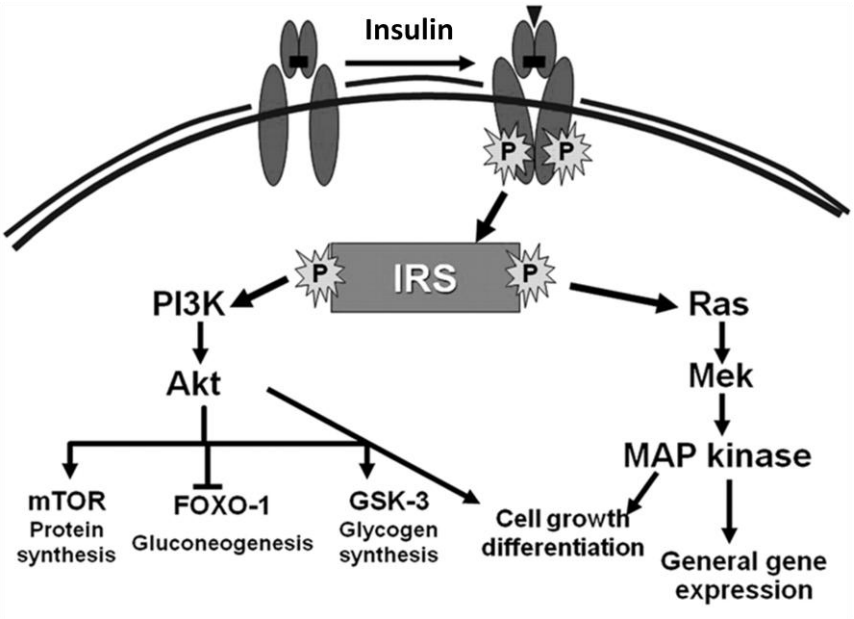

Figure 6. Model of the insulin signalling pathway. Insulin binds to the insulin receptor (IR) resulting in autophosphorylation of IR. Activated IR phosphorylates IRS which activates multiple downstream proteins including ERK/MAPK as well as AKT. Activated AKT phosphorylates and inactivates glycogen synthase kinase-3 (GSK-3) resulting in increased glycogen synthesis. Phosphorylated AKT also phosphorylates and inactivates FOXO1 which leads to decreased gluconeogenesis in the liver. Adapted from Eslam et al. 2011.

extracellular α subunits which, prior to ligand binding, inhibit the kinase activity of two transmembrane and intracellular β subunits. When insulin binds to the α subunits, the kinase activity of the β subunits is no longer inhibited leading to autophosphorylation of IR and subsequent phosphorylation of IRS proteins which activates multiple downstream pathways (Eslam et al., 2011; Saltiel and Kahn, 2001). Like leptin signalling, insulin activates ERK/MAPK as well as AKT. Phosphorylated IRS activates PI3K which, as discussed above, leads to the phosphorylation of AKT. Phospho-AKT phosphorylates and inactivates glycogen synthase kinase-3 (GSK-3). Activated GSK-3 phosphorylates and inhibits glycogen synthase, the enzyme which produces glycogen from glucose. Consequently, inactivation of GSK-3 resulting from insulin signalling leads to increased glycogen synthesis (Saltiel and Kahn, 2001). As previously mentioned, phospho-AKT also phosphorylates FOXO1 which leads to its inactivation via nuclear exclusion. In the liver, FOXO1 stimulates glucose production by activating expression of gluconeogenic genes such as glucose-6-phosphatase (*G6PC*) and phosphoenolpyruvate carboxykinase 1 (*PCK1*) (Puigserver et al., 2003). FOXO1 also inhibits beta cell proliferation. It represses expression of pancreas/duodenum homeobox-1 (*PDX1*) which encodes a transcription factor involved in the regulation of beta cell proliferation (Kitamura et al., 2002; Nakae et al., 2002). Both of these actions are inhibited by insulin signalling via FOXO1 phosphorylation by AKT.

1.4 FOXO1

1.4.1 FOXO protein family

FOXO1 is a member of the 'O' class of the Forkhead box (FOX) superfamily of transcription factors. There are more than 100 proteins in the FOX superfamily which all share a conserved DNA-binding domain of ~100 amino acids, referred to as the Forkhead domain (Huang and Tindall, 2007). The structure of the Forkhead domain is composed of three α-helices and 2 large loops that resemble wings, which is why FOX proteins are also referred to as winged helix transcription factors (Huang and Tindall, 2007). FOX proteins in the 'O'

class (FOXO) are considered the most divergent proteins of the FOX superfamily due to differences in the sequence of amino acids in the Forkhead domain which directly affects DNA binding site interactions (Barthel et al., 2005). FOXO transcription factors are involved in many cellular processes including differentiation, metabolism, proliferation, DNA damage repair, oxidative stress, cell cycle and apoptosis (Huang and Tindall, 2007; Accili and Arden, 2004). DAF-16, the FOXO homologue in *Caenorhabditis elegans*, has been implicated in longevity, stress resistance and arrest at the dauer diapause stage of nematode larval development. The FOXO homologue in *Drosophila melanogaster*, dFOXO, has also been found to be involved with resistance to oxidative stress (van der Heide et al., 2004). There are four mammalian FOXO proteins: FOXO1, FOXO3, FOXO4 and FOXO6 (Tzivion et al., 2011). A distinctive characteristic of FOXO proteins is that they are negatively regulated by the PI3K-AKT pathway. They all have highly conserved AKT phosphorylation sites which, when phosphorylated, inhibits their activity (Huang and Tindall, 2007; van der Heide et al., 2004).

1.4.2 Foxo1 expression pattern

FOXO1 was the first mammalian FOXO family protein to be identified. It was originally named Forkhead in rhabdomyosarcoma (FKHR) until the nomenclature for all FOX proteins was unified and updated (Kaestner et al., 2000). The *FOXO1* gene, located on chromosome 13 in humans, was found because of chromosomal translocations in rhabdomyosarcoma involving chromosome 2 and chromosome 13. These translocations resulted in a FOXO1/paired box 3 (PAX3) fusion protein which was found to have increased potency as a transcription factor when compared to wildtype PAX3 (Fredericks et al., 1995). Subsequently, translocations between chromosome 1 and 13 in some rhabdomyosarcomas were found to result in a FOXO1/paired box 7 (PAX7) fusion protein (Tzivion et al., 2011). Due to vasculature defects, homozygous *Foxo1* knock-in mice experience embryonic lethality at approximately E10. A heterozygous *Foxo1*$^{+/\beta\text{-}geo}$ mouse strain has subsequently been generated using

gene-targeting to insert an in-frame *β-geo* knock-in cassette, encoding β-galactosidase and Neo resistance, into the first intron of *Foxo1* (Villarejo-Balcells et al., 2011; Nakae et al., 2002). This mouse strain has been used to determine the embryonic expression pattern of *Foxo1*. In the developing mouse embryo, *Foxo1* expression can first be detected at E7 in the neuroepithelium, in the developing heart by E8 and in the rest of the developing vasculature at E9. By E11 *Foxo1* expression in the vasculature begins to decrease as expression in the developing muscle is first detected. At E12 *Foxo1* expression can no longer be detected in the vasculature and is primarily expressed in the developing muscle. Expression in most muscles decreases at E14 and at E16 *Foxo1* is strongly expressed in brown adipose tissue. By E18 *Foxo1* expression increases in the muscles, bone as well as part of the vasculature and epithelium (Villarejo-Balcells et al., 2011). In the adult mouse, *Foxo1* has been found by northern blot analysis to be strongly expressed in brown and white adipose tissue as well as the spleen. *Foxo1* is also expressed in the brain, skeletal muscle, lung, liver and kidney as well as low expression in the ovaries and testis (Villarejo-Balcells et al., 2011). *Foxo1* is also known to be expressed in the beta cells of the pancreas, skeleton and hypothalamus (Kousteni, 2012; Al-Masri et al., 2010).

1.4.3 FOXO1 function

FOXO1 has many roles in diverse tissues of the mammalian body. As a transcription factor, FOXO1 binds to the promoters of target genes in order to directly activate or repress their transcription. FOXO1 also affects transcription independently of DNA-binding via interactions with other transcription factors including nuclear receptors such as the estrogen receptor, progesterone receptor, androgen receptor, thyroid hormone receptor, glucocorticoid receptor, retinoic acid receptor and peroxisome-proliferator-activated receptor (PPAR) (van der Heide et al., 2004). Concurrently, many of these receptors also activate or repress FOXO1 activity. For example, FOXO1 both inhibits and is inhibited by PPARγ, a receptor which promotes adipocyte differentiation when activated (Dowell et al., 2003). FOXO1 promotes cell death by activating the expression of pro-apoptotic

genes including bcl-2 interacting mediator of cell death (*BIM*), Fas ligand (*FASL*) and tumour-necrosis-factor-related apoptosis-inducing ligand (*TRAIL*) (Gilley et al., 2003; Li et al., 2003; Modur et al., 2002). Additionally, acetylated FOXO1 promotes cell death independently of transcriptional activity by interacting with E1-like protein autophagy-related 7 (ATG7) to activate autophagy (Zhao et al., 2010). FOXO1 is also involved in skeletal muscle atrophy, activating the expression of the muscle-specific ubiquitin ligase atrogin-1. Transgenic mice overexpressing FOXO1 in skeletal muscle have significantly reduced skeletal muscle mass (Kamei et al., 2004). FOXO1 induces cell cycle arrest at the G1/S transition by activating expression of the cyclin-dependent kinase inhibitor $p27^{kip1}$, a cell cycle inhibitor protein (Nakamura et al., 2000). Stimulation by transforming growth factor-β leads to the phosphorylation and activation of SMAD proteins which can interact with FOXO1. The FOXO1-SMAD complex activates the expression of another cyclin-dependent kinase inhibitor, $p21^{cip1}$, which also functions in cell cycle arrest at the G1-phase (Seoane et al., 2004). FOXO1-mediated activation of these and other cell cycle inhibitors is associated with the role of FOXO1 in the inhibition of adipocyte differentiation (Nakae et al., 2003). FOXO1 is also involved in resistance to oxidative stress. Oxidative stress results from an increase in the level of reactive oxygen species (ROS) present in the cell. As ROS is able to induce damage to many parts of the cell, FOXO1 promotes stress resistance by activating the expression of manganese superoxide dismutase (MnSOD), a protein involved in oxidative detoxification (Huang and Tindall, 2007; Daitoku et al., 2004). As previously mentioned, FOXO1 is involved in promoting glucose production in the liver by interacting with PPARγ coactivator 1 (PGC-1α) to activate expression of *G6PC* and *PCK1* (Puigserver et al., 2003). In addition, FOXO1 inhibits pancreatic beta cell proliferation by repressing expression of *PDX1*. Accordingly, transgenic mice expressing constitutively active *Foxo1* in the liver and beta cells developed hyperglycemia and diabetes as a result of increased gluconeogenesis as well as decreased beta cell proliferation and functioning (Nakae et al., 2002). FOXO1 also inhibits beta cell proliferation through its activity in osteoblasts. Bone-forming osteoblast

cells release osteocalcin, a hormone which stimulates beta cell proliferation as well as insulin secretion and sensitivity (Kousteni, 2011). Osteocalcin is inactivated via carboxylation which is promoted by OST-PTP, a protein tyrosine phosphatase encoded by the *ESP* gene (Rached et al., 2010). FOXO1 has been shown to inhibit osteocalcin in two ways: by directly repressing transcription of osteocalcin and by increasing osteocalcin inactivation by activating *ESP* expression (Rached et al., 2010). FOXO1 is also involved in energy homeostasis. It activates the expression of *NPY* and *AgRP* in the ARC of the hypothalamus resulting in increased food intake and body weight (Kim et al., 2006). FOXO1 also represses the expression of anorexigenic *POMC* by binding with STAT3 and inhibiting STAT3-mediated POMC promoter activation (Yang et al., 2009).

1.4.4 Regulation of FOXO1

Much research has been done concerning the regulation of FOXO1. Numerous authors have found that stimulation by leptin, insulin or other growth factors leads to phosphorylation, cytoplasmic localization, inactivation and degradation of FOXO1 (Kim et al., 2006; Aoki et al., 2004; Matsuzaki et al., 2003). The nuclear export of FOXO1 involves passing through the nuclear-pore complex of the nuclear membrane which separates the nucleus from the cytoplasm (van der Heide et al., 2004). In the nucleus, the exportin chromosomal region maintenance protein 1 (CRM1) recognizes and binds to a nuclear export sequence (NES) located in the C-terminal region of FOXO1 (Figure 7). FOXO1 is then actively transported through the nuclear membrane to the cytoplasm by a complex composed of CRM1 and GTP-bound RAN, a small GTPase. FOXO1 can also be imported to the nucleus by importin proteins which recognize and bind to a nuclear localization sequence (NLS) located at the C-terminal end of the DNA-binding domain (Figure 7) (van der Heide et al., 2004). In the nucleus, FOXO1 binds directly to high-affinity DNA binding sites, such as the FOXO-recognized element (FRE) or the insulin response sequence (IRS), in the promoter region of target genes and activates their transcription (van der Heide et al., 2004). The subcellular localization of FOXO1, which largely influences its activity, is

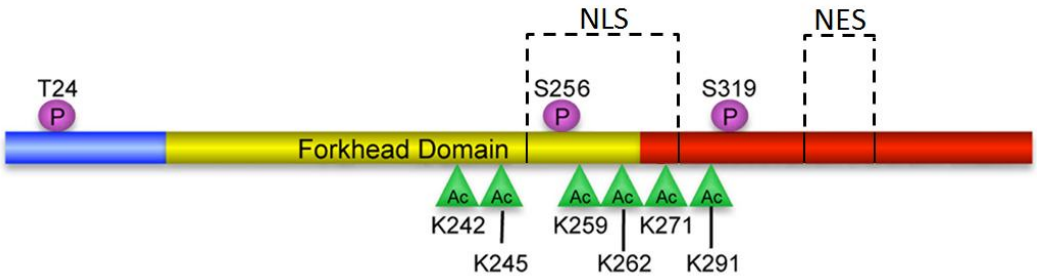

Figure 7. Schematic of the FOXO1 protein. FOXO1 contains the Forkhead domain, a nuclear localization sequence (NLS) as well as a nuclear export sequence (NES). The indicated FOXO1 residues are either phosphorylated by AKT (T24, S256 and S319) or acetylated by CBP (K242, K245, K259, K262, K271 and K291). Adapted from Qiang et al., 2010.

controlled by complex, multifaceted processes including intracellular signalling, post-translational modifications, protein-protein interactions and stress.

1.4.4.1 Phosphorylation

As previously discussed, FOXO1 is subject to PI3K-dependent AKT-mediated phosphorylation which is activated by growth factors such as leptin and insulin. Phosphorylated FOXO1 is shuttled to the cytoplasm which, consequently, abrogates its transcriptional activities in the nucleus (Biggs et al., 1999). This process of leptin- and insulin-induced cytoplasmic translocation of FOXO1 has also been shown in POMC and NPY neurons of the ARC (Fukuda et al., 2008). When activated, AKT phosphorylates FOXO1 at 3 highly conserved sites: threonine 24 (T24), serine 256 (S256) (S253 in murine FOXO1) and S319 (S316 in murine FOXO1) (Figure 7). T24 is located in the N-terminal region, S256 is in the C-terminal end of the DNA-binding domain and S319 is further downstream in the C-terminal area. Phosphorylation of the S256 site is required in order for phosphorylation of T24 and S319 to occur. This was determined through the use of FOXO1 phosphorylation mutants in which one of each of the three sites is replaced with alanine (A), rendering the site unphosphorylatable. Whereas neither the T24A nor the S319A mutants prevented phosphorylation of the other two sites when stimulated with insulin, the S256A mutant fully prevented phosphorylation of both the T24 and S319 sites (Rena et al., 2001; Nakae et al., 2000). In addition, phosphorylation of S256, but not T24 or S319, is necessary for insulin-mediated inhibition of FOXO1 transcriptional activity. Using a luciferase reporter construct driven by an IRS-containing promoter, insulin treatment caused decreased luciferase expression in cells transfected with either the T24A or S319A mutants. Insulin stimulation was not able to inhibit luciferase activity in cells transfected with the S256A mutant, suggesting that S256 phosphorylation is sufficient for insulin-mediated inhibition of FOXO1 transcriptional activity (Guo et al., 1999). However, there is also research which suggests that phosphorylation of T24 is also necessary to inhibit FOXO1-mediated gene expression (Nakae et al., 2000). With respect to localization, it has

been determined that the phosphorylation of both T24 and S256 are each required for FOXO1 nuclear exclusion. Both the S256A and T24A mutants remained in the nucleus and did not translocate to the cytoplasm after insulin stimulation as opposed to the S319A mutant which, although more slowly than wildtype FOXO1, did translocate to the cytoplasm after stimulation with insulin (Nakae et al., 2000). It is important to note that FOXO1 transcriptional activity is not entirely dependent on localization. A transiently transfected FOXO1 mutant, which cannot be exported to the cytoplasm due to a mutation in the NES, was still subject to insulin-mediated inhibition of its transcriptional activity in a rat hepatoma cell line (Tsai et al., 2003).

14-3-3 proteins, which bind to specific motifs containing phosphorylated serine or threonine residues, regulate the activity, interactions, stability and localization of the proteins they bind with (Tzivion et al., 2011). In order to shuttle to the cytoplasm, FOXO1 must bind with 14-3-3 protein dimers and this interaction requires phosphorylation of both T24 and S256. Unlike wildtype and S319A FOXO1, T24A and S256A FOXO1 did not bind with 14-3-3 proteins in co-immunoprecipitations or GST pull-down assays (Zhao et al., 2004; Rena et al., 2001). The phosphorylated T24 site is part of an optimal 14-3-3 binding site whereas the S256 site is not part of an optimal motif, however, optimal motifs are not necessary for interaction with 14-3-3 proteins (van der Heide et al., 2004). It has been proposed that the high affinity T24 site may first bind with one 14-3-3 subunit which then allows the other 14-3-3 subunit to bind with the lower affinity S256 site (van der Heide et al., 2004). Although the exact mechanism of how 14-3-3 proteins promote nuclear export is not fully understood, there is speculation that 14-3-3 binding may, in some way, enhance the functioning of the NES such as through facilitating the interaction of the NES with the RAN-CRM1 export complex (Brunet et al., 2002). In addition, multiple authors also suggest that, once exported, 14-3-3 binding functions to maintain cytoplasmic sequestration by masking or sterically inhibiting the NLS (Zhao et al., 2004; Brunet et al., 2002; Brownawell et al., 2001). Phosphorylation of S256 has been found to inhibit FOXO1 DNA binding. However, there are some conflicting results in the

literature concerning whether phosphorylated S256 inhibits FOXO1 DNA binding directly or if it inhibits DNA binding indirectly by enhancing FOXO1 binding affinity with 14-3-3 proteins (Tzivion et al., 2011, van der Hieide et al., 2004; Zhang et al., 2002).

In addition to the sites phosphorylated by AKT, FOXO1 is also phosphorylated at many other sites by multiple other proteins. Casein kinase 1 (CK1) requires phosphorylation of S319 in order to phosphorylate two subsequent serine residues on FOXO1, S322 and S325 (Rena et al., 2002). CK1, a serine/threonine kinase, is not activated directly by insulin. Rather, CK1 recognizes specific sites which have already been primed via phosphorylation by other proteins which allow it to phosphorylate adjacent residues (van der Heide et al., 2004). The S322 and S325 sites may be important for binding with the GTPase RAN, which forms a complex with CRM1 to facilitate nuclear export. Unlike wildtype or S319A FOXO1, S322A and S325A mutants did not co-immunoprecipitate with RAN (Rena et al., 2002).

The dual-specificity tyrosine-phosphorylated and regulated kinase 1A (DYRK1A) phosphorylates S329 immediately downstream of the CK1 sites of FOXO1 (Woods et al., 2001). Phosphorylation of S329 seems to be constitutive and is not affected by signalling via PI3K and AKT (Rena et al., 2002). A S329A FOXO1 mutant has increased transcriptional activity and has a higher proportion of nuclear localization as compared to wildtype FOXO1 indicating that the site does play a role in FOXO1 regulation (Woods et al., 2001).

Cyclin-dependent kinase 2 (CDK2), a cell cycle protein important for the transition to S phase, phosphorylates FOXO1 at S249 located in a known CDK consensus sequence. Phosphorylation of S249 results in decreased transcriptional activity and increased cytoplasmic localization of FOXO1 (Huang et al., 2006). Phosphorylation by CDK2 is independent of the PI3K pathway as inhibition of PI3K did not prevent the CDK2-mediated decrease in FOXO1 transcriptional activity. Consequently, inhibition of CDK2 resulting from DNA damage prevents FOXO1 inactivation. This leads to increased cell death via increased FOXO1-

mediated transcription of pro-apoptotic genes such as *BIM* and *TRAIL* (Huang et al., 2006; Gilley et al., 2003; Modur et al., 2002).

It has been suggested that the serum- and glucocorticoid-inducible kinase (SGK) may also phosphorylate the AKT recognition sites of FOXO1 via activation by PI3K and PDK1 (Brunet et al., 2001). SGK and AKT are related proteins which both belong to the AGC kinase family. However, it has been determined that FOXO1 is similarly phosphorylated with or without activated SGK (Collins et al., 2003).

1.4.4.2 Acetylation

FOXO1 is also regulated by acetylation. However the role of acetylation on FOXO1 regulation is highly complex and controversial, with much left to be elucidated. CREB-binding protein (CBP) binds to and acetylates FOXO1 on multiple lysine residues including K242, K245 and K262, which are located in or immediately downstream of the DNA-binding domain (Figure 7). FOXO1 is deacetylated at these same sites by sirtuin 1 (SIRT1), a NAD-dependent deacetylase (Daitoku et al., 2004). The effect of reversible acetylation on FOXO1 activity has generated conflicting experimental results. Some researchers have found that acetylation increases FOXO1 transcriptional activity whereas others have found that deacetylated FOXO1 is more active. In one study, SIRT1-mediated deacetylation of a constitutively active FOXO1 phospho-mutant resulted in decreased expression from a luciferase reporter construct under the control of the *BIM* promoter (Motta et al., 2004). Furthermore, this repression of luciferase activity by SIRT1 was relieved by treatment with the deacetylase inhibitor nicotinamide. In addition, using Northern blot analysis, expression of the FOXO1 target genes *PCK1* and insulin-like growth factor binding protein-1 (*IGFBP-1*) were found to be higher in SIRT1 knock-out mice as compared to wildtype mice. In another study, four and a half LIM 2 (FHL2) was found to enhance SIRT1-mediated deacetylation of FOXO1 in prostate cancer cells, resulting in decreased expression from a luciferase reporter linked to the *IGFBP-1* promoter containing three copies of the IRS (Yang et al., 2005). This repression of FOXO1 activity

was also mitigated by nicotinamide. Depletion of SIRT1 via SIRT1 siRNA resulted in higher levels of acetylated FOXO1 as well as increased protein abundance of the FOXO1 transcriptional targets BIM and FASL. In HEK293A cells, the MAGE protein necdin was found to form a complex with SIRT1 and FOXO1, facilitating SIRT1-mediated deacetylation and inactivation of FOXO1. Using a luciferase reporter driven by a promoter containing three copies of the IRS (3xIRS-luciferase), repression of luciferase activity by necdin and SIRT1 was diminished by SIRT1 siRNA. Furthermore, acetylated FOXO1 levels as well as expression of the FOXO1 target genes *Agrp* and *Npy* were found to be increased in the hypothalamus of *Ndn*-null mice as compared to wildtype mice (Hasegawa et al., 2012).

There is also a lot of evidence to suggest that deacetylated FOXO1 is more active than acetylated FOXO1. In a rat hepatoma cell line transiently transfected with FOXO1, treatment with the SIRT1 activator resveratrol resulted in increased expression of the FOXO1 target genes *G6PC*, *PCK1* and *IGFBP-1* as well as increased glucose release into the culture medium (Frescas et al., 2005). In another study, two FOXO1 acetylation mutants were used: one mimicking a constitutively acetylated FOXO1 in which six lysine residues (K242, K245, K259, K262, K271 and K291) are replaced with glutamines (6KQ) as well as one mimicking a constitutively deacetylated FOXO1 in which those same six lysines are mutated to arginines (6KR) (Kitamura et al., 2005). Replacing the positively charged lysine residues with uncharged glutamines mimics acetylation via neutralization of the positive charges associated with the lysine residues. Replacing the positively charged lysine residues with positively charged arginines mimics a deacetylated state in that the positive charges are preserved but the amino acids are not able to be acetylated. In a luciferase assay using the pancreatic insulinoma cell line βTC-3, significantly increased expression was detected from a luciferase reporter construct driven by the *IGFBP-1* promoter with FOXO1-6KR than with wildtype FOXO1. In addition, expression was reduced with the FOXO1-6KQ mutant as compared with wildtype FOXO1 (Kitamura et al., 2005). In HEK293 cells, inhibition of SIRT1 via nicotinamide

treatment reduced the expression of the FOXO1 transcriptional targets MnSOD and the cell cycle inhibitor protein $p27^{kip1}$ indicating that acetylation of FOXO1 decreases its transcriptional activity (Daitoku et al., 2004).

Many attribute these seemingly contradictory results to the distinct tissue- and target-gene-specific effects of FOXO1. Accordingly, the complex role of acetylation in proper FOXO1 regulation may play a significant part in what allows for the precise and diverse functions of FOXO1 *in vivo*. For example, it has been suggested that SIRT1-mediated deacetylation of FOXO transcription factors leads to increased expression of FOXO target genes which promote cell cycle arrest and resistance to oxidative stress such as $p27^{kip1}$ but decreased expression of pro-apoptotic genes such as *BIM* (Brunet et al. 2004). Thus, due to the different effects of FOXO1 deacetylation on transcriptional regulation, downstream events which promote cellular survival are activated whereas those which promote cell death are not.

Another hypothesis which helps to reconcile the conflicting results concerning FOXO1 acetylation and activity proposes that CBP-mediated acetylation has a twofold effect on FOXO1 transcriptional activity and that the failure to distinguish between these two roles accounts for the inconsistencies found in the literature (Daitoku et al. 2004). CBP is a histone acetyl-transferase which functions to increase transcription by acetylating nucleosomal histones. Histone acteylation weakens its interaction with DNA which allows transcription factors access to the DNA to augment transcription (van der Heide and Smidt, 2005). CBP also directly acetylates transcription factors including the tumour suppressor protein p53, GATA-binding protein 1 (GATA-1) as well as FOXO1 (Daitoku et al, 2011). In view of this bimodal role, CBP-mediated histone acetylation would initially grant FOXO1 access to target genes in the DNA but subsequent acetylation of FOXO1 would inhibit its transcriptional activity. In support of this hypothesis CBP was found to increase expression from a 3xIRS-luciferase plasmid stably transfected in HEK293 cells when co-transfected with an acetylation-deficient FOXO1 mutant as compared with wildtype FOXO1 or the acetylation-deficient FOXO1 without CBP (Daitoku et al. 2004). Increased

luciferase activity was also detected with wildtype FOXO1 co-transfected with both CBP and SIRT1 suggesting that histone acetylation combined with FOXO1 deacetylation results in enhanced FOXO1 activity.

In order the elucidate the mechanisms behind how acetylation affects FOXO1 activity, a series of experiments were performed which support a model in which acetylation of FOXO1 decreases its transcriptional activity via impaired DNA-binding and increased sensitivity to phosphorylation (Matsuzaki et al. 2005). Through electrophoretic mobility shift assays (EMSA) and chromatin immunoprecipitation, the authors determined that acetylated FOXO1 binds to DNA with less affinity than wildtype or deacetylated FOXO1. In a separate study also using EMSA experiments, acetylation of FOXO1 was again found to reduce its DNA-binding affinity (Brent et al. in 2008). Furthermore, FOXO1 acetylation was also found to increase its sensitivity to phosphorylation as inhibition of deacetylation by nicotinamide resulted in increased phosphorylation at S253 of FOXO1 (Matsuzaki et al. 2005). In addition, the authors generated two acetylation mutants similar to Kitamura et al., an acetylation-mimicking FOXO1 mutant in which three lysine residues known to be acetylated by CBP (K242, K245 and K262) are replaced with glutamines (3KQ) and an acetylation-deficient FOXO1 mutant, in which those same three lysine residues are mutated to arginines (3KR). The FOXO1-3KQ mutant mimicking constitutive acetylation was found to be more highly phosphorylated than wildtype FOXO1 or the FOXO1-3KR mutant mimicking constitutive deacetylation. The authors also found that FOXO1-3KR is much more transcriptionally active than FOXO1-3KQ in a luciferase assay. Lastly, by performing *in vitro* kinase assays the authors found that preincubation with a DNA fragment containing the IRS reduced AKT-mediated phosphorylation of FOXO1-3KR and wildtype FOXO1 but not of FOXO1-3KQ and not of wildtype FOXO1 incubated with a mutated IRS fragment (Matsuzaki et al. 2005). These experiments suggest that acetylation of FOXO1 reduces its DNA-binding ability and, consequently, decreases FOXO1 transcriptional activity and allows for AKT-mediated phosphorylation. Research by other groups has supported this hypothesis. The acetylation-mimicking

FOXO1-6KQ was found to be more sensitive to AKT-mediated phosphorylation and subsequent nuclear exclusion than the acetylation-deficient FOXO1-6KR (Qiang et al. 2010). Also in support of this, knock-down of the cytoplasmic sirtuin SIRT2 in 3T3-L1 preadipocytes was found to increase FOXO1 acetylation, phosphorylation and cytoplasmic localization (Jing et al. 2007). In addition, treatment of cultured hepatocytes with the SIRT1 activator resveratrol resulted in increased nuclear localization of FOXO1 suggesting that deacetylated FOXO1 accumulates in the nucleus (Frescas et al., 2005). However, research by other authors has indicated that acetylated FOXO1 may also be localized in the nucleus (Hasegawa et al., 2012; Kitamura et al., 2005). In another study, after performing fluorescence recovery after photobleaching (FRAP) and fluorescence loss in photobleaching (FLIP) analysis with GFP-tagged FOXO1, the authors proposed that SIRT1-deacetylated FOXO1 is retained in the nucleus and does not undergo nucleocytoplasmic shuttling whereas acetylated FOXO1 is able to shuttle back and forth between the nucleus and the cytoplasm (Frescas et al., 2005).

1.4.4.3 Ubiquitination and proteasomal degradation

FOXO1 is also regulated by polyubiquitination and subsequent degradation by the proteasome. FOXO1 interacts with and is polyubiquitinated by the Skp2 subunit of the Skp1/Cul1/F-box protein complex (SCF^{Skp2}), an E3 ubiquitin ligase complex (Huang et al, 2005). Multiple authors have found that FOXO1 ubiquitination and degradation is dependent upon phosphorylation of FOXO1 by AKT (Huang et al., 2005; Matsuzaki et al. 2003). In HepG2 cells, insulin stimulation resulted in reduced levels of FOXO1 over time and this effect was abrogated by the proteasome inhibitor MG132 as well as the PI3K inhibitor wortmannin (Matsuzaki et al., 2003). FOXO1 ubiquitination was also shown to be increased with insulin stimulation as compared to without. Phosphorylation-deficient FOXO1, in which all three AKT phosphorylation sites are replaced with alanines (FOXO1-3A), was ubiquitinated significantly less than wildtype FOXO1 suggesting that phosphorylation of FOXO1 is necessary for effective FOXO1 ubiquitination. In addition, a phosphorylatable FOXO1 mutant with a mutated

nuclear export sequence (NES) was found to have predominantly nuclear localization and reduced ubiquitination as compared to wildtype FOXO1. This indicates that in order for FOXO1 to be ubiquitinated, it may have to be localized in the cytoplasm. A non-phosphorylatable FOXO1-3A mutant containing a mutated nuclear localization sequence (NLS) was found to have mainly cytoplasmic localization but was also ubiquitinated much less than wildtype FOXO1 (Matsuzaki et al., 2003). This further suggests that phosphorylation, even independent of cellular localization, is required for complete ubiquitination of FOXO1. In addition, acetylated FOXO1 has been found to be ubiquitinated significantly less than deacetylated FOXO1 indicating that acetylation may protect FOXO1 from ubiquitination and degradation (Kitamura et al., 2005).

1.4.4.4 Methylation

Methylation is another post-translational modification involved in the regulation of FOXO1. FOXO1 is methylated by protein arginine methyltransferase 1 (PRMT1) at R250 and R252 (murine R248 and R250) of the DNA-binding domain. PRMT1-mediated methylation of FOXO1 has been shown to inhibit phosphorylation by AKT which subsequently prevents nuclear export, polyubiquitination and proteasomal degradation of FOXO1. Accordingly, in a luciferase assay, co-transfection of PRMT1 with FOXO1 resulted in increased FOXO1 transcriptional activity compared to FOXO1 alone (Yamagata et al., 2008).

1.4.4.5 Stress

In response to oxidative or genotoxic stress, FOXO transcription factors will translocate to or remain in the nucleus, regardless of the presence of growth factors such as insulin (Huang and Tindall, 2007). Oxidative stress, caused by treatment with H_2O_2, resulted in increased nuclear localization of FOXO1 in cultured hepatocytes and HEK293 cells, even when treated with insulin (Qiang et al., 2010; Frescas et al., 2005). H_2O_2 also promoted nuclear translocation in βTC-

3 cells and primary islet cells (Kitamura et al., 2005). The effect of stress on FOXO1 localization may be facilitated by SIRT1-mediated deacetylation of FOXO1. Pre-treating cells with the deacetylase inhibitor nicotinamide prevents H_2O_2-induced nuclear translocation of FOXO1 (Qiang et al., 2010; Frescas et al., 2005). However, treatment with H_2O_2 has also been shown to increase acetylation of FOXO transcription factors (Brunet et al., 2004; Motta et al., 2004; van der Horst et al., 2004). Kitamura et al., in 2005 suggested that conditions which induce oxidative stress such as hyperglycemia result in increased acetylation of FOXO1. As acetylated FOXO1 is less likely to be ubiquitinated and subsequently degraded by the proteosome, it is able to accumulate and interact with PML bodies in the nucleus where it is deacetylated by SIRT1. SIRT1-mediated deacetylation of FOXO1 enhances its transcriptional activity but concurrently, increases its likelihood of ubquitination and degradation. Thus oxidative stress overrides AKT-mediated inactivation and cytoplasmic sequestration of FOXO1 in order to promote the expression of FOXO1 target genes involved oxidative detoxification, cell cycle arrest and DNA damage repair. However, as this process also involves deacetylation of FOXO1 which is more readily ubiquitinated and degraded, it prevents prolonged activation of FOXO1 which is known to result in apoptosis (Huang and Tindall, 2007; Kitamura et al., 2005).

In addition to acetylation, oxidative stress also increases methylation of FOXO1. As methylation increases FOXO1 transcriptional activity, PRMT1-mediated methylation of FOXO1 has been shown to mediate apoptosis induced by oxidative stress. In cells treated with H_2O_2, *PRMT1* knock-down via transfection of siRNA targeted against *PRMT1* resulted in significantly less apoptosis than cells transfected with control siRNA (Yamagata et al., 2008).

Camptothecin-induced genotoxic stress has been shown to reduce FOXO1 phosphorylation at S249 (Huang et al., 2006). Additionally, H_2O_2-induced oxidative stress has been shown to reduce phosphorylation of FOXO1 at S253 as well as T24 (Qiang et al., 2010; Frescas et al., 2005). As reduced phosphorylation was also detected in the 6KQ and 6KR FOXO1 acetylation mutants, it has been

suggested that the effect of H_2O_2-induced stress on FOXO1 phosphorylation may be independent of acetylation (Qiang et al., 2010).

H_2O_2-induced oxidative stress activates mammalian Ste20-like kinase 1 (MST1), a protein known to be involved in apoptosis. MST1 phosphorylates S212, S218, S234 and S235 in the Forkhead domain of FOXO1. MST1-mediated phosphorylation of FOXO transcription factors has been found to disrupt their interaction with 14-3-3 proteins. This, in turn, results in increased nuclear translocation and transcriptional activity of FOXO proteins leading to increased cell death (Lehtinen et al., 2006).

1.5 Hypothesis and Aims

The chronic energy imbalance characteristic of PWS is strongly indicative of hypothalamic dysfunction. One of the genes lacking expression in PWS, *MAGEL2*, is highly expressed in the hypothalamus, the body's main energy regulator. Concordantly, *Magel2*-null mice also display symptoms of energy dysregulation. The Forkhead box transcription factor FOXO1 has been found to promote increased food intake and body weight when activated in the hypothalamus (Kim et al., 2006). As individuals with PWS experience insatiable hunger leading to hyperphagia and weight gain, I hypothesized that MAGEL2 may play a role in energy homeostasis specifically via the negative regulation of FOXO1. Consequently, I aimed to determine if there is any relationship between MAGEL2 and FOXO1 regulation by examining the effect of MAGEL2 on the subcellular localization, abundance, leptin- and insulin-signalling-induced inactivation and post-translational modifications of FOXO1and by testing whether MAGEL2 and FOXO1 can interact. Long term, the aim is to increase understanding of the energy dysregulation apparent in PWS with the hopes of improving treatment of this complex genetic obesity disorder.

Chapter 2: Materials and Methods

2.1 Plasmids

Murine *Magel2* was cloned into the mammalian expression vector pcDNA4/HisMax version B (Invitrogen, Carlsbad, CA) producing pcDNA4HisMaxXpress*Magel2* (referred to as Xpress-*Magel2*) with an Xpress epitope tag on the N-terminus (Lee et al., 2005). *FOXO1* expression constructs pcDNA3GFP*FKHR* (referred to as GFP-*FOXO1*), pcDNA3GFP*FKHR*AAA in which 3 amino acids known to be phosphorylated by AKT (Thr24, Ser256 and Ser 319) were mutated to alanines (referred to as GFP-*FOXO1*AAA) (Nakamura et al., 2000), and pSG5LHA*FKHR* (referred to as HA-*FOXO1*) were generously donated by Dr. Fred Berry from the University of Alberta. Other *Foxo1* constructs were obtained from Dr. Domenico Accili through Addgene including pCMV5FLAG*Foxo1* (Addgene plasmid 12148, referred to as FLAG-*Foxo1*), pCMV5FLAG*Foxo1*WT6KR in which 6 lysine residues (K242, K245, K259, K262, K271 and K291) have been replaced with arginines (Addgene plasmid 17560, referred to as FLAG-*Foxo1*-KR) and pCMV5FLAG*Foxo1*WT6KQ in which 6 lysine residues (K242, K245, K259, K262, K271 and K291) have been replaced with glutamines (Addgene plasmid 17562, referred to as FLAG-*Foxo1*-KQ) (Kitamura et al., 2005). An expression plasmid for murine CBP (pRc/RSVm*Crebbp*HA, referred to as *Crebbp*-HA) was acquired from Dr. Richard Goodman, also through Addgene (Addgene plasmid 16701) (Chrivia et al., 1993). A murine *Per2* construct, pcDNA3.1*Per2*V5His (referred to as *Per2*-V5), was obtained from Dr. Joseph Takahashi from Northwestern University (Kume et al., 1999). The expression plasmid for murine BMAL1, pcDNA3HA*Bmal1* (referred to as HA-*Bmal1*), was from Dr. Marina Antoch at the Roswell Park Insitute (Kondratov et al. 2003).

2.2 Antibodies

The primary antibodies used for immunoblotting, immunofluorescence and immunoprecipitation include mouse monoclonal anti-Xpress (Invitrogen), rabbit polyclonal anti-V5 (Milipore, Billerica, MA), rabbit polyclonal anti-HA (Y-11) , anti-Ac-FKHR (D-19) and anti-ERK1 (K-23) (Santa Cruz

Biotechnology, Santa Cruz, CA), rabbit polyclonal anti-FLAG and mouse monoclonal anti-gamma tubulin (Sigma-Aldrich, Oakville, ON) and rabbit monoclonal anti-FOXO1 (C29H4) and rabbit polyclonal anti-Phospho-FOXO1 (Ser256), anti-Phospho-AKT (Ser473), anti-AKT, anti-Phospho-AMPKα (Thr172), anti-AMPKα, anti-Phospho-STAT3 (Tyr705), anti-STAT3 and Phospho-p44/42 MAPK (ERK1/2) (Thr202/Tyr204) antibody (Cell Signaling Technology, Pickering, ON). The secondary antibodies used for immunoblotting were sheep anti-mouse and goat anti-rabbit IgG HRP-linked whole antibodies (GE Healthcare). The fluorescently tagged secondary antibodies used for immunofluorescence were goat anti-mouse Alexa Fluor 594 and goat anti-rabbit Alexa Fluor 488 and 594 antibodies (Invitrogen).

2.3 Cell culture and transient transfection

HEK293, HEK293/ELR and HEK293/ELR/MAGEL2 cell lines were cultured in Dulbecco's modified Eagle medium (DMEM) (Invitrogen) and kept in an incubator at 37°C with 5% CO_2. The HEK293/ELR cell line was generously donated by Dr. Martin G. Myers from the University of Michigan (Banks et al., 2000). Under normal culture conditions the cells were grown in DMEM supplemented with 10% Fetal Bovine Serum (FBS) (Invitrogen). Prior to transfection, cells were plated on 6-well or 100 mm plates. For cells used for immunofluorescence, coverslips were placed in the wells of a 6-well plate prior to plating the cells. HEK293 cells were transfected the day after plating with Attractene Transfection Reagent (Qiagen, Mississauga, ON) according to the Attractene Transfection Reagent Handbook. In particular, 1.2 μg of DNA per well of a 6-well plate was diluted into 60 μl of serum-free DMEM. Subsequently, 1.5 μl of Attractene Transfection Reagent was added to this solution and mixed by vortexing. The mixture was then incubated at room temperature for 15 minutes before being added drop-wise onto the cells. After gently swirling the plates, the HEK293 cells were incubated at 37°C for 18-24 hours before being collected for immunoblotting or immunoprecipitation. The procedure was the same for 100 mm plates except 4 μg of DNA was diluted in 300 μl of serum-free DMEM with

15 µl of Attractene Transfection Reagent subsequently added. HEK293/ELR cells were transfected the day after plating using polyethylenimine (PEI). Per well of a 6-well plate, 3 µg of DNA was diluted into 400 µl of serum-free DMEM. For 100 mm plates, 10 µg of DNA was diluted into 600 µl of serum-free DMEM. PEI was added to the diluted DNA at a ratio of 4 µl PEI to 1 µg DNA, vortexed and subsequently incubated for 15 minutes before being added dropwise to the HEK293/ELR cells plated in DMEM with 10% FBS (DMEM-FBS). After gently swirling the plates, the cells were incubated at 37°C for 15-16 hours before replacing the DMEM-FBS. Cells were then collected or treated for immunofluorescence the day after that. The suitable empty vector plasmids were used if necessary in order to keep the total amount of DNA transfected into the cells constant for every transfection in an experiment.

2.4 Stable transfection

HEK293/ELR cells were used to make a cell line stably expressing Xpress-*Magel2* (HEK293/ELR/MAGEL2). The restriction enzyme XhoI was used to linearize Xpress-*Magel2* plasmid. HEK293/ELR cells were plated on 100 mm plates and the following day linearized Xpress-*Magel2* plasmid was transfected into HEK293/ELR cells using PEI. After 48 hours, the transfected cells were re-plated onto new 100 mm plates and incubated with DMEM-FBS containing 600 µg/mL of the selective antibiotic Zeocin (Invitrogen). The cells were incubated at 37°C with 5% CO_2 and the Zeocin-containing DMEM-FBS was replaced every 3-4 days. Colonies of cells resistant to Zeocin were plated onto 24-well plates with selective DMEM-FBS. When cells were close to confluent they were re-plated onto 6-well plates, followed by Corning 25cm^2 and 75cm^2 cell culture flasks. Stable expression of Xpress-*Magel2* was determined by detection of Xpress-MAGEL2 via immunofluorescence and immunoblotting.

2.5 Immunofluoresence

HEK293/ELR cells were used for immunofluorescence experiments. After being plated on coverslips in 6-well plates and transfected with PEI, the cells were washed 48 hours later with phosphate-buffered saline (PBS) and then incubated for 1 hour in serum-free-DMEM. The cells were subsequently incubated for 1 hour at 37°C with either serum-free medium or serum-free medium containing 50 ng/mL of mouse erythropoietin (Epo) recombinant protein (BD Biosciences, Mississauga, ON). Alternatively, cells were incubated in 20 μm wortmannin (Sigma-Aldrich) in serum-free DMEM with and without Epo for 1 hour. Subsequently, cells were washed twice with PBS, fixed with 4% paraformaldehyde and washed three times with PBS containing 0.05% Triton X-100 (PBSX). Afterward, the cells were blocked in PBSX with 2% Boehringer Mannheim Blocking reagent (BMB) for 15 minutes at room temperature. The cells were then incubated for 1 hour with the relevant primary antibodies in PBSX with 2% BMB, washed twice with PBSX and incubated with the suitable fluorescently tagged secondary antibodies for 1 hour. The cells were again washed twice with PBSX and then treated for 15 minutes with PBSX containing the nuclear stain Hoechst 33342 (Invitrogen) at a ratio of 0.24 μL Hoechst 33342 per 10 ml PBSX. The cells were washed twice with PBSX before the coverslips were mounted onto glass microscope slides using VectaMount Permanent Mounting Medium (Vector Laboratories, Burlington, ON). Subcellular localization was examined by recording the number of cells with exclusively nuclear, nuclear and cytoplasmic or exclusively cytoplasmic expression of fluorescent proteins. Approximately 100-200 cells were counted from each slide. For experiments in which two expression constructs encoding proteins were transfected into cells, only the cells in which both of the fluorescent proteins could be visibly detected were counted. Fisher's exact tests were used to determine statistical differences in subcellular localization. A value of $P<0.05$ was considered statistically significant. When statistically analyzing the subcellular localization of FOXO1, the number of cells with nuclear as well as nuclear and cytoplasmic FOXO1 expression was compared to the number of cells

with cytoplasmic expression alone. For the statistical analysis of MAGEL2 localization, the number of cells with nuclear expression of MAGEL2 was compared to the number of cells with cytoplasmic as well as nuclear and cytoplasmic expression.

2.6 Immunoprecipitation

HEK293 and HEK293/ELR cells plated on 100 mm plates were used for immunoprecipitation experiments. The day after transfection with Attractene, or 48 hours after transfection with PEI, cells were lysed using 300 µL of lysis buffer containing 50 mM Tris-Cl pH 8.0, 150 nM NaCl, 0.5% IGEPAL (Sigma-Aldrich), Complete Mini EDTA-free protease inhibitor cocktail tablets (Roche, Laval, QC) and PhosSTOP phosphatase inhibitor cocktail tablets (Roche). After centrifuging the lysates at a rate of 20,800 x g for 15 minutes at 4°C, 100 µL of the supernatant was aliquoted into each of two 1.5 mL microcentrifuge tubes for the co-immunoprecipitation protocol while the rest of the supernatant was pipetted into a separate microcentrifuge tube and kept at -20°C. The frozen aliquots were used as inputs when immunoblotting in order to verify the presence of transfected proteins in the lysates. To each of the two unfrozen tubes with 100 µL of lysate, 400 µL of an extra buffer, consisting of 12.5 mM Tris-Cl pH 8.0, 87.5 mM NaCl and 0.125% IGEPAL, was added. The lysates were subsequently pre-cleared for 2 hours by adding 10 µL of 50% protein G-agarose slurry (Sigma-Aldrich) to the tubes and mixing them end-over-end at 4°C. The beads of the protein G-agarose slurry were then pelleted via centrifugation at 3000 x g for 1 minute and the supernatant was transferred to clean tubes. The lysates were pre-cleared so that any proteins which would nonspecifically stick to the beads would be removed. This was followed by an overnight incubation of the lysates with the appropriate primary antibodies, mixed end-over-end at 4°C. The next day, 30 µL of protein G-agarose slurry was added to the lysates and mixed end-over-end at 4°C for 4 hours. The agarose beads were subsequently pelleted at 3000 x g and washed 4 times with 1 mL of wash buffer consisting of 20 mM Tris-Cl pH 8.0, 100-150

mM NaCl and 0.2% IGEPAL. After the final wash, the supernatant was removed and the agarose beads were kept overnight at -20°C. Thirty μL of sample buffer, composed of 20% glycerol, 4% SDS and 0.13 M Tris-Cl pH 6.8, was added to the pelleted beads along with 2% β-mercaptoethanol and 1% saturated bromophenol blue. Immediately prior to SDS-polyacrylamide gel electrophoresis (SDS-PAGE) and immunoblotting, the beads were boiled for 5 minutes in order to extract the bound proteins from the agarose beads.

2.7 Immunoblotting

Experiments involving phosphorylation, acetylation, protein abundance and co-immunoprecipitation were performed in triplicate and analyzed by SDS-PAGE and protein immunoblotting in order to detect specific proteins from the cellular lysates. Depending on the particular experiment, some plated cells were treated with either 50 ng/mL Epo or 100 nM insulin (Sigma-Aldrich) in serum-free DMEM prior to harvesting for immunoblotting. Cells in 6-well plates were lysed in 60 μL of the previously described lysis buffer and centrifuged at a rate of 20,800 x g for 15 minutes at 4°C. Sample buffer as well as 2% β-mercaptoethanol and 1% saturated bromophenol blue was added to the lysates before being boiled for 5 minutes and then loaded onto 7.5% acrylamide gels along with Precision Plus Protein Dual Color Standard (BIO-RAD, Mississauga, ON). The lysates were subsequently electrophoresed at 80 milliamps in order to separate the proteins. The proteins on the gels were then transferred onto Immobilon-P polyvinylidene fluoride membranes (Millipore) at 100 volts for 60-90 minutes. The membranes were subsequently blocked for 1 hour with TBST (137 mM NaCl, 0.1% Tween-20 and 20 mM Tris pH 7.5) containing 5% skim milk powder (TBSTM) or TBST containing 3% BSA (Sigma-Aldrich). The membranes were then incubated overnight with the relevant primary antibodies in either TBSTM or TBST with 3% BSA at 4°C. After three 10 minute washes in TBST, the membranes were incubated for 1 hour at 4°C with the suitable HRP-linked secondary antibodies in TBSTM and then washed 3 times with TBST again. Finally, the membranes were immersed in Immobilon Western Chemiluminescent

HRP Substrate solution (Millipore) and imaged using the Kodak Image Station. Kodak Image Station software was used to quantify the intensity of the protein bands on the membranes. Two-tailed t-tests with *P* values of <0.05 were considered statistically significant.

Chapter 3: Results

3.1 MAGEL2 increases cytoplasmic localization of FOXO1

People suffering from PWS are known to have insatiable hunger leading to overeating and obesity. This strongly points to a dysfunctional homeostatic regulation of energy. Thus *MAGEL2*, one of the genes deleted in PWS, may be involved in or even necessary to maintaining energy homeostasis. The Forkhead box transcription factor FOXO1 plays a significant role in the proper regulation of food intake and energy balance (Kim et al, 2006). In hypothalamic neurons important for energy homeostasis, FOXO1 functions to increase food intake and decrease energy expenditure by increasing expression of the orexigenic hormones NPY and AgRP and decreasing the expression of the anorexigenic hormone POMC. FOXO1 is inactivated by two major energy regulating pathways: the leptin receptor and insulin receptor signalling pathways. When leptin or insulin signal through their respective receptors, a cascade of downstream phosphorylation events is initiated including the activation of PI3K. Activated PI3K leads to the phosphorylation of AKT at the plasma membrane. Phosphorylated AKT translocates to the nucleus and phosphorylates FOXO1. Phosphorylated FOXO1 is then excluded from the nucleus, its sequestration in the cytoplasm consequently inhibiting its actions as a transcription factor. Accordingly, the leptin and insulin receptor signalling pathways function to decrease FOXO1 activity which leads to decreased food intake and body weight. Interestingly another MAGE protein, necdin, has been found to interact with FOXO1 as part of a complex with SIRT1 (Hasegawa et al. 2012). Since localization in the nucleus is critical to the ability of FOXO1 to carry out its transcriptional activities and MAGEL2 is known to be involved in the subcellular localization of various proteins (Devos et al, 2011), I hypothesized that MAGEL2 may be involved in energy homeostasis via regulation of FOXO1 subcellular localization.

In order to determine whether MAGEL2 is involved in the regulation of FOXO1, I started working with an HEK293 cell line which stably expresses a chimeric erythropoietin:leptin receptor (ELR) (Figure 8A) (Banks et al., 2000). This receptor is made up of the extracellular and transmembrane domains of the

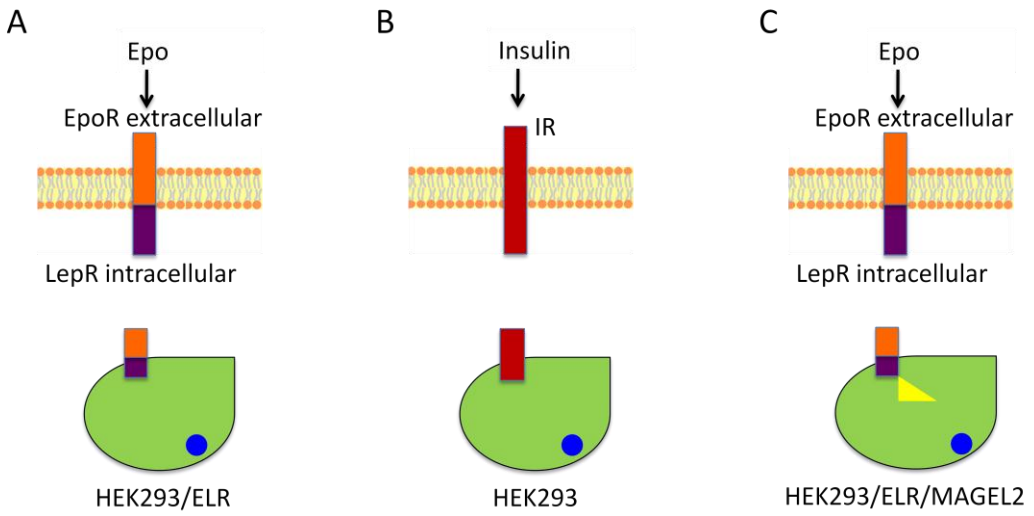

Figure 8. Schematic of cell lines used to test receptor signalling pathways. (A) HEK293/ELR cell line stably expresses a chimeric erythropoietin (Epo)/leptin receptor which can be activated by Epo. This receptor is made up of the extracellular and transmembrane domains of the Epo receptor and the intracellular domain of the leptin receptor. (B) HEK293 cell line endogenously expresses the insulin receptor which can be activated by insulin. (C) HEK293/ELR/MAGEL2 cell line stably expresses the Epo/leptin receptor as well as Xpress-*Magel2*. The blue circle represents the nucleus and the yellow triangle represents MAGEL2.

erythropoietin receptor and the intracellular domain of the leptin receptor, and is stimulated by erythropoietin (Epo). The chimeric ELR receptor expresses more robustly than the leptin receptor (Dunn et al., 2005) and allowed me to study the potential role of MAGEL2 in FOXO1 localization on a cellular level and in the context of leptin receptor signalling. I used immunofluoresence to test whether the presence of MAGEL2, with and without Epo stimulation, had any effect on the localization of FOXO1 within the cell. I transfected HEK293/ELR cells plated on coverslips with GFP-tagged *FOXO1* (GFP-*FOXO1*) and either Xpress-*Magel2* or empty vector. Then after serum starving the cells for 1 hour I incubated the cells in serum-free DMEM with or without Epo for 1 hour. After processing the cells for immunofluorescence I noted the subcellular localization of GFP-FOXO1 in individual cells. The localization was categorized as nuclear, nuclear and cytoplasmic or cytoplasmic. Since I wanted to determine if MAGEL2 is involved in the localization of FOXO1 in terms of whether it affects its role as a transcription factor in receptor signalling pathways, the number of cells with exclusively nuclear as well as both nuclear and cytoplasmic FOXO1 localization was compared to the number of cells with exclusively cytoplasmic localization for the statistical analysis, with the reasoning that complete FOXO1 transcriptional inactivation would only happen when the entire pool of FOXO1 protein is excluded from the nucleus. Using those classifications I found that, in unstimulated cells, GFP-FOXO1 was localized in the cytoplasm in 37% of cells (Figure 9A, lane 1 in 9E). When stimulated with Epo, 51% of cells had cytoplasmic GFP-FOXO1 (Figure 9B, lane 2 in 9E). This was a significant difference ($P<0.0001$, Fisher's exact test) which demonstrated that the signalling of Epo through the ELR receptor is able to bring about increased nuclear exclusion of GFP-FOXO1. With co-transfection of Xpress-*Magel2*, GFP-FOXO1 was found exclusively in the cytoplasm of 55% of cells without Epo stimulation (Figure 9C, lane 3 in 9E). This was a significant increase ($P<0.0001$) when compared to unstimulated cells expressing GFP-FOXO1 and empty vector. There was not a significant difference in localization between Epo-stimulated cells transfected with GFP-*FOXO1* and empty vector or unstimulated cells transfected

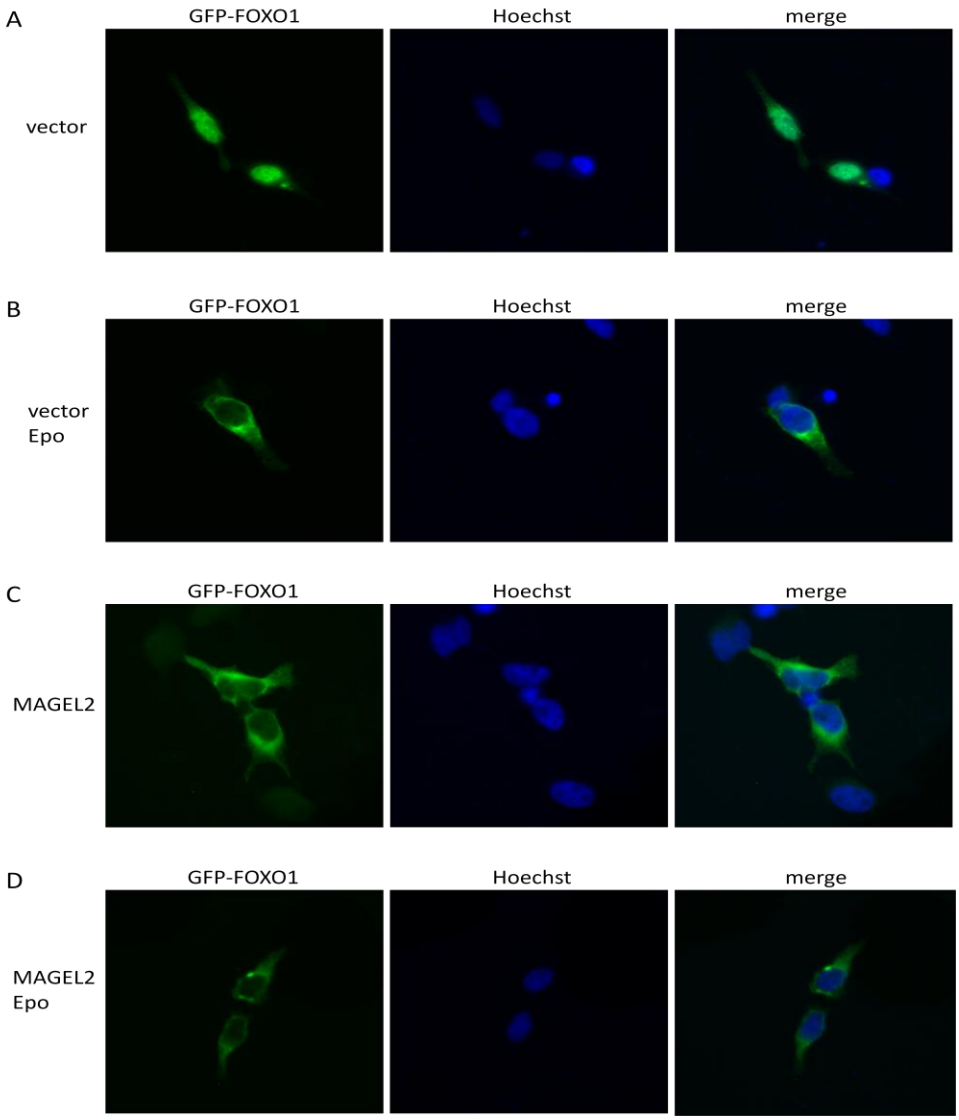

Figure 9. The proportion of cells with cytoplasmic GFP-FOXO1 is significantly increased when co-transfected with Xpress-*Magel2*.
HEK293/ELR cells plated on coverslips were transfected with GFP-*FOXO1* and either empty vector or Xpress-*Magel2*, serum-starved and subsequently incubated in the presence or absence of Epo for 1 hour. Proteins were visualized via immunofluorescence with representative examples of cells shown in (A)-(D). Stimulation with Epo resulted in increased cytoplasmic GFP-FOXO1 with either empty vector (lane 2 versus lane 1 in (E)) or Xpress-MAGEL2 (lane 4 versus lane 3 in (E)). Co-transfected Xpress-*Magel2* significantly increased cytoplasmic GFP-FOXO1 without Epo (lane 3 versus lane 1 in (E)) and with Epo (lane 4 versus lane 2 in (E)). A * indicates a significant difference from unstimulated cells co-transfected with empty vector ($P<0.0001$). A # indicates a significant difference from Epo stimulated cells co-transfected with empty vector ($P<0.0001$) as well as unstimulated cells co-transfected with Xpress-*Magel2* ($P<0.0001$).

E

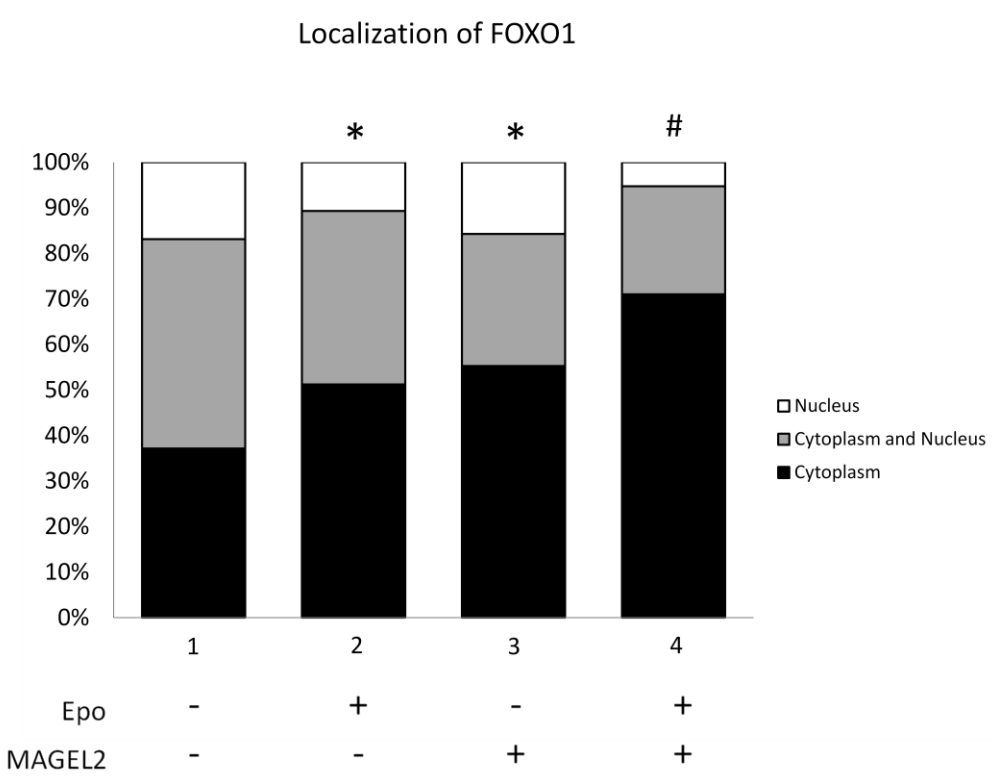
Localization of FOXO1
*
*
#
100%
90%
80%
70%
60%
50%
40%
30%
20%
10%
0%
1
2
3
4
Epo
- + - +
MAGEL2
- - + +
Nucleus
Cytoplasm and Nucleus
Cytoplasm

with GFP-*FOXO1* and Xpress-*Magel2*. Cells with both Xpress-MAGEL2 and GFP-FOXO1 which were stimulated with Epo had 71% cytoplasmic GFP-FOXO1 (Figure 9D, lane 4 in 9E). This was significant as compared to cells with GFP-FOXO1 alone with and without Epo as well as compared to cells with GFP-FOXO1 and Xpress-MAGEL2 without Epo stimulation ($P<0.0001$). This suggests that MAGEL2 itself increases shuttling of FOXO1 from the nucleus to the cytoplasm with or without stimulation of the receptor signalling pathway. Consequently there is a significant additive effect of MAGEL2 on FOXO1 nuclear exclusion coupled with Epo-induced activation of the leptin signalling pathway.

In order to verify whether this effect on FOXO1 localization is specific to MAGEL2 and not a consequence of any co-transfected protein, I repeated the experiment using V5-tagged *Per2* (*Per2*-V5) instead of Xpress-*Magel2*. Co-transfection of GFP-*FOXO1* with *Per2*-V5 resulted in 33% cytoplasmic GFP-FOXO1 without Epo stimulation which is not significantly different from cells with GFP-FOXO1 and empty vector (Figure 10A, lane 3 versus lane 1 in 10C). In cells transfected with *Per2*-V5 and treated with Epo 48% had cytoplasmic GFP-FOXO1 which is a significant increase from unstimulated cells but not significantly different from Epo-stimulated cells with GFP-FOXO1 and empty vector (Figure 10B, lane 4 versus lane 2 in 10C). This helps to confirm that the results seen with MAGEL2 are indeed specific to MAGEL2 and not a spurious result stemming from any protein that is co-transfected with GFP-FOXO1 in HEK293/ELR cells.

3.2 MAGEL2 does not alter the subcellular localization of dephosphorylated FOXO1

Next I wanted to determine whether the effect of MAGEL2 on FOXO1 localization is dependent on FOXO1 phosphorylation. Using a GFP-tagged triple A phospho-mutant FOXO1 (GFP-FOXO1AAA) in which 3 AKT phosphorylation sites (Thr24, Ser256 and Ser 319) have been mutated to alanines (Nakamura et al., 2000), I transfected HEK293/ELR cells with either GFP-*FOXO1*AAA and

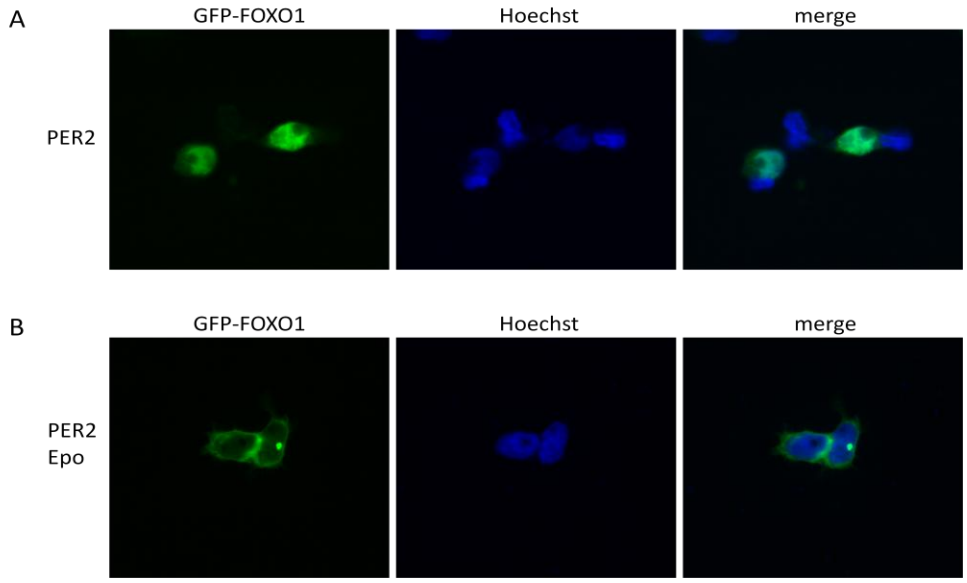

Figure 10. Subcellular localization of GFP-FOXO1 is not significantly different when co-transfected with *Per2*-V5. HEK293/ELR cells plated on coverslips were transfected with GFP-*FOXO1* and *Per2*-V5, serum-starved and subsequently incubated in the presence or absence of Epo for 1 hour. Proteins were visualized via immunofluorescence with representative examples of cells shown in (A) and (B). Stimulation with Epo resulted in increased cytoplasmic GFP-FOXO1 with either empty vector (lane 2 versus lane 1 in (C)) or PER2-V5 (lane 4 versus lane 3 in (C)). Co-transfected *Per2*-V5 did not have a significant effect on the subcellular distribution of GFP-FOXO1 without Epo (lane 3 versus lane 1 in (C)) or with Epo (lane 4 versus lane 2 in (C)). A * indicates a significant difference from unstimulated cells transfected with empty vector ($P<0.0001$). A # indicates a significant difference from unstimulated cells transfected with *Per2*-V5 ($P=0.0019$).

C

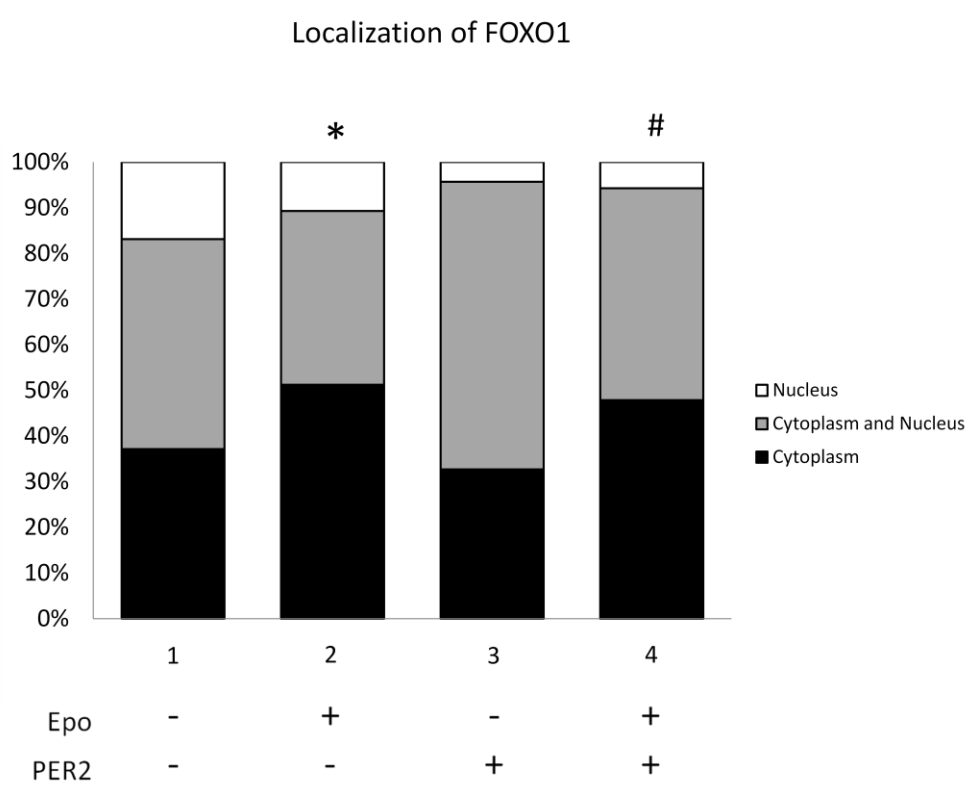
Localization of FOXO1
*
#
100%
90%
80%
70%
60%
50%
40%
30%
20%
10%
0%
1
2
3
4
Epo
- + - +
PER2
- - + +
Nucleus
Cytoplasm and Nucleus
Cytoplasm

Xpress-*Magel2* or GFP-*FOXO1*AAA and empty vector, with and without Epo stimulation. As expected, I found that 0% of cells had exclusively cytoplasmic GFP-FOXO1AAA either with or without Epo stimulation (Figure 11A and B, lane 1 and lane 2 in 11E). Co-expression of Xpress-*Magel2* also did not significantly affect the localization of GFP-FOXO1AAA (Figure 11C and D, lane 3 and lane 4 in 11E). In further analysis, there also was not a significant difference in the number of cells with exclusively nuclear GFP-FOXO1AAA as compared to cells with both nuclear and cytoplasmic GFP-FOXO1AAA among any of the groups. This result shows that MAGEL2 is unable to affect the localization of non-phosphorylatable FOXO1, suggesting that MAGEL2 either assists in the phosphorylation of FOXO1 or requires that FOXO1 be phosphorylated in order to be able to exert its effect.

3.3 MAGEL2 does not alter the phosphorylation of FOXO1 at S256

Since MAGEL2 is not able to affect the localization of a constitutively dephosphorylated FOXO1 phospho-mutant, I next tested whether MAGEL2 promotes increased cytoplasmic localization of wildtype FOXO1 by facilitating enhanced FOXO1 phosphorylation. Stimulation of HEK293/ELR cells with Epo did not significantly increase phosphorylation of FOXO1, either endogenously or with transfected FLAG-*Foxo1* (data not shown). Consequently, as HEK293 cells endogenously express the insulin receptor and insulin also activates AKT to phosphorylate FOXO1, I tried using insulin to stimulate HEK293 cells (Figure 8B). I transfected HEK293 cells with FLAG-*Foxo1* and either Xpress-*Magel2* or empty vector, incubated the cells for 1 hour with serum-free medium and then incubated them in serum-free medium with and without insulin for 1 hour. I then immunoblotted the cell lysates with a rabbit polyclonal anti-Phospho-FOXO1 antibody, which detects FOXO1 phosphorylated at S256, and compared it to the total amount of FLAG-FOXO1 using rabbit anti-FLAG polyclonal antibody. Since MAGEL2 was able to increase cytoplasmic FOXO1 levels even without stimulation of the receptor with Epo I also tested the effect of MAGEL2 on FOXO1 phosphorylation without insulin stimulation. I found that insulin is able

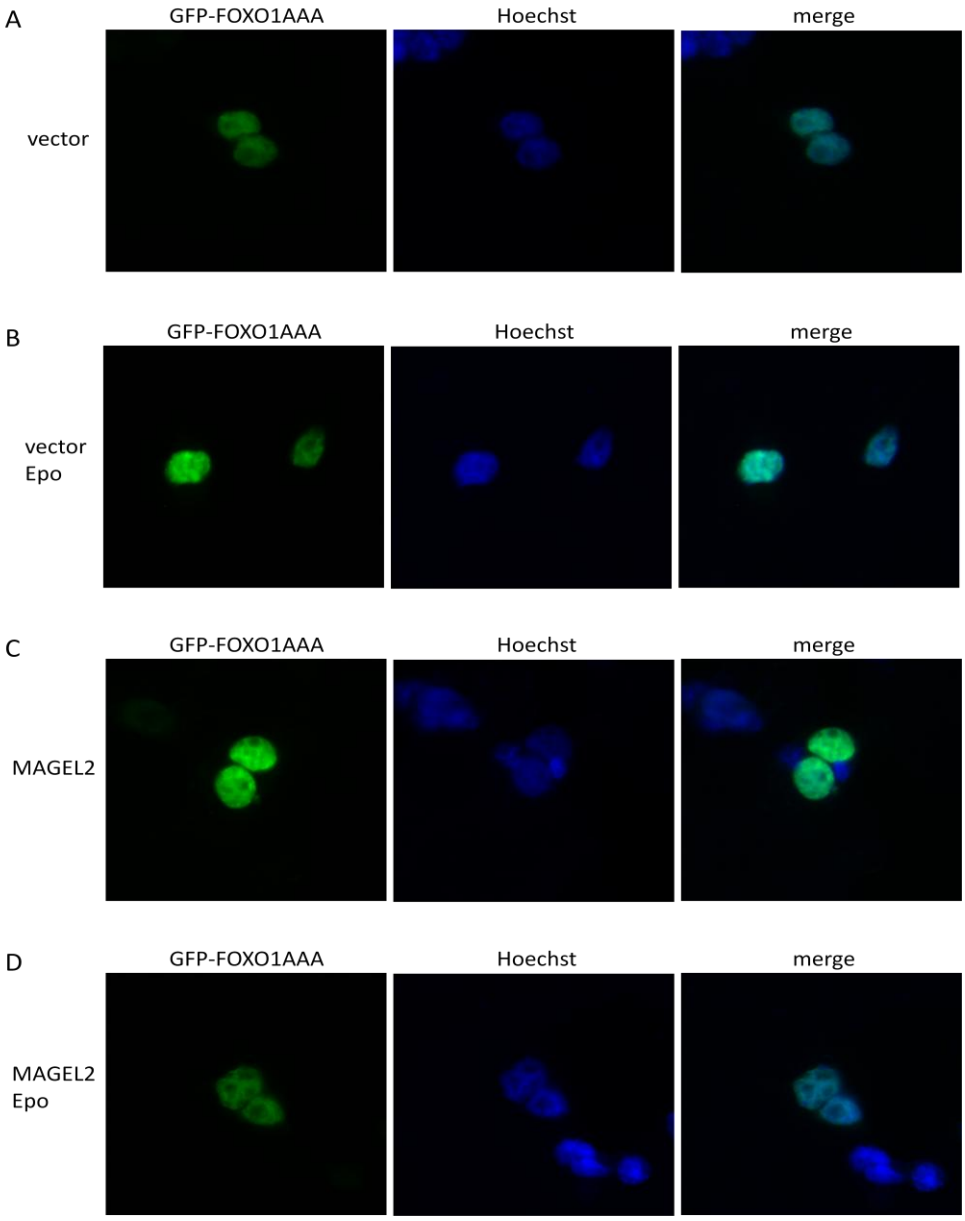

Figure 11. Subcellular localization of GFP-FOXO1AAA phospho-mutant is not significantly different when co-transfected with Xpress-*Magel2*. HEK293/ELR cells plated on coverslips were transfected with GFP-*FOXO1*AAA and either empty vector or Xpress-*Magel2*, serum-starved and subsequently incubated in the presence or absence of Epo for 1 hour. Proteins were visualized via immunofluorescence with representative examples of cells shown in (A)-(D). Stimulation with Epo did not result in increased cytoplasmic GFP-FOXO1AAA with either empty vector (lane 2 versus lane 1 in (E)) or Xpress-MAGEL2 (lane 4 versus lane 3 in (E)). Co-transfected Xpress-*Magel2* did not have a significant effect on the subcellular distribution of GFP-FOXO1AAA without Epo (lane 3 versus lane 1 in (E)) or with Epo (lane 4 versus lane 2 in (E)).

E

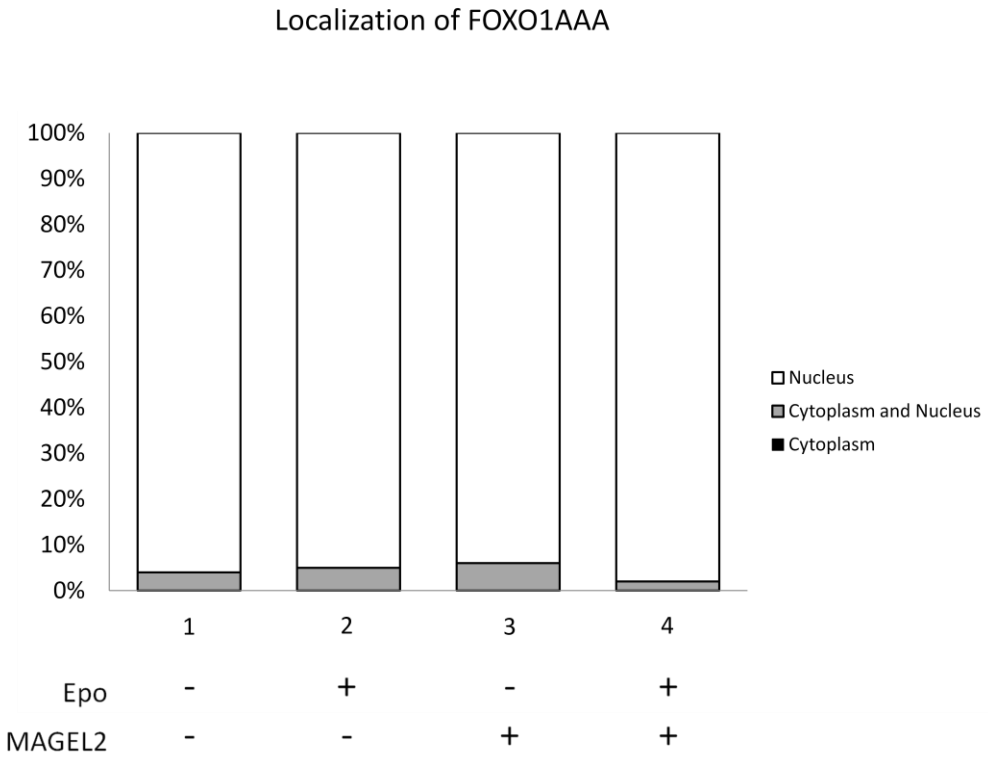
Localization of FOXO1AAA
100%
90%
80%
70%
60%
50%
40%
30%
20%
10%
0%
Nucleus
Cytoplasm and Nucleus
Cytoplasm
1
2
3
4
Epo
-
+
-
+
MAGEL2
-
-
+
+

to significantly increase the phosphorylation of FOXO1 as compared to unstimulated cells (Figure 12, lane 2 versus lane 1; P=0.008, t-test on triplicate samples). However, the presence of MAGEL2 did not cause a significant difference in FOXO1 phosphorylation, either with or without insulin stimulation (Figure 12, lane 4 versus lane 2 and lane 3 versus lane 1). These results indicate that MAGEL2 is not involved in the phosphorylation of FOXO1 at S256. Rather, as MAGEL2 is unable to affect the localization of the FOXO1AAA phospho-mutant, it is more likely that MAGEL2 requires the phosphorylation of FOXO1 in order to exert its effect on localization. Previous research has established that FOXO1 must be phosphorylated in order to be exported from the nucleus and concordantly the presence of MAGEL2 does not negate this requirement (Nakae et al., 2000; Biggs et al., 1999).

3.4 The effect of MAGEL2 on FOXO1 localization is PI3K-dependent

Since MAGEL2 appears to require the phosphorylation of FOXO1 in order to be able to influence its localization, I further sought to determine whether the effect of MAGEL2 on FOXO1 localization was specifically dependent on the PI3K-AKT-FOXO1 pathway of receptor signalling or if MAGEL2 is to be able to influence FOXO1 localization independently from it. I transfected HEK293/ELR cells with GFP-*FOXO1* and either Xpress-*Magel2* or empty vector. Then, after serum starving the cells for 1 hour, I incubated them with the PI3K inhibitor wortmannin either with or without Epo. Wortmannin blocks the phosphorylation of AKT which would subsequently inhibit the phosphorylation of FOXO1. This would allow me to determine whether or not FOXO1 must be phosphorylated specifically through the PI3K-AKT-FOXO1 pathway in order for MAGEL2 to be able to influence its localization. In cells with and without MAGEL2 as well as with and without Epo 0% had exclusively cytoplasmic GFP-FOXO1 (Figure 13A-D, quantification in 13E). In addition, there was not a significant difference in cells with only nuclear versus both nuclear and cytoplasmic FOXO1 between any of the groups. This suggests that MAGEL2 requires the PI3K-AKT-FOXO1 signalling pathway in order to exert its effect on FOXO1 localization in the cell.

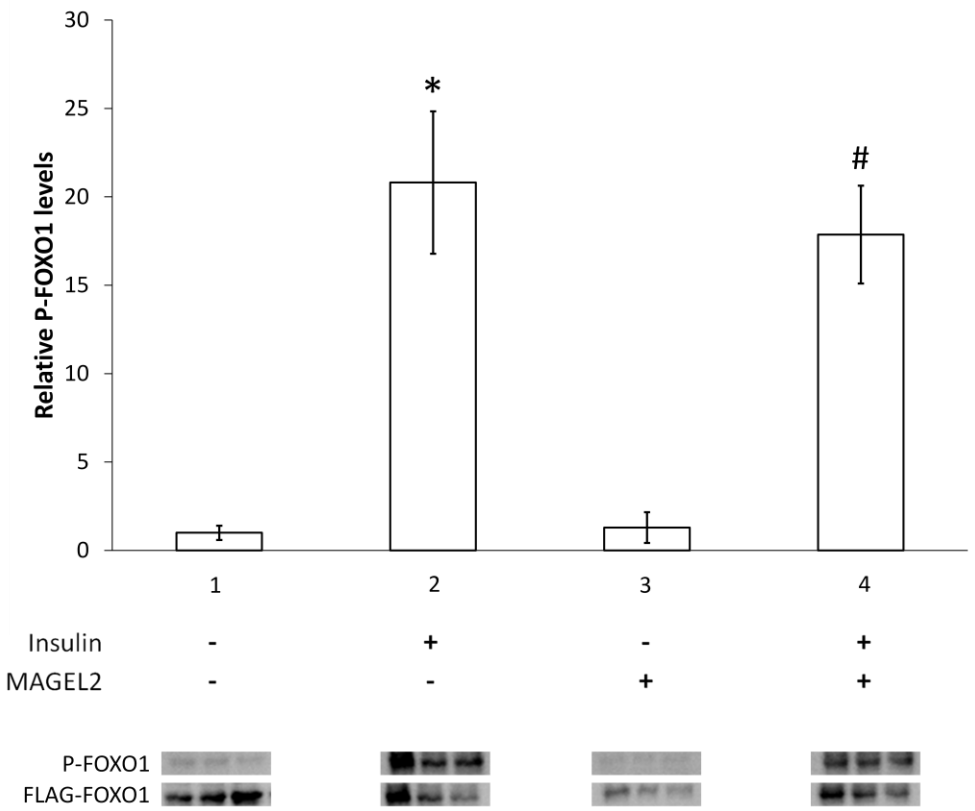

Figure 12. Phosphorylation of FOXO1 at S256 is not significantly different when co-expressed with *Magel2*. HEK293 cells were transfected in triplicate with FLAG-*Foxo1*and either empty vector or Xpress-*Magel2*, serum-starved and subsequently incubated in the presence or absence of insulin for 1 hour. Proteins were immunoblotted with the appropriate antibodies and analyzed using Kodak Image Station software. Protein quantities were calculated as a ratio of the pixel intensity of phosphorylated FOXO1 to FLAG-FOXO1. Levels of phosphorylated FOXO1 were significantly increased after 1 hour of insulin stimulation as compared to unstimulated cells, with either empty vector (lane 2 versus lane 1) or Xpress-MAGEL2 (lane 4 versus lane 3). Phosphorylated FOXO1 levels were not significantly different with Xpress-MAGEL2 as compared to empty vector, without insulin (lane 3 versus lane 1) or with insulin (lane 4 versus lane 2). A * indicates a significant difference from unstimulated cells transfected with empty vector (P=0.008) and a # indicates a significant difference from unstimulated cells transfected with Xpress-*Magel2* (P=0.005). Representative examples of blots with samples in triplicate are shown.

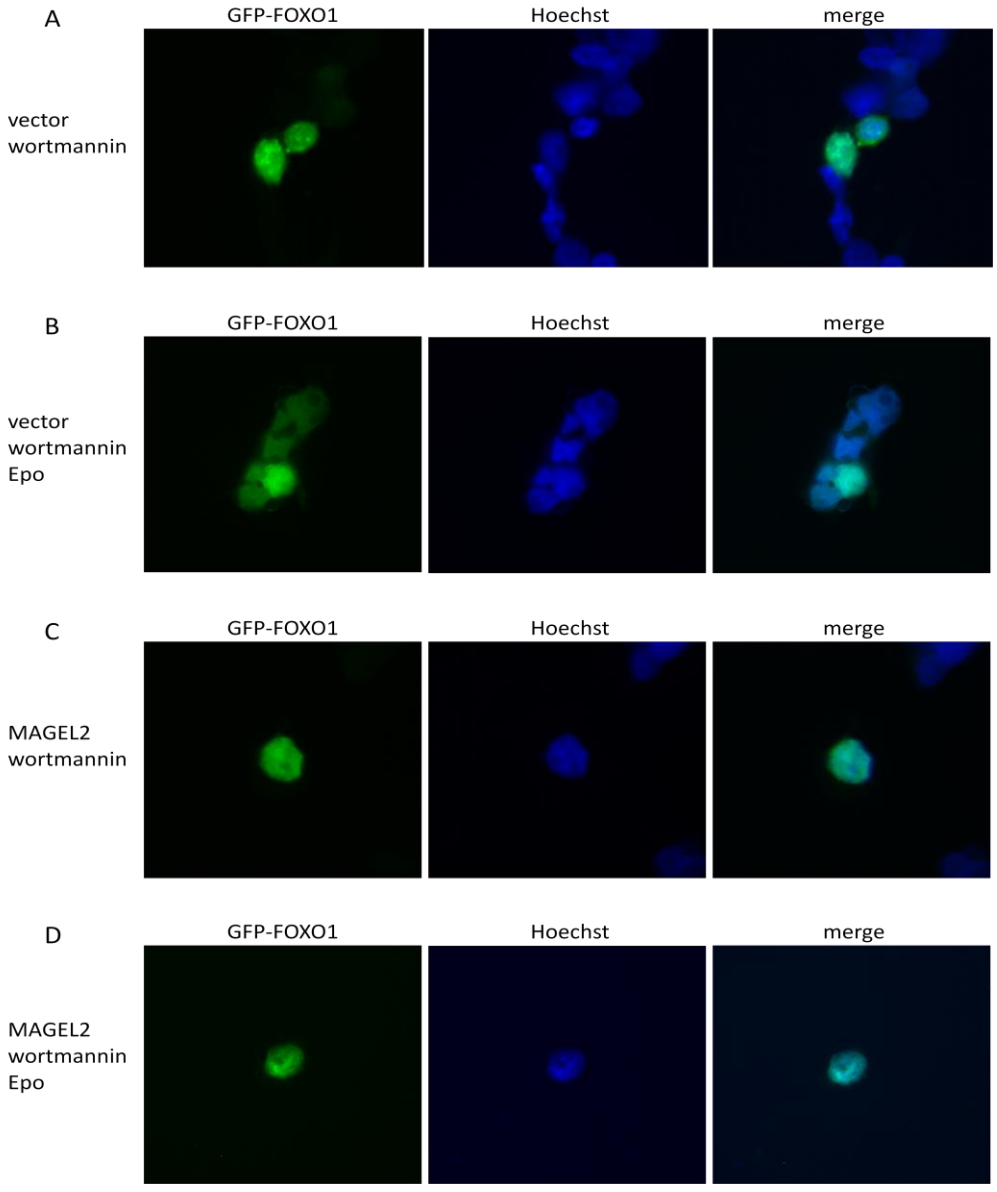

Figure 13. Subcellular localization of GFP-FOXO1 is not significantly different when co-transfected with Xpress-*Magel2* after treatment with the PI3K inhibitor wortmannin. HEK293/ELR cells plated on coverslips were transfected with GFP-*FOXO1* and either empty vector or Xpress-*Magel2*, serum-starved and subsequently incubated in wortmannin as well the presence or absence of Epo for 1 hour. Proteins were visualized via immunofluorescence with representative examples of cells shown in (A)-(D). **S**timulation with Epo did not result in increased cytoplasmic GFP-FOXO1 with wortmannin present, either with empty vector (lane 2 versus lane 1 in (E)) or Xpress-MAGEL2 (lane 4 versus lane 3 in (E)). Co-transfected Xpress-*Magel2* did not have a significant effect on the subcellular distribution of GFP-FOXO1 with wortmannin present, either without Epo (lane 3 versus lane 1 in (E)) or with Epo (lane 4 versus lane 2 in (E)).

E

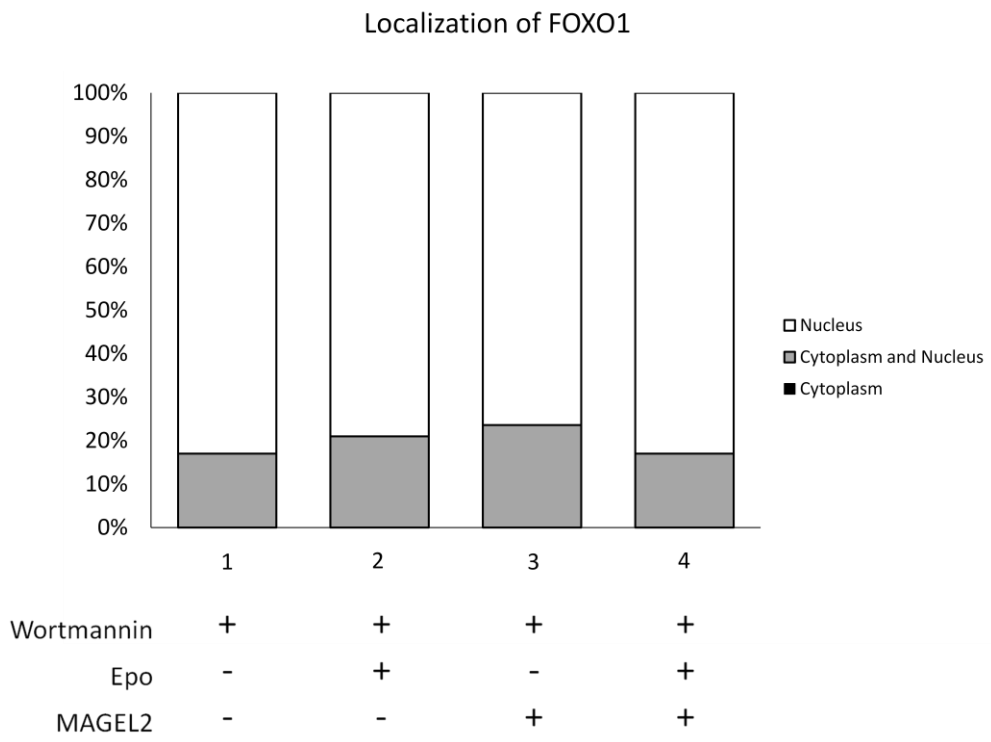
Localization of FOXO1
100%
90%
80%
70%
60%
50%
40%
30%
20%
10%
0%
Nucleus
Cytoplasm and Nucleus
Cytoplasm
1
2
3
4
Wortmannin + + + +
Epo - + - +
MAGEL2 - - + +

3.5 MAGEL2 does not alter the phosphorylation of leptin and insulin signalling proteins

Since the effect of MAGEL2 on FOXO1 localization is dependent upon the PI3K-AKT-FOXO1 pathway I wanted to determine if MAGEL2 functions to increase the activation of the overall leptin receptor and/or specific downstream proteins by examining protein phosphorylation. When leptin activates the leptin receptor many downstream proteins are activated or inactivated via post-translational modifications. This includes phosphorylation of STAT3, ERK and AKT as well as dephosphorylation of AMPK (Morris and Rui, 2009). In order to test whether MAGEL2 is increasing the overall activation of the leptin receptor or affecting a specific protein in receptor signalling, I first wanted to establish if stimulation of the HEK293/ELR cells with Epo results in significant phosphorylation of the downstream signalling proteins STAT3, ERK and AKT and dephosphorylation of AMPK. HEK293/ELR cells were incubated for 1 hour with serum-free medium and subsequently stimulated in serum-free medium with or without Epo for 1 hour. Gel electrophoresis and immunoblotting was done using the resulting lysates and the relevant proteins were detected using the appropriate antibodies. The intensity of the phosphorylated protein signals were normalized to the total amount of endogenous protein for each protein tested. The level of phosphorylated STAT3 to total STAT3 was found to be significantly increased with Epo as compared to without Epo (Figure 14A; P=0.0022). ERK phosphorylation was also significantly increased with the presence of Epo (Figure 15A; P=0.0024). The levels of phosphorylated AMPK and AKT however, were not significantly different in Epo stimulated cells as compared to unstimulated cells (data not shown). Since stimulation with Epo in HEK293/ELR cells did not significantly increase phosphorylation of AKT, I tried using insulin to stimulate HEK293 cells. After stimulation of the HEK cells with or without insulin for 1 hour, I found that AKT was significantly phosphorylated in cells treated with insulin compared to without insulin (Figure 16A; P<0.0001).

After affirming that Epo causes significantly increased phosphorylation of STAT3 and ERK in HEK293/ELR cells and that insulin significantly increases

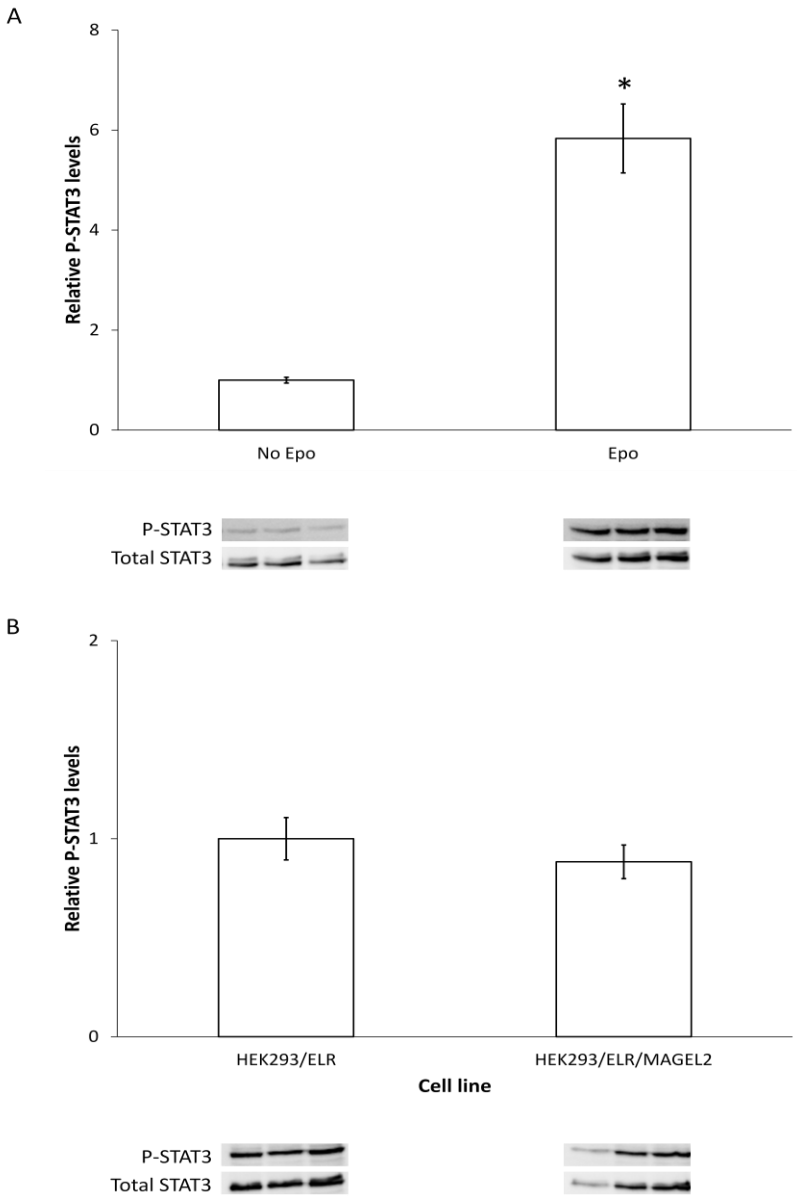

Figure 14. Phosphorylation of STAT3 after Epo stimulation is not significantly different when co-expressed with *Magel2*. HEK293/ELR cells and HEK293/ELR/MAGEL2 cells were serum-starved and subsequently incubated in the presence or absence of Epo for 1 hour. Proteins were immunoblotted with the appropriate antibodies and analyzed using Kodak Image Station software. Protein quantities were calculated as a ratio of the pixel intensity of phosphorylated STAT3 to total STAT3. (A) Phosphorylation of STAT3 was significantly increased with Epo stimulation as compared to unstimulated cells. (B) Levels of phosphorylated STAT3 were not significantly different between HEK293/ELR and HEK293/ELR/MAGEL2 cells. A * indicates a significant difference from unstimulated cells (P=0.0022). Representative examples of blots with samples in triplicate are shown.

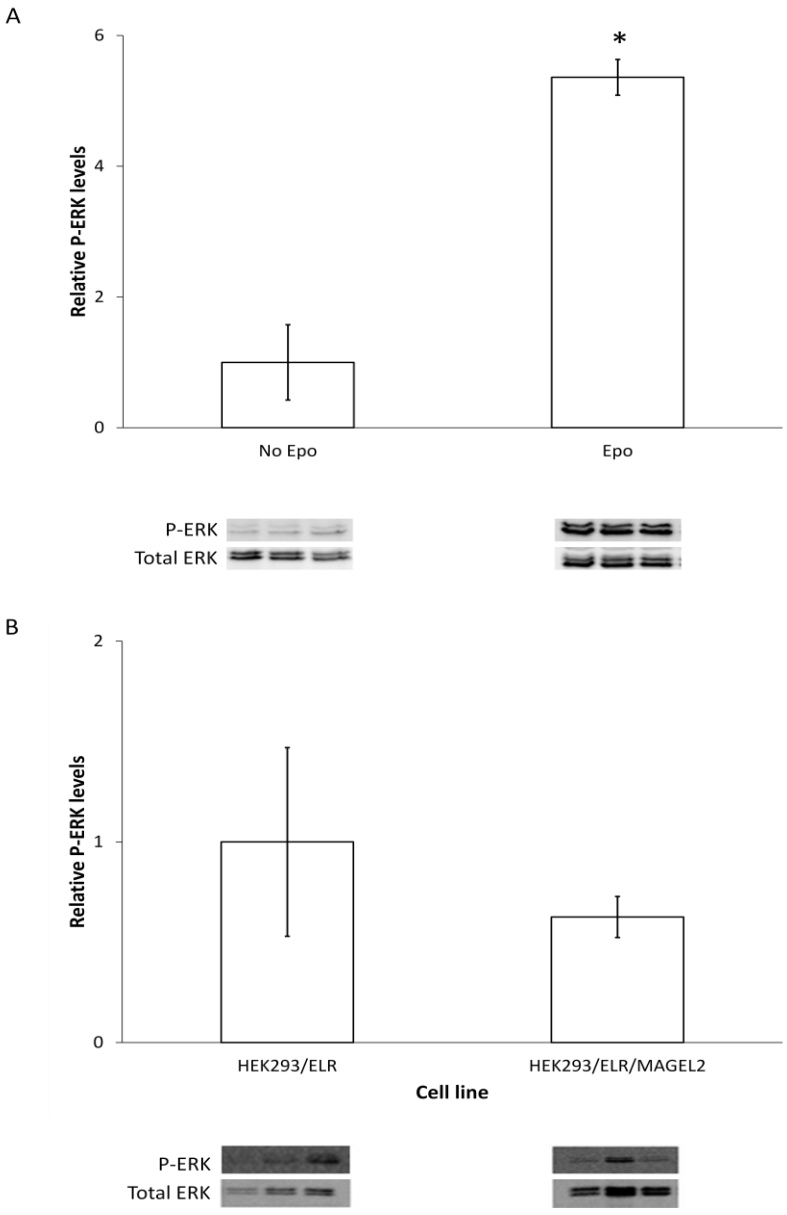

Figure 15. Phosphorylation of ERK after Epo stimulation is not significantly different when co-expressed with *Magel2*. HEK293/ELR cells and HEK293/ELR/MAGEL2 cells were serum-starved and subsequently incubated in the presence or absence of Epo for 1 hour. Proteins were immunoblotted with the appropriate antibodies and analyzed using Kodak Image Station software. Protein quantities were calculated as a ratio of the pixel intensity of phosphorylated ERK to total ERK. (A) Phosphorylation of ERK was significantly increased after stimulation with Epo as compared to unstimulated cells. (B) Levels of phosphorylated ERK were not significantly different between HEK293/ELR and HEK293/ELR/MAGEL2 cells. A * indicates a significant difference from unstimulated cells (P=0.0024). Representative examples of blots with samples in triplicate are shown.

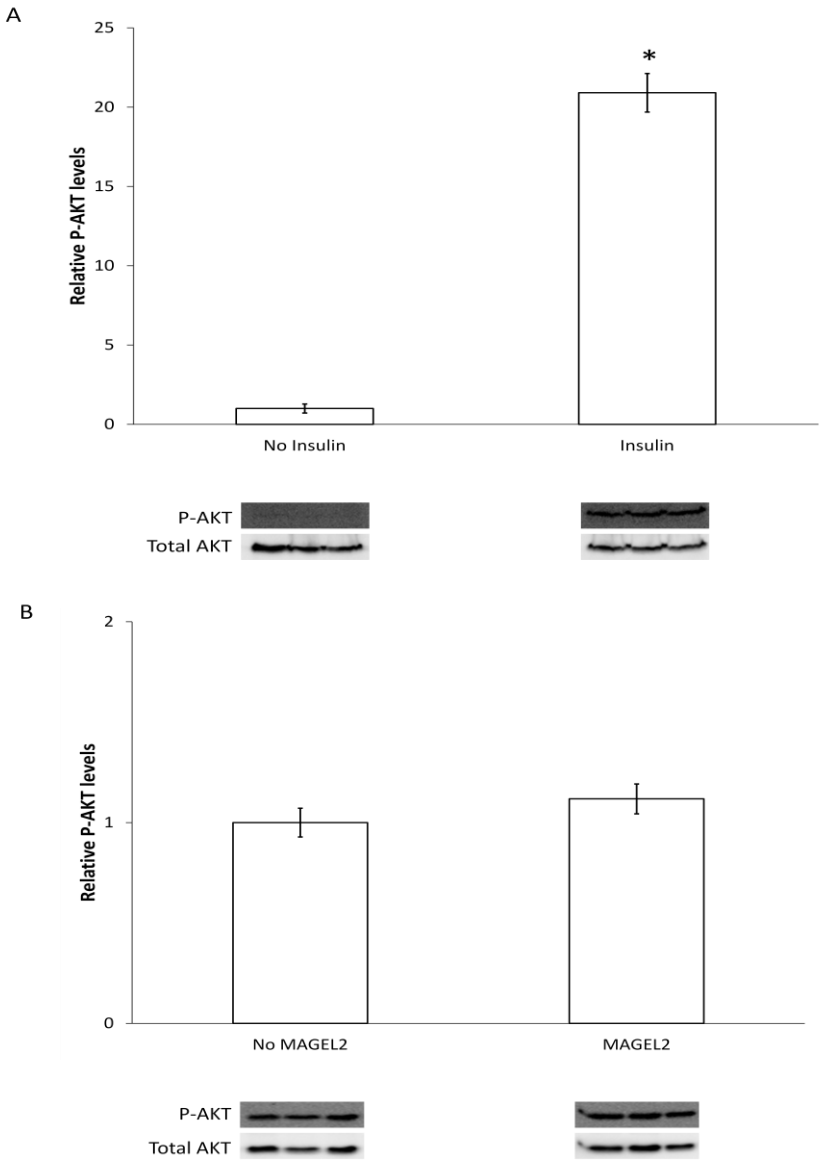

Figure 16. Phosphorylation of AKT after insulin stimulation is not significantly different when co-expressed with *Magel2*. Untransfected HEK293 cells (A) or HEK293 cells transfected with empty vector or Xpress-*Magel2* (B) were serum-starved and subsequently incubated in the presence or absence of insulin for 1 hour. Proteins were immunoblotted with the appropriate antibodies and analyzed using Kodak Image Station software. Protein quantities were calculated as a ratio of the pixel intensity of phosphorylated AKT to total AKT. (A) Phosphorylation of AKT was significantly increased after stimulation with insulin as compared to unstimulated cells. (B) Levels of phosphorylated AKT after insulin stimulation were not significantly different with transfected Xpress-*Magel2* as compared to empty vector. A * indicates a significant difference from unstimulated cells ($P<0.0001$). Representative examples of blots with samples in triplicate are shown.

phosphorylation of AKT in HEK293 cells, I tested the effect of MAGEL2 on the phosphorylation of these signalling proteins. From the HEK293/ELR cell line I made another cell line which stably expresses both the ELR receptor and Xpress-*Magel2* (Figure 8C). After incubating HEK293/ELR and HEK293/ELR/MAGEL2 cells in serum-free medium for 1 hour followed by treating both cell lines with Epo for 1 hour I found no significant difference in the phosphorylation of STAT3 or ERK with or without the presence of MAGEL2 (Figure 14B and 15B). I transiently transfected HEK293 cells with either Xpress-*Magel2* or empty vector, incubated the cells for 1 hour with serum-free medium and then stimulated them with insulin for 1 hour. I found no significant difference in the phosphorylation of AKT with or without MAGEL2 (Figure 16B). Since none of the proteins tested were affected by the presence of MAGEL2 this indicates that MAGEL2 is not involved in the phosphorylation of specific leptin and insulin signalling proteins and, by extension, is most likely not involved in the overall activation of the leptin or insulin receptor.

3.6 MAGEL2 does not alter the acetylation of FOXO1

FOXO1 subcellular localization is a very complex ongoing process involving many different factors including post-translational modifications such as phosphorylation and acetylation. The regulation of FOXO1 activity by post-translational modification is still not fully understood and in fact not all of the literature on the matter is in agreement. According to some authors, acetylated FOXO1 is more sensitive to phosphorylation by AKT and is thus more readily shuttled to the cytoplasm (Matsuzaki et al., 2005 and Qiang et al., 2010). With this in mind I wanted to see if MAGEL2 is involved in increasing the acetylation of FOXO1, thus rendering it more susceptible to phosphorylation by AKT and increasing its likelihood of being excluded from the nucleus. I transfected HEK293 cells with FLAG-*Foxo1* and either empty vector or Xpress-*Magel2* in triplicate. After immunoblotting the cell lysates with an acetylated-FOXO1 antibody, which detects acetylation at K259, K262 and K271, and comparing it to the total amount of FLAG-FOXO1 using rabbit anti-FLAG polyclonal antibody, I

found that Xpress-MAGEL2 does not significantly affect the acetylation of FOXO1 (Figure 17, lane 3 versus lane 1). However, perhaps the cellular availability of CREB-binding protein (CBP), the protein known to acetylate FOXO1, is a limiting factor. If MAGEL2 is involved as an adaptor protein, increasing the likelihood of FOXO1 acetylation by facilitating the interaction of CBP with FOXO1, then maybe co-transfection with *Crebbp*, the gene encoding CBP, is required in order to generate a measurable difference in acetylation. Thus I also transfected the cells with and without *Crebbp*-HA. The presence of CBP-HA resulted in a significant increase in acetylated FOXO1, without co-transfected Xpress-*Magel2* (Figure 17, lane 2 versus lane 1; P=0.035) as well as with Xpress-*Magel2* (Figure 17, lane 4 versus lane 3; P=0.02). However, the presence of Xpress-MAGEL2 did not cause any further difference in FOXO1 acetylation than transfection with *Crebbp*-HA alone (Figure 17, lane 4 versus lane 2). This indicates that MAGEL2 does not enhance FOXO1 acetylation and is most likely not an adaptor protein for CBP-mediated acetyltransferase activity.

3.7 MAGEL2 increases cytoplasmic localization of acetylation-mimicking FOXO1 and increases nuclear localization of acetylation-deficient FOXO1

Although co-expression of *Magel2* does not increase acetylation of FOXO1, acetylation could still be playing a role in the ability of MAGEL2 to influence FOXO1 localization. Acetylation of FOXO1 could be what signals MAGEL2 to affect its localization. In particular, MAGEL2 could be specifically sensing acetylated FOXO1 and subsequently targeting it to the cytoplasm. With this hypothesis in mind, I performed immunofluorescence with FOXO1 acetylation mutants to test if the acetylation status of FOXO1 has any bearing on the involvement of MAGEL2 in FOXO1 localization. I used a FLAG-tagged FOXO1 mimicking constitutively acetylated FOXO1 in which 6 lysine residues (K242, K245, K259, K262, K271 and K291) are replaced with glutamines (FLAG-FOXO1-KQ) as well as a FLAG-tagged FOXO1 mimicking constitutively deacetylated FOXO1 in which those same 6 lysines are mutated to

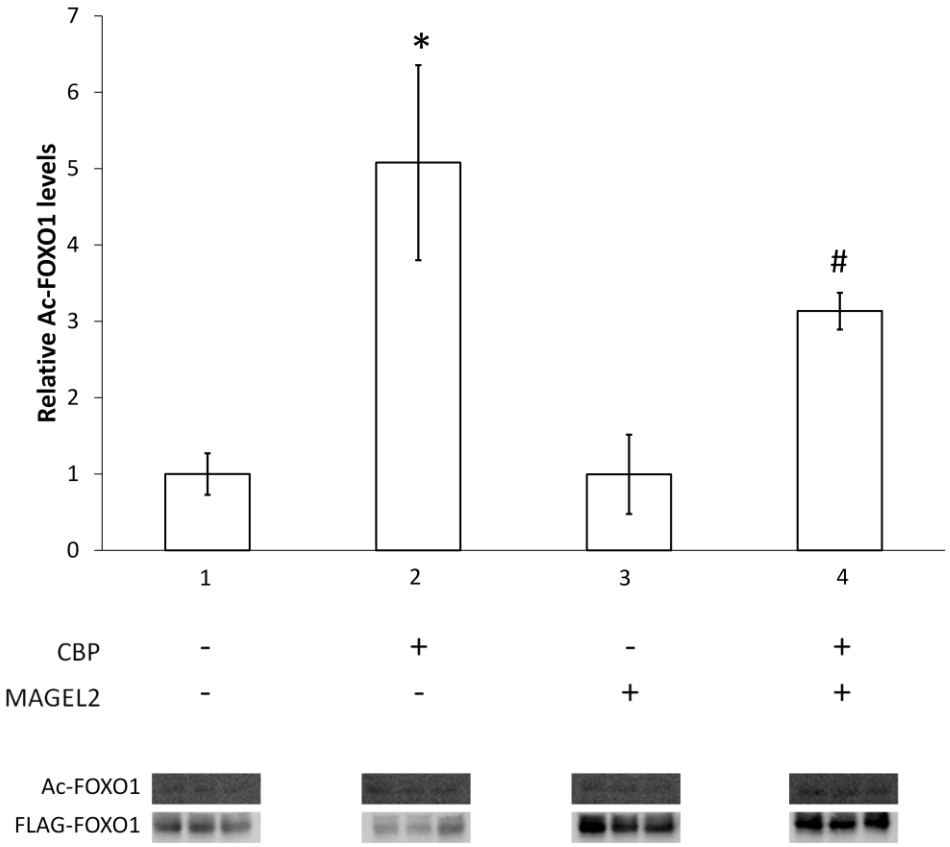

Figure 17. Acetylation of FOXO1 is not significantly different when co-expressed with *Magel2*. HEK293 cells were transfected in triplicate with FLAG-*Foxo1* and either *Crebbp*-HA and/or Xpress-*Magel2*. Proteins were immunoblotted with the appropriate antibodies and analyzed using Kodak Image Station software. Protein quantities were calculated as a ratio of the pixel intensity of acetylated FOXO1 to FLAG-FOXO1. CBP-HA caused a significant increase in acetylated FOXO1 with either empty vector (lane 2 versus lane 1) or Xpress-MAGEL2 (lane 4 versus lane 3). Levels of acetylated FOXO1 were not significantly different when transfected with Xpress-*Magel2* as compared to empty vector, either without CBP-HA (lane 3 versus lane 1) or with CBP-HA (lane 4 versus lane 2). A * indicates a significant difference from cells transfected without *Crebbp*-HA or Xpress-*Magel2* (P=0.035) and a # indicates a significant difference from cells transfected without *Crebbp*-HA and with Xpress-*Magel2* (P=0.02). Representative examples of blots with samples in triplicate are shown.

arginines (FLAG-FOXO1-KR) (Kitamura et al. 2005). I transfected the HEK293/ELR cells with either FLAG-*Foxo1*-KQ or FLAG-*Foxo1*-KR and either Xpress-*Magel2* or empty vector. I found that 39% of cells had cytoplasmic FLAG-FOXO1-KQ (Figure 18A, quantification in 18E). When Xpress-MAGEL2 was present the level of cytoplasmic FLAG-FOXO1-KQ significantly increased to 74% (Figure 18B, lane 2 versus lane 1 in 18E; $P<0.0001$). This strongly suggests that MAGEL2 increases the nuclear exclusion of acetylated FOXO1. Interestingly, I found that MAGEL2 also has a significant effect on constitutively deacetylated FOXO1. When FLAG-*Foxo1*-KR was transfected with empty vector, 9% of cells had exclusively cytoplasmic FLAG-FOXO1-KR and 40% of cells had both nuclear and cytoplasmic expression (Figure 18C, quantification in 18E). Co-transfection with Xpress-*Magel2* resulted in 1% cytoplasmic FLAG-FOXO1-KR and 26% nuclear and cytoplasmic FLAG-FOXO1-KR (Figure 18D, lane 4 versus lane 3 in 18E; $P<0.0001$). This drop in cytoplasmic FLAG-FOXO1-KR with MAGEL2 is statistically significant as compared to cytoplasmic FLAG-FOXO1-KR levels without MAGEL2. This suggests that the presence of MAGEL2 causes increased nuclear accumulation of deacetylated FOXO1. These results indicate that MAGEL2 may affect FOXO1 subcellular localization specifically in response to the particular acetylation state of FOXO1. Accordingly, in the presence of MAGEL2, acetylation of FOXO1 may serve as a trigger for increased cytoplasmic localization whereas deacetylation may serve as a trigger for increased nuclear localization of FOXO1.

3.8 Acetylation-mimicking FOXO1 increases cytoplasmic localization of MAGEL2 and acetylation-deficient FOXO1 increases nuclear localization of MAGEL2

To further confirm these results, the subcellular localization of MAGEL2 was also quantified using immunofluorescence. As complete nuclear exclusion of MAGEL2 is not necessary to its involvement in shuttling FOXO1 to the cytoplasm, I compared the number of cells that were found to have Xpress-MAGEL2 in both the nucleus and the cytoplasm as well as in the cytoplasm alone

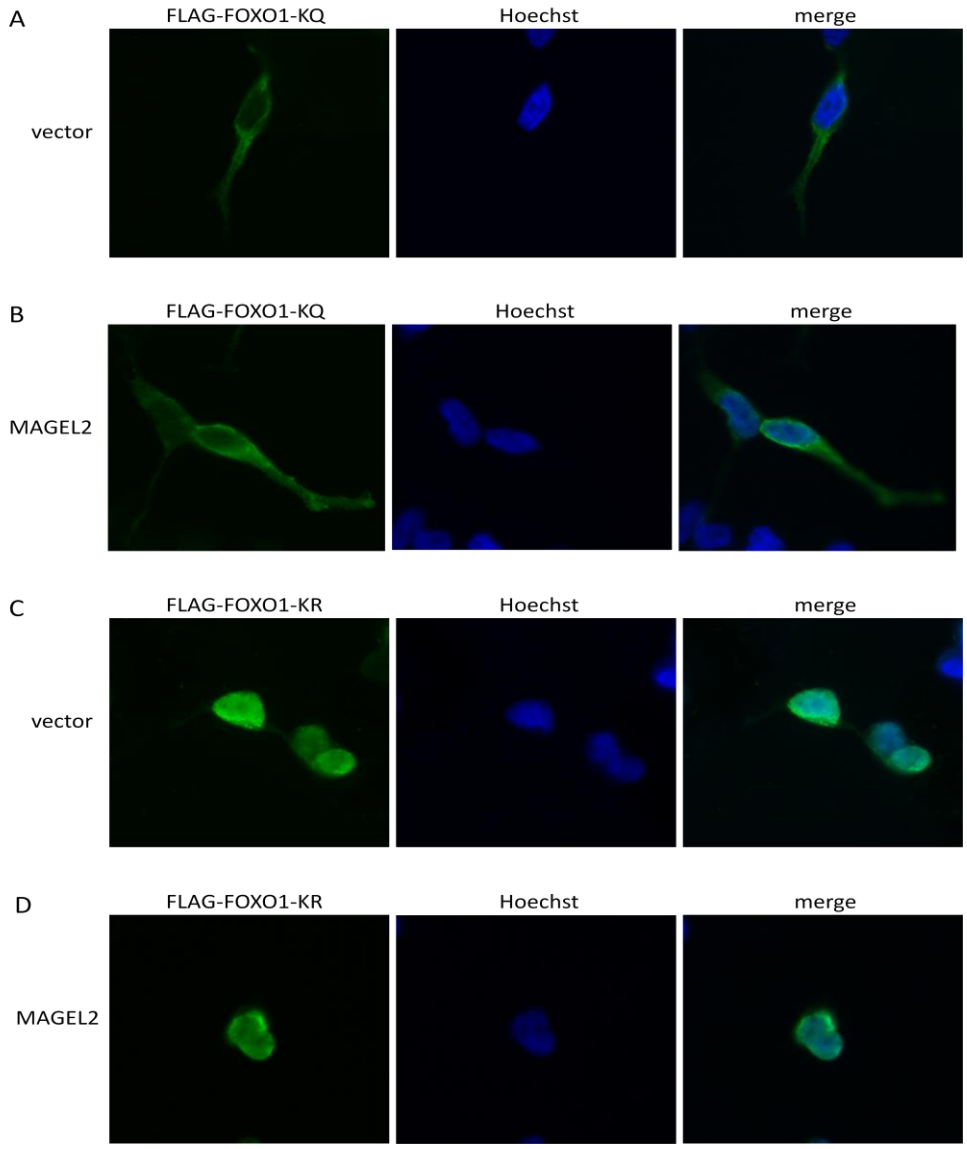

Figure 18. Subcellular localization of FLAG-FOXO1-KQ and FLAG-FOXO1-KR is significantly different in cells co-transfected with Xpress-*Magel2*. HEK293/ELR cells plated on coverslips were transfected with either FLAG-*Foxo1*-KQ or FLAG-*Foxo1*-KR and either empty vector or Xpress-*Magel2*. Proteins were visualized via immunofluorescence with representative examples of cells shown in (A)-(D). The percentage of cells with cytoplasmic FLAG-FOXO1-KQ was significantly increased when co-transfected with Xpress-*Magel2* (lane 2 versus lane 1 in (E)). The percentage of cells with cytoplasmic FLAG-FOXO1-KR was significantly decreased when co-transfected with Xpress-*Magel2* (lane 4 versus lane 3 in (E)). A * indicates a significant difference from cells transfected with empty vector and FLAG-*Foxo1*-KQ ($P<0.0001$). A # indicates a significant difference from cells transfected with empty vector and FLAG-*Foxo1*-KR ($P<0.0001$).

E

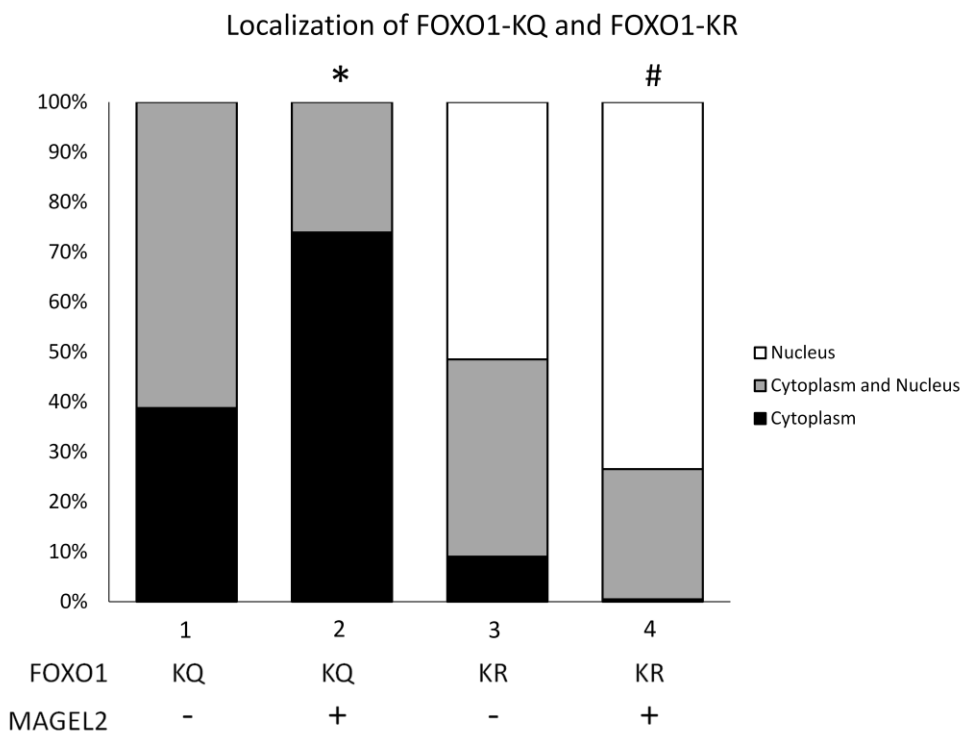
Localization of FOXO1-KQ and FOXO1-KR
*
#
100%
90%
80%
70%
60%
50%
40%
30%
20%
10%
0%
Nucleus
Cytoplasm and Nucleus
Cytoplasm
1
2
3
4
FOXO1
KQ
KQ
KR
KR
MAGEL2
-
+
-
+

to the number of cells with exclusively nuclear localization when doing the statistics. This allowed me to see whether it is possible for MAGEL2 to be directly shuttling FOXO1 from the nucleus to the cytoplasm. HEK293/ELR cells were transfected with Xpress-*Magel2* and either empty vector or GFP-*FOXO1*. I found that, when transfected with empty vector, 49% of cells had exclusively nuclear localization of Xpress-MAGEL2 (Figure 19A, lane 1 in 19E). With co-transfected GFP-*FOXO1*, 41% of cells had exclusively nuclear localization of Xpress-MAGEL2 which was not statistically significant from the results with Xpress-MAGEL2 and empty vector (Figure 19B, lane 2 versus lane 1 in 19E). When Xpress-*Magel2* was co-transfected with FLAG-*Foxo1*-KQ, the level of exclusively nuclear Xpress-MAGEL2 decreased dramatically to 11% (Figure 19C, lane 3 versus lane 2 or lane 1 in 19E, $P<0.0001$). This is an extremely significant decrease in nuclear Xpress-MAGEL2 as compared to the results with empty vector or wildtype GFP-FOXO1. This demonstrates that the localization of MAGEL2 is substantially altered in the presence of acetylation-mimicking FOXO1 and so it further strengthens the results of the FLAG-FOXO1-KQ localization experiment as both proteins significantly re-localize to the cytoplasm when transfected together. When Xpress-*Magel2* was co-transfected with FLAG-*Foxo1*-KR, the percentage of cells with exclusively nuclear Xpress-MAGEL2 was 86% (Figure 19D, lane 4 versus lane 2 or lane 1 in 19E; $P<0.0001$). Compared to when Xpress-*Magel2* was transfected with wildtype GFP-*FOXO1* or empty vector, this is a very significant increase in nuclear Xpress-MAGEL2. This further supports the results seen in the localization of FLAG-FOXO1-KR as both proteins significantly re-localize to the nucleus when transfected together. When co-transfected, the subcellular localization of MAGEL2 and acetylation-mimicking FOXO1 becomes significantly more cytoplasmic compared to when each is transfected with empty vector, or in the case of MAGEL2, even when transfected with wildtype *FOXO1*. Remarkably, the subcellular localization of MAGEL2 and acetylation-deficient FOXO1 becomes significantly more nuclear when co-transfected as compared to when each is transfected with empty vector, or when *Magel2* is transfected with wildtype *FOXO1*. Combined, these results

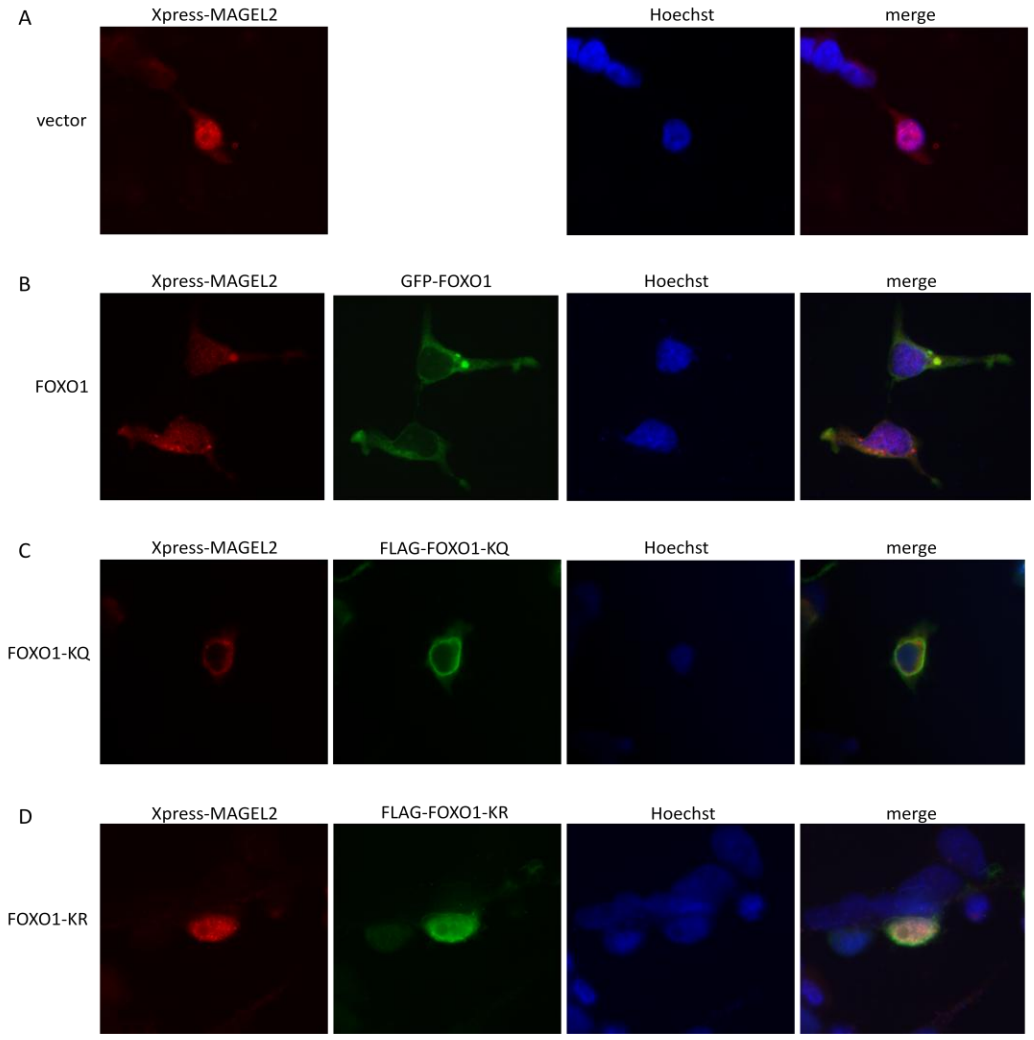

Figure 19. Subcellular localization of Xpress-MAGEL2 is significantly different when co-transfected with either FLAG-*Foxo1*-KQ or FLAG-*Foxo1*-KR. HEK293/ELR cells were plated on coverslips and transfected with Xpress-*Magel2* and either empty vector, GFP-*FOXO1*, FLAG-*Foxo1*-KQ or FLAG-*Foxo1*-KR. Proteins were visualized via immunofluorescence with representative examples of cells shown in (A)-(D). The percentage of cells with cytoplasmic Xpress-MAGEL2 was not significantly different when co-transfected with wildtype GFP-*FOXO1* as compared to empty vector (lane 2 versus lane 1 in (E)). The percentage of cells with cytoplasmic Xpress-MAGEL2 was significantly increased when co-transfected with FLAG-*Foxo1*-KQ as compared to empty vector (lane 3 versus lane 1 in (E)) or wildtype GFP-*FOXO1* (lane 3 versus lane 2 in (E)). The percentage of cells with cytoplasmic Xpress-MAGEL2 was significantly decreased when co-transfected with FLAG-*Foxo1*-KR as compared to empty vector (lane 4 versus lane 1 in (E)) or wildtype GFP-*FOXO1* (lane 4 versus lane 2 in (E)). A * indicates a significant difference from cells transfected with either empty vector or GFP-*FOXO1* ($P<0.0001$).

E

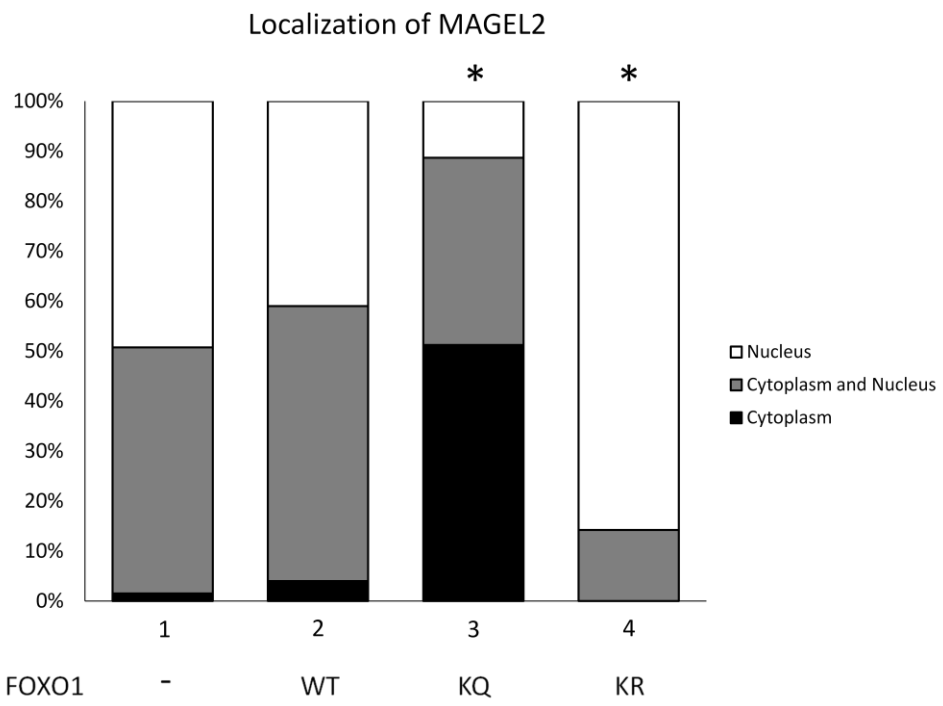
Localization of MAGEL2
*
*
100%
90%
80%
70%
60%
50%
40%
30%
20%
10%
0%
1
2
3
4
FOXO1
-
WT
KQ
KR
Nucleus
Cytoplasm and Nucleus
Cytoplasm

are suggestive of another layer of regulation for FOXO1. The acetylation state of FOXO1 appears to act as a switch for MAGEL2-mediated nucleocytoplasmic shuttling. FOXO1 acetylation signals MAGEL2 to promote the export and/or sequestration of FOXO1 to the cytoplasm whereas deacetylation signals MAGEL2 to promote the import and/or sequestration of FOXO1 to the nucleus.

3.9 MAGEL2 does not co-immunoprecipitate with FOXO1

As previously mentioned, Hasegawa et al. in 2012 have found, through co-immunoprecipitation (co-IP) experiments, that FOXO1 and necdin interact with each other along with the deacetylase SIRT1 in order to increase deacetylation of FOXO1. Since necdin and MAGEL2 are both MAGE proteins they share a conserved MHD (Doyle et al., 2010). Perhaps MAGEL2 is also able to interact with FOXO1 as both necdin and MAGEL2 share this ~170 amino acid domain and since the preceding results indicate that MAGEL2 has a strong influence on FOXO1 localization. In previous work, I found that MAGEL2 co-immunoprecipitated with the circadian rhythm proteins BMAL1 and PER2 (Figure 20A and B). The subcellular localization of BMAL1 and its heterodimerization partner CLOCK was also found to be altered by co-expression with MAGEL2 (Devos et al., 2011). MAGEL2 promoted the cytoplasmic accumulation of both BMAL1 and CLOCK when each was separately transfected with *Magel2* compared to without *Magel2*. Interestingly, MAGEL2 promoted increased nuclear accumulation of both proteins when they were co-transfected together with *Magel2* compared to without *Magel2*. Thus MAGEL2 has the ability to affect the localization of proteins with which it interacts. I performed co-IPs with FOXO1 and MAGEL2 in order to determine if these two proteins can interact. I transfected HEK293/ELR cells with HA-tagged *FOXO1* (HA-*FOXO1*), Xpress-*Magel2* or both HA-*FOXO1* and Xpress-*Magel2*. I incubated the lysates overnight with either rabbit anti-HA polyclonal antibody or mouse anti-Xpress monoclonal antibody and subsequently incubated them with protein G agarose. After running the input samples and the immunoprecipitation (IP) samples on gels and transferring onto blots, I used the appropriate reciprocal antibodies to detect if

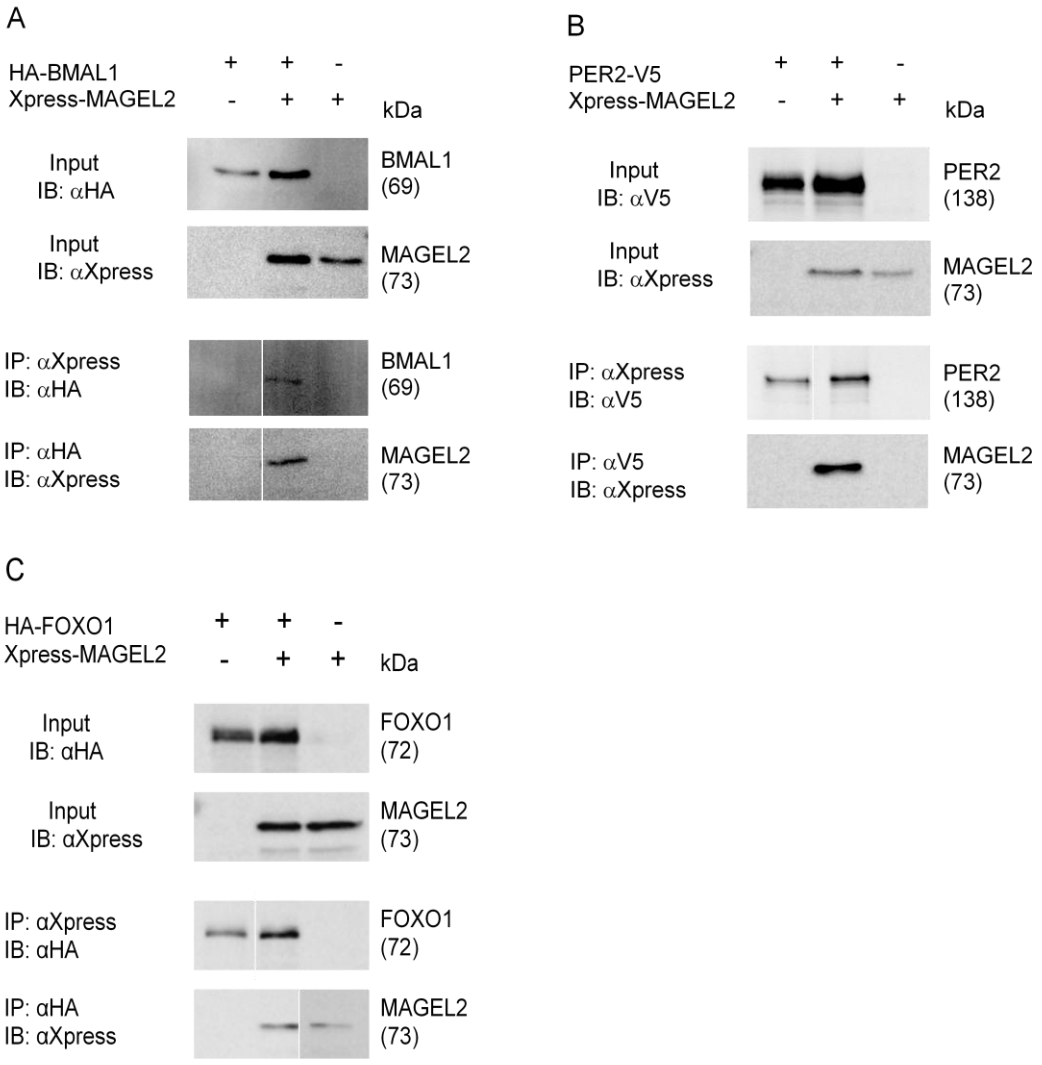

Figure 20. MAGEL2 does not co-immunoprecipitate with FOXO1 but does co-immunoprecipitate with transcription factors involved in circadian rhythm. (A) Xpress-MAGEL2 co-immunoprecipitates with HA-BMAL1. HEK293 cells were transfected with HA-*Bmal1* and Xpress-*Magel2* either together or on their own with the appropriate empty vector. Five percent of the volume of cell lysate used for immunoprecipitation was immunoblotted to confirm the presence of HA-BMAL1 and Xpress-MAGEL2 in the appropriate input lanes (top). The proteins were immunoprecipitated with rabbit anti-HA and mouse anti-Xpress antibodies and the immunoprecipitates detected by immunoblotting with antibodies directed against the reciprocal tag (bottom). (B) Xpress-MAGEL2 immunoprecipitates with PER2-V5. The same co-immunoprecipitation experiment as (A) was done with *Per2*-V5 plasmid in place of HA-*Bmal1* and rabbit anti-V5 in place of rabbit anti-HA antibody. (C) Xpress-MAGEL2 does not co-immunoprecipitate with HA-FOXO1. The same co-immunoprecipitation experiment as (A) was done in HEK293/ELR cells with HA-*FOXO1* plasmid in place of HA-*Bmal1*.

HA-FOXO1 had been immunoprecipitated along with Xpress-MAGEL2 and vice versa. From this experiment I was unable to detect an interaction between FOXO1 and MAGEL2 (Figure 20C). Both Xpress-MAGEL2 and HA-FOXO1 were present in the appropriate input lanes as well as the IP sample lanes in which Xpress-*Magel2* and HA-*FOXO1* were co-expressed. However there are also bands visible in IP sample lanes which only had expression of either Xpress-*Magel2* or HA-*FOXO1*. This is indicative of nonspecific binding of HA-FOXO1 and Xpress-MAGEL2 to the protein G agarose and so since all of the bands are of about the same intensity it suggests that IP of Xpress-MAGEL2 by HA-FOXO1 and vice versa most likely did not occur. When I repeated the co-IPs, higher stringency washes of the immunoprecipitation samples did not change these results. Although I did not find that FOXO1 and MAGEL2 co-immunoprecipitate with each other in HEK293 cells this only means that it is unlikely that these two proteins interact with each other directly. MAGEL2 may be functioning in a manner that does not require an interaction with FOXO1 or indirectly interacting with FOXO1 via some unknown adaptor protein, thus facilitating the significant effect of MAGEL2 on FOXO1 localization.

3.10 MAGEL2 does not alter FOXO1 protein abundance

Both Kim et al. in 2006 as well as Matsuzaki et al. in 2003 have found that stimulation by leptin and insulin not only leads to AKT-mediated phosphorylation and nuclear exclusion of FOXO1, but also to increased FOXO1 degradation. In particular, growth factor stimulation has been found to increase FOXO1 ubiquitination and proteasomal degradation (Aoki et al., 2004; Matsuzaki et al., 2003). Intriguingly, MAGE proteins have been found to interact with E3 ubiquitin ligases in order to facilitate the degradation of target proteins. Since the presence of MAGEL2 results in increased cytoplasmic localization of wildtype FOXO1 in a phosphorylation dependent manner I wanted to test whether the presence of MAGEL2 also results in increased FOXO1 protein degradation. First I sought to establish that activation of leptin/insulin receptor signalling pathways causes significant degradation of FOXO1. However, neither stimulation of

HEK293/ELR cells with Epo nor HEK293 cells with insulin resulted in decreased levels of either endogenous or transfected FOXO1 (data not shown). Since MAGEL2 increases levels of FOXO1 in the cytoplasm even without stimulation by Epo, I tested FOXO1 protein levels with and without the presence of MAGEL2, without any activation of receptor signalling pathways. HEK293 cells were transfected with HA-*FOXO1* and either empty vector or Xpress-*Magel2*. Total HA-FOXO1 protein levels were measured relative to gamma tubulin levels after immunoblotting the resulting lysates. I found that the presence of Xpress-MAGEL2 does not have a significant effect on the abundance of transfected HA-FOXO1 protein (Figure 21). Therefore although MAGEL2 increases the cytoplasmic localization of wildtype FOXO1, it does not have a significant effect on the abundance of FOXO1 protein.

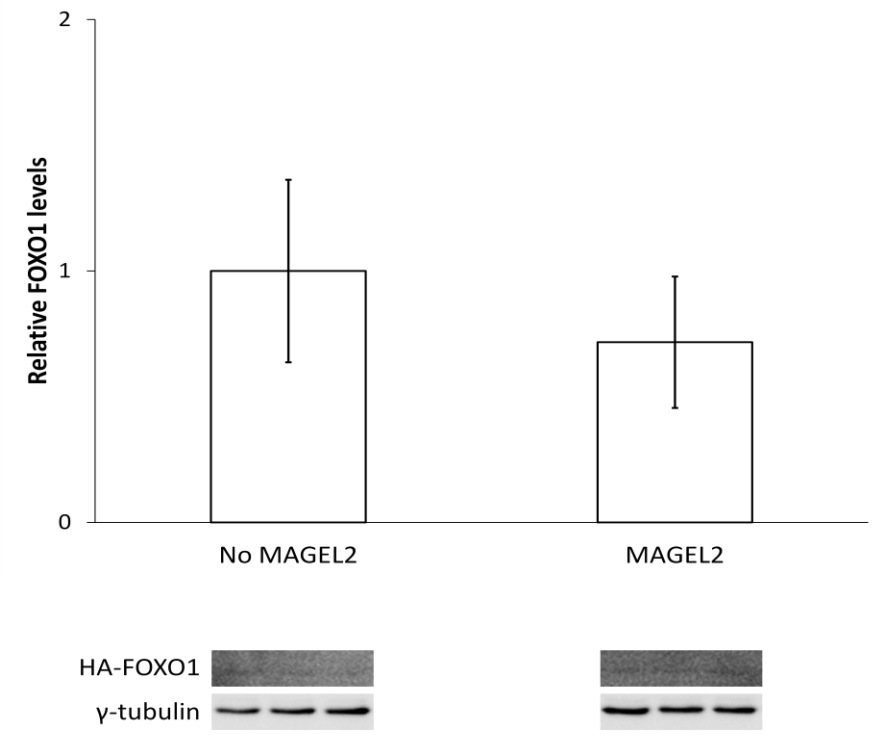

Figure 21. FOXO1 protein abundance is not significantly different when co-expressed with *Magel2*. HEK293 cells were transfected in triplicate with HA-*FOXO1*and either empty vector or Xpress-*Magel2*. Proteins were immunoblotted with the appropriate antibodies and analyzed using Kodak Image Station software. Protein quantities were calculated as a ratio of the pixel intensity of HA-FOXO1 to γ-tubulin. No significant difference in the relative levels of transfected HA-FOXO1was observed when cells were co-transfected with Xpress-*Magel2* as compared to empty vector. Representative examples of blots with samples in triplicate are shown.

Chapter 4: Discussion

4.1 Introduction

People with PWS must deal with severely dysfunctional energy homeostasis, manifesting in insatiable hunger, overeating and obesity. Through this research I have found a role for *MAGEL2*, one the genes deleted in PWS, in the regulation of the Forkhead box transcription factor FOXO1. FOXO1 is a protein known to stimulate increased food intake and body weight. Activation of two major energy regulating pathways in the hypothalamus, the leptin and insulin receptor signalling pathways, lead to inactivation of FOXO1 via phosphorylation and nuclear exclusion. The effect of acetylation on FOXO1 activity, however, remains controversial. Some researchers have observed that acetylation of FOXO1 increases its transcriptional activity (Hasegawa et al., 2012; Yang et al., 2005; Motta et al., 2004) whereas others claim that acetylation decreases its activity (Frescas et al., 2005; Kitamura et al., 2005; Daitoku et al., 2004). Several authors have found that acetylation of FOXO1 reduces its DNA-binding ability and increases its sensitivity to AKT-mediated phosphorylation (Qiang et al., 2010; Brent et al., in 2008; Matsuzaki et al., 2005). My experiments in cultured cells indicate that MAGEL2, which is strongly expressed in the hypothalamus, increases the cytoplasmic localization of acetylated FOXO1 in a manner also dependent upon AKT-mediated FOXO1 phosphorylation. In addition, I found that the presence of MAGEL2 increases the nuclear localization of deacetylated FOXO1. How this translates to the regulation of FOXO1 activity *in vivo* is as yet unknown. However, this research suggests that MAGEL2 may function as an additional regulatory component of FOXO1 localization and, as such, its loss may have a significant impact on energy balance and could play a part in explaining the dysfunctional regulation of energy seen in PWS.

4.2 MAGEL2 promotes the accumulation of phosphorylated FOXO1 in the cytoplasm

The nucleocytoplasmic shuttling of FOXO1 is pivotal to its activity and function as a transcription factor. The subcellular localization of FOXO1 is thoroughly dependent upon its post-translational modifications and interactions

with other proteins which are intricately controlled by many different factors including intracellular signalling pathways and oxidative stress. As seen in Figure 9, co-expression of *Magel2* with wildtype *FOXO1* results in siginificantly increased nuclear exclusion of FOXO1. Without stimulation of the intracellular leptin signalling pathway via Epo treatment, the presence of MAGEL2 increased the levels of cytoplasmic FOXO1 from 37% to 55% of cells counted (Figure 9E, lane 1 versus lane 3). In Epo stimulated cells, the percentage of cells with cytoplasmic FOXO1 increased from 51% without MAGEL2 to 71% when MAGEL2 was present (Figure 9E, lane 2 versus lane 4). Thus, regardless of Epo, co-expression of *Magel2* with wildtype *FOXO1* results in an approximately 20% increase in cytoplasmic FOXO1. Most likely, the increased nuclear export of FOXO1 promoted by MAGEL2 would reduce FOXO1 transcriptional activity as cytoplasmic localization prevents access to DNA-binding in the nucleus. However, I could not provide evidence for or against this hypothesis as luciferase assays using reporter constructs driven by either the *POMC* promoter or the *IGFBP-1* promoter, which contain FOXO1 binding sites, were unsuccessful.

As phosphorylation and, according to some authors, acetylation are thought to increase the likelihood of FOXO1 nuclear exclusion, I tested to see if the presence of MAGEL2 altered the levels of either of these post-translational modifications. Via immunoblotting I discovered that MAGEL2 did not affect the phosphorylation of FOXO1 at S256 either directly (Figure 12) or indirectly through enhancing the activation of other pathways downstream of leptin or insulin receptors, such as ERK or AKT (Figures 14-16). In addition, MAGEL2 did not significantly alter the levels of acetylated FOXO1 with or without CBP (Figure 17). However, MAGEL2 was unable to affect the localization of either the FOXO1AAA phospho-mutant (Figure 11) or of wildtype FOXO1 in cells treated with the PI3K-inhibitor wortmannin (Figure 13). As MAGEL2 does not significantly affect FOXO1 phosphorylation, these results indicate that in accordance with previous research, AKT-mediated phosphorylation of FOXO1 is required in order for FOXO1 to be excluded from the nucleus and, consequently, MAGEL2 can only exert its affect on phosphorylated FOXO1. Since MAGEL2

could affect the localization of FOXO1 with or without Epo stimulation, this suggests that there is some level of FOXO1 phosphorylation occurring regardless of specific activation of leptin signalling. This is supported by the fact that, as seen in lane 1 of Figure 9E, 37% of unstimulated cells without MAGEL2 had exclusively cytoplasmic localization of FOXO1.

All of the immunofluorescence work performed was done using HEK293/ELR cells. Stimulation with Epo significantly increased levels of cytoplasmic wildtype FOXO1 without co-expression of *Magel2* (from 37% to 51% of cells, Figure 9E, lane 1 versus lane 2) as well as with *Magel2* (from 55% to 71% of cells, Figure 9E, lane 3 versus lane 4). Thus, Epo was able to significantly activate nuclear exclusion resulting in an approximately 15% increase in cytoplasmic FOXO1. I determined through immunoblotting experiments however, that Epo does not significantly increase the phosphorylation of either AKT or FOXO1 in HEK293/ELR cells. This may result from being able to visualize differences in localization intracellularly which are not able to be measured grossly via differences in phosphorylation levels on immunoblots. Even so, insulin was able to significantly activate phosphorylation of both AKT and FOXO1 in HEK293 cells. Hence, repeating the immunofluorescence experiments in HEK293 cells with and without insulin stimulation may produce more significant results with regards to FOXO1 nuclear exclusion.

4.3 MAGEL2 promotes the accumulation of acetylation-mimicking FOXO1 in the cytoplasm

Interestingly, co-expression of *Magel2* with the constitutively acetylated *Foxo1* mimic, *Foxo1*-KQ, results in considerably increased localization of both of these proteins in the cytoplasm as compared to when each is transfected with empty vector. The percentage of cells with cytoplasmic localization of FOXO1-KQ increased from 39% without MAGEL2 to 74% with MAGEL2 (Figure 18E, lane 1 versus lane 2). Likewise, the percentage of cells expressing exclusively cytoplasmic or nuclear and cytoplasmic MAGEL2 increased from 51% with

empty vector to 89% when co-expressed with *Foxo1*-KQ (Figure 19E, lane 1 versus lane 3). Thus FOXO1-KQ and MAGEL2 underwent a 35% and 38% increase in cytoplasmic localization respectively.

The increase in FOXO1 cytoplasmic localization with co-expression of *Magel2* is considerably greater with FOXO1-KQ compared to wildtype FOXO1. This disparity could perhaps be explained by the difference in 'acetylated' FOXO1 levels. Experiments using FOXO1-KQ create an artificial environment in which the entire pool of transfected FOXO1 mimicks constitutive acetylation. Wildtype FOXO1 has the ability to be reversibly acetylated and so the ratio of acetylated to deacetylated FOXO1 would be constantly changing. If MAGEL2 specifically targets acetylated FOXO1 to the cytoplasm, this may account for why a lower percentage of wildtype FOXO1 is translocated to the cytoplasm in the presence of MAGEL2 than the constitutively acetylation-mimicking FOXO1-KQ mutant (Figure 9E lane 3 versus Figure 18E lane 2). Concurrently, this vulnerability of wildtype FOXO1 to deacetylation may also explain why although the localization of MAGEL2 was significantly altered when co-expressed with *Foxo1*-KQ (Figure 19E, lane 3 versus lane 1), its localization was not significantly different when co-transfected with wildtype *FOXO1* as compared to empty vector (Figure 19E, lane 2 versus lane 1).

Continued experimentation is required in order to elucidate the exact mechanism behind how MAGEL2 affects FOXO1 localization. I propose that MAGEL2 may have a direct influence on the physical transport of FOXO1 and that this influence is specifically dependent upon the post-translational modifications of FOXO1. As MAGEL2 co-localizes with FOXO1 in the same cellular compartments based on FOXO1 acetylation status, this indicates that they may be shuttling together as part of a complex. However, it is as yet unknown whether MAGEL2 functions specifically to promote FOXO1 nuclear export, to retain FOXO1 n the cytoplasm, or if MAGEL2 functions in both of these capacities. This could be studied using immunofluorescence with cells transfected with and without *Magel2* and treated with leptomycin B, an inhibitor of the exportin CRM1, in order to block the nuclear export of FOXO1. If the

presence of MAGEL2 still results in increased cytoplasmic localization of FOXO1 after leptomycin B treatment then either MAGEL2 increases FOXO1 nuclear export independently of CRM1 or, more likely, MAGEL2 functions to maintain the cytoplasmic sequestration of FOXO1.

As previously mentioned, FOXO1 nuclear export requires passage through the nuclear-pore complex of the nuclear membrane via interaction with an export complex made up of GTP-bound RAN and CRM1. This complex recognizes and binds to the NES located in the C-terminal region of FOXO1 and subsequently shuttles FOXO1 out of the nucleus and into the cytoplasm (van der Heide et al., 2004). Potentially, MAGEL2 may be increasing the likelihood of acetylated FOXO1 interacting with the export complex by enhancing the function of the NES. Although FOXO1 and MAGEL2 most likely do not interact as they did not immunoprecipitate with each other in co-IP experiments (Figure 20C), perhaps one or more adaptor proteins facilitates this interaction allowing MAGEL2 to promote export complex-mediated nuclear exclusion of specifically acetylated FOXO1. It is possible that these unknown adaptor proteins may include 14-3-3 proteins as it is suspected that they enhance functioning of the NES. It is known that FOXO1 must bind with 14-3-3 dimers in order to be shuttled out of the nucleus and that this interaction requires phosphorylation of T24 and S256 of FOXO1 (Tzivion et al., 2011; van der Heide et al., 2004). MAGEL2, which was also found to require phosphorylation of FOXO1 at the conserved AKT-recognized S256 site in order to be able to affect FOXO1 localization, may increase the sensitivity or specificity of 14-3-3 proteins binding to acetylated FOXO1. Or, upon binding, MAGEL2 may enhance the function of 14-3-3 proteins exclusively in regards to acetylated FOXO1. Once in the cytoplasm, MAGEL2 may also function to keep FOXO1 in the cytoplasm by promoting continued binding of 14-3-3 proteins or other adaptor proteins to FOXO1 which may mask or sterically inhibit the NLS of FOXO1. Blocking the NLS, located at the C-terminal end of the DNA-binding domain, would prevent FOXO1 from being transported back into the nucleus via NLS-recognizing importin proteins. Although there is conflict in the literature about whether acetylated FOXO1 is

more transcriptionally active or less active, I hypothesize that since the presence of MAGEL2 increases the cytoplasmic localization of acetylated FOXO1 that this would decrease the transcriptional activity of FOXO1.

4.4 MAGEL2 promotes the accumulation of acetylation-deficient FOXO1 in the nucleus

Co-expression of *Magel2* with the constitutively acetylation-deficient *Foxo1* mutant, *Foxo1*-KR, was found to have the absolute opposite effect on the localization of these two proteins. When transfected together, MAGEL2 and FOXO1-KR both had considerably increased nuclear localization as compared to when each was transfected with empty vector. Without MAGEL2, FOXO1-KR was localized exclusively in the nucleus in 52% of cells (Figure 18E, lane 3). Likewise, without FOXO1-KR, MAGEL2 was localized exclusively in the nucleus in 49% of cells (Figure 19E, lane 1). When co-expressed, however, FOXO1-KR was localized in the nucleus in 74% of cells (Figure 18E, lane 4) and MAGEL2 was localized exclusively in the nucleus in 86% of cells (Figure 19E, lane 4). Respectively, this represents a 22% and 37% increase in exclusively nuclear localization of these two proteins when expressed together. These results indicate a significant swing in localization of both of these proteins toward the nucleus, which is a complete reversal of the results documented when expressing *Magel2* with *Foxo1*-KQ. However, these results may be somewhat less convincing than the results with FOXO1-KQ as there is not a significant difference in exclusively cytoplasmic localization of MAGEL2 with and without co-transfected *Foxo1*-KR.

A question remains as to why a significant increase in cytoplasmic wildtype FOXO1 occurs when co-transfected with *Magel2* if indeed MAGEL2 increases nuclear localization of deacetylated FOXO1 while at the same time increasing nuclear exclusion of acetylated FOXO1. I would suggest that perhaps the pool of wildtype FOXO1 is skewed towards increased acetylation in HEK293/ELR cells. Consequently, due to increased acetylated FOXO1 levels, the net effect of MAGEL2 on wildtype FOXO1 localization would be increased

nuclear exclusion. Also, it has been found that serum starving cultured cells results in increased acetylation of FOXO1 (Zhao et al., 2010). Higher proportions of acetylated versus deacetylated FOXO1 may therefore have come as a result of serum starving the cells prior to fixing them for immunofluorescence. This could be tested by serum starving cells for increasing timepoints and comparing the levels of acetylated FOXO1 by immunoblotting the resulting cell lysates.

I suggest that, mechanistically, MAGEL2 may affect the localization of deacetylated FOXO1 also via FOXO1 localization sequences. Instead of promoting nuclear export and/or sequestration in the cytoplasm, MAGEL2 promotes nuclear accumulation of acetylation-deficient FOXO1. Whether MAGEL2 is influencing deacetylated FOXO1 by limiting its nuclear export, enhancing its nuclear import or both remains unknown. However, as fellow MAGE protein necdin has been found to directly interact with multiple importin proteins including transportin 1, transportin 2 and importin β1, perhaps MAGEL2 also interacts with importins and thereby enhances FOXO1 nuclear localization (Lavi-Itzkovitz et al., 2012). SIRT1 is widely known to deacetylate FOXO1 in the nucleus (Daitoku et al., 2004). Perhaps MAGEL2 functions to retain nuclear localization of deacetylated FOXO1 by reducing NES function. In the cytoplasm, FOXO1 has been found to be deacetylated by SIRT2 (Daitoku et al., 2011; Jing et al., 2007). Potentially, upon SIRT2-mediated deacetylation of cytoplasmic FOXO1, MAGEL2 functions to increase nuclear import of deacetylated FOXO1 by enhancing or sterically disinhibiting the NLS. This would give importin proteins, which recognize and bind to the NLS, access to FOXO1 and allow for nuclear inclusion. Again, as I was unable to detect an interaction between FOXO1 and MAGEL2, this effect may instead be mediated through one or more unknown adaptor proteins. As FOXO1 phosphorylation promotes 14-3-3 proteins to interact with FOXO1, it has also been established that dephosphorylation by the protein phosphatase PP2A promotes the dissociation of these binding partners and increased nuclear localization of FOXO1 (Tzivion et al., 2011; Yan et al., 2008). Perhaps MAGEL2 functions to promote dissociation of 14-3-3 protein binding after dephosphorylation and deacetylation of FOXO1. It would be interesting to

test whether MAGEL2 requires dephosphorylation of FOXO1 in order to target deacetylated FOXO1 to the nucleus seeing that MAGEL2 requires phosphorylation of FOXO1 in order to promote increased cytoplasmic localization of acetylated FOXO1. This could be tested via immunofluorescence using cells transfected with and without MAGEL2 and treated with PP2A inhibitors, such as microcystin-LR, okadaic acid or fostriecin, to block FOXO1 dephosphorylation. If MAGEL2 is unable to increase the nuclear localization of deacetylated FOXO1, as it does without PP2A inhibitors, then it would be clear that MAGEL2 requires FOXO1 dephosphorylation in order to increase nuclear import.

There are conflicts in the literature concerning the activity of deacetylated FOXO1. Some authors have shown evidence that deacetylated FOXO1 is more active and some have shown that it is less active. The transcriptional activity of deacetylated FOXO1 may be tissue and target-gene specific. Since the presence of MAGEL2 results in increased nuclear localization of deacetylated FOXO1, this may actually function to increase the transcriptional activity of FOXO1, or at least give FOXO1 the opportunity to become more transcriptionally active. However, experiments by Hasegawa et al. in 2012 appear to show that deacetylation of FOXO1 in fact reduces its transcriptional activity in the murine hypothalamus. Ultimately, more testing is needed in order to understand how changes in acetylation affect FOXO1 activity as well as how MAGEL2-mediated alteration of FOXO1 localization affects its activity.

4.5 MAGEL2 and the regulation of FOXO1 in the hypothalamus: translation to energy dysregulation in Prader-Willi syndrome

Based on my results, I propose that the loss of MAGEL2 expression in PWS contributes to the energy imbalance in this disorder. As the hypothalamus is the main area of the body responsible for the homeostatic regulation of energy, it makes sense that MAGEL2, which is so highly expressed in the hypothalamus, would somehow be involved. The extent to which *MAGEL2*, as only one of several deleted genes in PWS, actually contributes to energy homeostasis is yet to

be entirely elucidated. The results of this investigation indicate that MAGEL2 is involved in the regulation of the Forkhead box transcription factor FOXO1 via its subcellular localization. In the hypothalamus, FOXO1 promotes increased food intake and decreased energy expenditure by activating the transcription of the orexigenic neuropeptides NPY and AgRP as well as inhibiting the expression of anorexigenic POMC. Signals such as leptin and insulin stimulate anorexigenic pathways which lead to the phosphorylation, nuclear exclusion and, consequently, the inactivation of FOXO1. Under conditions in which FOXO1 is both acetylated as well as phosphorylated, MAGEL2 functions to increase the movement of FOXO1 into the cytoplasm and/or increase FOXO1 cytoplasmic sequestration (Figure 22A and 23), thus potentiating the appetite-suppressing effect of leptin and insulin signalling by reducing FOXO1 transcriptional activity. The loss of *MAGEL2* in PWS could therefore result in increased nuclear localization of FOXO1 (Figure 22B) potentially leading to a concomitant increase in FOXO1 transcriptional activity, rendering the leptin and insulin signalling pathways as less potent mediators of energy regulation in the body. Without MAGEL2, the possible increased expression of the FOXO1 target genes *NPY* and *AgRP* and decreased expression of *POMC* could to some degree contribute to the extreme overeating and excessive weight gain characteristic of PWS.

Alternatively, under conditions which promote deacetylation of FOXO1, MAGEL2 increases the nuclear import of FOXO1 and/or FOXO1 nuclear sequestration (Figure 22C and 23). FOXO1 deacetylation may be increased by dietary restriction, fasting and nutrient-poor conditions as these have been found to increase the activity of SIRT1 (Baur et al., 2010; Imai and Guarente, 2010). Increased nuclear localization of deacetylated FOXO1 would potentially allow for increased FOXO1 transcriptional activity. In this situation, the loss of MAGEL2 expression could increase cytoplasmic localization of FOXO1 (Figure 22D) and thereby reduce its activity. How this may relate functionally to energy regulation in PWS is currently unclear. Perhaps conditions which may promote FOXO1 deacetylation, such as nutrient deprivation, require increased FOXO1 activity. This would be logical, from an evolutionary perspective, as it would be important

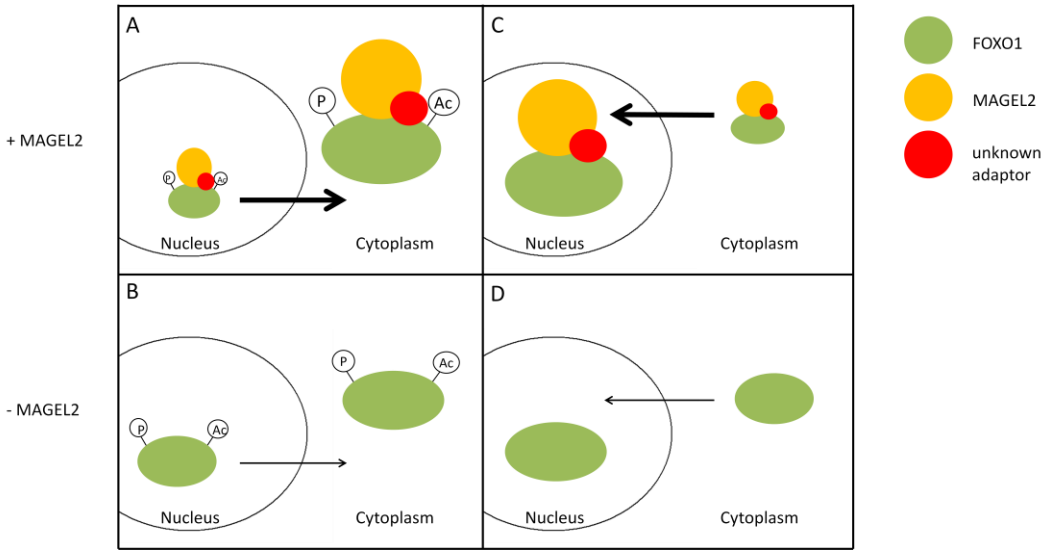

Figure 22. Comparative illustration of FOXO1 subcellular localization with and without MAGEL2. (A) When FOXO1 is both acetylated and phosphorylated, MAGEL2 functions to increase the cytoplasmic localization of FOXO1. (B) Without MAGEL2, acetylated and phosphorylated FOXO1 also localizes to the cytoplasm but to a lesser extent. (C) When FOXO1 is deacetylated, MAGEL2 increases the nuclear localization of FOXO1. (D) Without MAGEL2, deacetylated FOXO1 also localizes to the nucleus but to a lesser extent. The interaction between MAGEL2 and FOXO1 may be facilitated by an unknown adaptor protein.

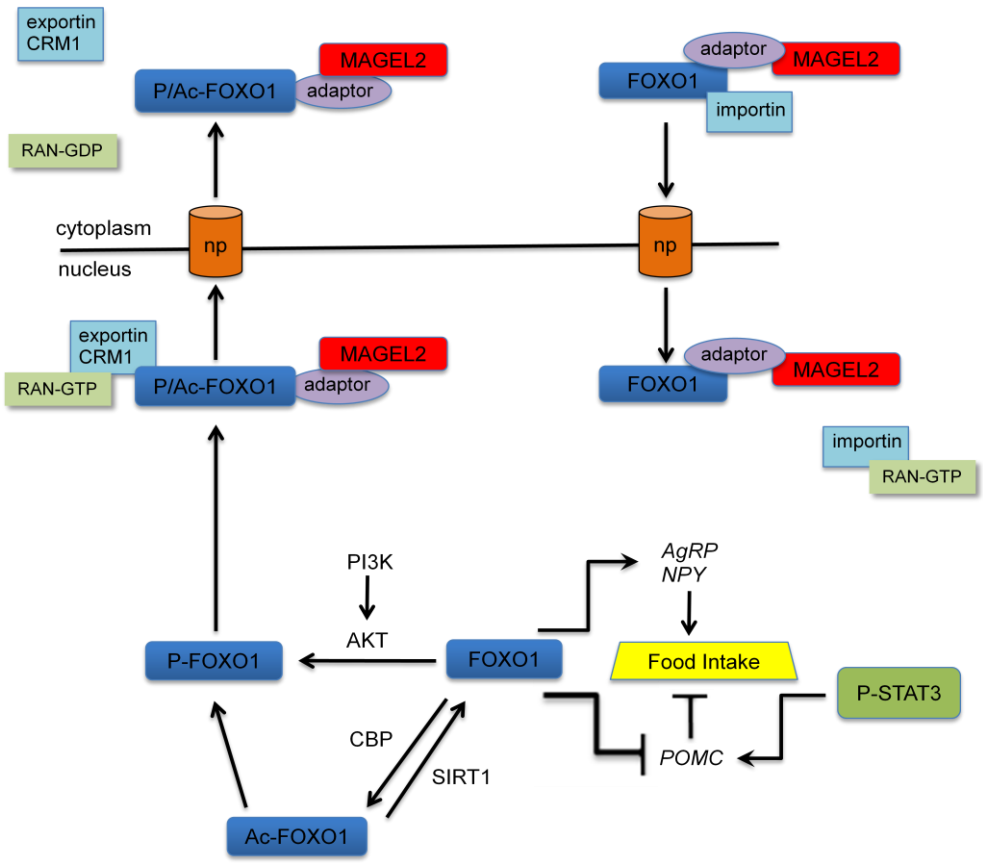

Figure 23. Model of the proposed role of MAGEL2 in the regulation of FOXO1 in hypothalamic neurons. In the nucleus, phosphorylated FOXO1 forms an export complex with the exportin protein CRM1 and GTP-bound RAN. The export complex is transported through the nuclear pore complex (np) to the cytoplasm where it is then disassembled. MAGEL2 may function to increase cytoplasmic localization of acetylated forms of phosphorylated FOXO1 by enhancing the export process and/or retaining FOXO1 in the cytoplasm once exported, potentially via an unknown adaptor protein. In the cytoplasm, FOXO1 interacts with importin proteins which transport it to the nucleus. MAGEL2 may function to increase nuclear localization of deacetylated FOXO1 by enhancing nuclear import and/or retaining FOXO1 in the nucleus, again this may possibly be mediated by an unknown adaptor protein. FOXO1 functions as a transcription factor in the nucleus, promoting the expression of the orexigenic genes *NPY* and *AgRP* as well as inhibiting the expression of the anorexigenic *POMC*, which is activated by phosphorylated STAT3. The MAGEL2-mediated increase in the nuclear exclusion of phosphorylated and acetylated FOXO1 in the hypothalamus may decrease FOXO1 transcriptional activity leading to decreased food intake. The MAGEL2-mediated increase in nuclear localization of deacetylated FOXO1 may result in increased FOXO1 transcriptional activity leading to increased food intake. AKT-mediated phosphorylation of FOXO1 is activated by PI3K. FOXO1 is acetylated by the acetyltransferase CBP and deacetylated by SIRT1.

to stimulate increased appetite and food intake in situations of nutrient deprivation. An aspect crucial to the *in vivo* outcomes of MAGEL2-mediated changes in FOXO1 localization involves the acetylation status of the pool of FOXO1 protein in hypothalamic neurons. In order to understand the ultimate effect of MAGEL2 on FOXO1 localization it would be important to know the composition of acetylated versus deacetylated FOXO1 under various conditions in the hypothalamus. As the influence of MAGEL2 on FOXO1 is largely dependent on the acetylation status of FOXO1, whichever signals, pathways or conditions that promote variation in FOXO1 acetylation, such as oxidative stress, would be important in clarifying the overall extent and specificity with which MAGEL2 is able to alter FOXO1 localization. Taken together, the alterations in FOXO1 localization facilitated by MAGEL2 are suggestive of an additional component in the post-translational modification-status dependent model of FOXO1 regulation. In addition, knowledge of the complexity surrounding the link between the loss of *MAGEL2* expression and the apparent energy dysregulation symptomatic of PWS has been further illuminated through this research.

4.6 Future work and Conclusions

There is much left to be elucidated with respect to the relationship between MAGEL2 and FOXO1. Further experimentation is necessary in order to address some unanswered questions including how the loss of MAGEL2 affects FOXO1 localization and activity *in vivo*. Also, it remains to be determined how MAGEL2 alters FOXO1 localization mechanistically. As it is unlikely that MAGEL2 and FOXO1 directly interact with each other, it will be helpful to establish whether or not adaptor proteins are involved and, if they are, which protein(s) in particular are facilitating the effects that these two proteins have on each other. Moving forward, the research begun here in cultured cells could be expanded and confirmed in mice. The expression of the FOXO1 target-genes *NPY, AgRP* and *POMC* could be measured and compared between *Magel2*-null and wildtype mice using RT-PCR or *in situ* hybridization. As luciferase assays were unsuccessful, this would provide alternative means for determining whether

the loss of MAGEL2 results in altered FOXO1 transcriptional activity. In addition, the subcellular localization of FOXO1 could also be studied using immunofluorescence with hypothalamic sections of *Magel2*-null versus wildtype mice after they have been either fasted or fed and treated with or without leptin or insulin, allowing for an *in vivo* characterization of how MAGEL2 and its loss affect FOXO1 localization.

Through the analysis of initial experiments in cultured cells, I have discovered as well as begun to decipher the relationship between MAGEL2 and the regulation of FOXO1. As MAGEL2 not only acts to promote increased cytoplasmic localization of acetylated and phosphorylated FOXO1 but also functions to increase nuclear localization of deacetylated FOXO1, I propose that MAGEL2 plays dual roles in FOXO1 regulation and that these dual roles are specifically performed in response to FOXO1 acetylation status. Since *Magel2* is almost exclusively expressed in the hypothalamus but *Foxo1* is expressed and functions in many tissues of the body, it is clear that MAGEL2 is not absolutely required for the regulation of FOXO1. Rather, I suggest that MAGEL2 functions as an additional regulator of FOXO1 activity in the hypothalamus in order to fine tune the regulation of energy balance and thereby allow for improved adjustments in food intake and energy expenditure in response to the body's constantly monitored energy stores. Hopefully, this research can be used as a springboard for continued study concerning the relationship between MAGEL2 and FOXO1 as well as how the loss of *MAGEL2* ultimately contributes to the PWS phenotype.

References

Accili, D., and Arden, K.C. (2004). FoxOs at the crossroads of cellular metabolism, differentiation, and transformation. Cell *117,* 421-426.

Aja, S., Sahandy, S., Ladenheim, E.E., Schwartz, G.J., and Moran, T.H. (2001). Intracerebroventricular CART peptide reduces food intake and alters motor behavior at a hindbrain site. Am. J. Physiol. Regul. Integr. Comp. Physiol. *281,* R1862-7.

Al-Masri, M., Krishnamurthy, M., Li, J., Fellows, G.F., Dong, H.H., Goodyer, C.G., and Wang, R. (2010). Effect of forkhead box O1 (FOXO1) on beta cell development in the human fetal pancreas. Diabetologia *53,* 699-711.

Aoki, M., Jiang, H., and Vogt, P.K. (2004). Proteasomal degradation of the FoxO1 transcriptional regulator in cells transformed by the P3k and Akt oncoproteins. Proc. Natl. Acad. Sci. U. S. A. *101,* 13613-13617.

Banks, A.S., Davis, S.M., Bates, S.H., and Myers, M.G.,Jr. (2000). Activation of downstream signals by the long form of the leptin receptor. J. Biol. Chem. *275,* 14563-14572.

Barker, P.A., and Salehi, A. (2002). The MAGE proteins: emerging roles in cell cycle progression, apoptosis, and neurogenetic disease. J. Neurosci. Res. *67,* 705-712.

Barsh, G.S., and Schwartz, M.W. (2002). Genetic approaches to studying energy balance: perception and integration. Nat. Rev. Genet. *3,* 589-600.

Barthel, A., Schmoll, D., and Unterman, T.G. (2005). FoxO proteins in insulin action and metabolism. Trends Endocrinol. Metab. *16,* 183-189.

Batterham, R.L., Cowley, M.A., Small, C.J., Herzog, H., Cohen, M.A., Dakin, C.L., Wren, A.M., Brynes, A.E., Low, M.J., Ghatei, M.A., Cone, R.D., and Bloom, S.R. (2002). Gut hormone PYY(3-36) physiologically inhibits food intake. Nature *418,* 650-654.

Baur, J.A., Chen, D., Chini, E.N., Chua, K., Cohen, H.Y., de Cabo, R., Deng, C., Dimmeler, S., Gius, D., Guarente, L.P., *et al.* (2010). Dietary restriction: standing up for sirtuins. Science *329,* 1012-3; author reply 1013-4.

Biggs, W.H.,3rd, Meisenhelder, J., Hunter, T., Cavenee, W.K., and Arden, K.C. (1999). Protein kinase B/Akt-mediated phosphorylation promotes nuclear exclusion of the winged helix transcription factor FKHR1. Proc. Natl. Acad. Sci. U. S. A. *96,* 7421-7426.

Bischof, J.M., Stewart, C.L., and Wevrick, R. (2007). Inactivation of the mouse Magel2 gene results in growth abnormalities similar to Prader-Willi syndrome. Hum. Mol. Genet. *16,* 2713-2719.

Bjorbaek, C., Buchholz, R.M., Davis, S.M., Bates, S.H., Pierroz, D.D., Gu, H., Neel, B.G., Myers, M.G.,Jr, and Flier, J.S. (2001). Divergent roles of SHP-2 in ERK activation by leptin receptors. J. Biol. Chem. *276,* 4747-4755.

Boccaccio, I., Glatt-Deeley, H., Watrin, F., Roeckel, N., Lalande, M., and Muscatelli, F. (1999). The human MAGEL2 gene and its mouse homologue are paternally expressed and mapped to the Prader-Willi region. Hum. Mol. Genet. *8,* 2497-2505.

Boguszewski, C.L., Paz-Filho, G., and Velloso, L.A. (2010). Neuroendocrine body weight regulation: integration between fat tissue, gastrointestinal tract, and the brain. Endokrynol. Pol. *61,* 194-206.

Brambilla, P., Bosio, L., Manzoni, P., Pietrobelli, A., Beccaria, L., and Chiumello, G. (1997). Peculiar body composition in patients with Prader-Labhart-Willi syndrome. Am. J. Clin. Nutr. *65,* 1369-1374.

Brent, M.M., Anand, R., and Marmorstein, R. (2008). Structural basis for DNA recognition by FoxO1 and its regulation by posttranslational modification. Structure *16,* 1407-1416.

Brownawell, A.M., Kops, G.J., Macara, I.G., and Burgering, B.M. (2001). Inhibition of nuclear import by protein kinase B (Akt) regulates the subcellular distribution and activity of the forkhead transcription factor AFX. Mol. Cell. Biol. *21,* 3534-3546.

Brunet, A., Kanai, F., Stehn, J., Xu, J., Sarbassova, D., Frangioni, J.V., Dalal, S.N., DeCaprio, J.A., Greenberg, M.E., and Yaffe, M.B. (2002). 14-3-3 Transits to the Nucleus and Participates in Dynamic Nucleocytoplasmic Transport. J. Cell Biol. *156,* 817-828.

Brunet, A., Park, J., Tran, H., Hu, L.S., Hemmings, B.A., and Greenberg, M.E. (2001). Protein kinase SGK mediates survival signals by phosphorylating the forkhead transcription factor FKHRL1 (FOXO3a). Mol. Cell. Biol. *21,* 952-965.

Brunet, A., Sweeney, L.B., Sturgill, J.F., Chua, K.F., Greer, P.L., Lin, Y., Tran, H., Ross, S.E., Mostoslavsky, R., Cohen, H.Y., *et al.* (2004). Stress-dependent regulation of FOXO transcription factors by the SIRT1 deacetylase. Science *303,* 2011-2015.

Bruning, J.C., Gautam, D., Burks, D.J., Gillette, J., Schubert, M., Orban, P.C., Klein, R., Krone, W., Muller-Wieland, D., and Kahn, C.R. (2000). Role of brain insulin receptor in control of body weight and reproduction. Science *289,* 2122-2125.

Buiting, K. (2010). Prader-Willi syndrome and Angelman syndrome. Am. J. Med. Genet. C. Semin. Med. Genet. *154C,* 365-376.

Bush, J.R., and Wevrick, R. (2008). The Prader-Willi syndrome protein necdin interacts with the E1A-like inhibitor of differentiation EID-1 and promotes myoblast differentiation. Differentiation *76,* 994-1005.

Carrel, A.L., Myers, S.E., Whitman, B.Y., Eickhoff, J., and Allen, D.B. (2010). Long-term growth hormone therapy changes the natural history of body composition and motor function in children with prader-willi syndrome. J. Clin. Endocrinol. Metab. *95,* 1131-1136.

Cassidy, S.B., and Driscoll, D.J. (2009). Prader-Willi syndrome. Eur. J. Hum. Genet. *17,* 3-13.

Cataletto, M., Angulo, M., Hertz, G., and Whitman, B. (2011). Prader-Willi syndrome: A primer for clinicians. Int. J. Pediatr. Endocrinol. *2011,* 12.

Cavaille, J., Buiting, K., Kiefmann, M., Lalande, M., Brannan, C.I., Horsthemke, B., Bachellerie, J.P., Brosius, J., and Huttenhofer, A. (2000). Identification of brain-specific and imprinted small nucleolar RNA genes exhibiting an unusual genomic organization. Proc. Natl. Acad. Sci. U. S. A. *97,* 14311-14316.

Chrivia, J.C., Kwok, R.P., Lamb, N., Hagiwara, M., Montminy, M.R., and Goodman, R.H. (1993). Phosphorylated CREB binds specifically to the nuclear protein CBP. Nature *365,* 855-859.

Collins, B.J., Deak, M., Arthur, J.S., Armit, L.J., and Alessi, D.R. (2003). In vivo role of the PIF-binding docking site of PDK1 defined by knock-in mutation. EMBO J. *22,* 4202-4211.

Cowley, M.A., Smart, J.L., Rubinstein, M., Cerdan, M.G., Diano, S., Horvath, T.L., Cone, R.D., and Low, M.J. (2001). Leptin activates anorexigenic POMC neurons through a neural network in the arcuate nucleus. Nature *411,* 480-484.

Daitoku, H., Hatta, M., Matsuzaki, H., Aratani, S., Ohshima, T., Miyagishi, M., Nakajima, T., and Fukamizu, A. (2004). Silent information regulator 2 potentiates Foxo1-mediated transcription through its deacetylase activity. Proc. Natl. Acad. Sci. U. S. A. *101,* 10042-10047.

Daitoku, H., Sakamaki, J., and Fukamizu, A. (2011). Regulation of FoxO transcription factors by acetylation and protein-protein interactions. Biochim. Biophys. Acta *1813,* 1954-1960.

de Smith, A.J., Purmann, C., Walters, R.G., Ellis, R.J., Holder, S.E., Van Haelst, M.M., Brady, A.F., Fairbrother, U.L., Dattani, M., Keogh, J.M., *et al.* (2009). A deletion of the HBII-85 class of small nucleolar RNAs (snoRNAs) is associated with hyperphagia, obesity and hypogonadism. Hum. Mol. Genet. *18,* 3257-3265.

Devos, J., Weselake, S.V., and Wevrick, R. (2011). Magel2, a Prader-Willi syndrome candidate gene, modulates the activities of circadian rhythm proteins in cultured cells. J. Circadian Rhythms *9,* 12.

Dowell, P., Otto, T.C., Adi, S., and Lane, M.D. (2003). Convergence of peroxisome proliferator-activated receptor gamma and Foxo1 signaling pathways. J. Biol. Chem. *278,* 45485-45491.

Doyle, J.M., Gao, J., Wang, J., Yang, M., and Potts, P.R. (2010). MAGE-RING protein complexes comprise a family of E3 ubiquitin ligases. Mol. Cell *39,* 963-974.

Dunn, S.L., Bjornholm, M., Bates, S.H., Chen, Z., Seifert, M., and Myers, M.G.,Jr. (2005). Feedback inhibition of leptin receptor/Jak2 signaling via Tyr1138 of the leptin receptor and suppressor of cytokine signaling 3. Mol. Endocrinol. *19,* 925-938.

Eslam, M., Khattab, M.A., and Harrison, S.A. (2011). Insulin resistance and hepatitis C: an evolving story. Gut *60,* 1139-1151.

Fredericks, W.J., Galili, N., Mukhopadhyay, S., Rovera, G., Bennicelli, J., Barr, F.G., and Rauscher, F.J.,3rd. (1995). The PAX3-FKHR fusion protein created by the t(2;13) translocation in alveolar rhabdomyosarcomas is a more potent transcriptional activator than PAX3. Mol. Cell. Biol. *15,* 1522-1535.

Frescas, D., Valenti, L., and Accili, D. (2005). Nuclear trapping of the forkhead transcription factor FoxO1 via Sirt-dependent deacetylation promotes expression of glucogenetic genes. J. Biol. Chem. *280,* 20589-20595.

Fukuda, M., Jones, J.E., Olson, D., Hill, J., Lee, C.E., Gautron, L., Choi, M., Zigman, J.M., Lowell, B.B., and Elmquist, J.K. (2008). Monitoring FoxO1 localization in chemically identified neurons. J. Neurosci. *28,* 13640-13648.

Gale, S.M., Castracane, V.D., and Mantzoros, C.S. (2004). Energy homeostasis, obesity and eating disorders: recent advances in endocrinology. J. Nutr. *134,* 295-298.

Gallagher, R.C., Pils, B., Albalwi, M., and Francke, U. (2002). Evidence for the role of PWCR1/HBII-85 C/D box small nucleolar RNAs in Prader-Willi syndrome. Am. J. Hum. Genet. *71*, 669-678.

Gao, Q., and Horvath, T.L. (2008). Neuronal control of energy homeostasis. FEBS Lett. *582*, 132-141.

Gao, S., Kinzig, K.P., Aja, S., Scott, K.A., Keung, W., Kelly, S., Strynadka, K., Chohnan, S., Smith, W.W., Tamashiro, K.L., *et al.* (2007). Leptin activates hypothalamic acetyl-CoA carboxylase to inhibit food intake. Proc. Natl. Acad. Sci. U. S. A. *104*, 17358-17363.

Gillespie, A.M., and Coleman, R.E. (1999). The potential of melanoma antigen expression in cancer therapy. Cancer Treat. Rev. *25*, 219-227.

Gilley, J., Coffer, P.J., and Ham, J. (2003). FOXO transcription factors directly activate bim gene expression and promote apoptosis in sympathetic neurons. J. Cell Biol. *162*, 613-622.

Goldstone, A.P., Holland, A.J., Hauffa, B.P., Hokken-Koelega, A.C., Tauber, M., and speakers contributors at the Second Expert Meeting of the Comprehensive Care of Patients with PWS. (2008). Recommendations for the diagnosis and management of Prader-Willi syndrome. J. Clin. Endocrinol. Metab. *93*, 4183-4197.

Gunay-Aygun, M., Schwartz, S., Heeger, S., O'Riordan, M.A., and Cassidy, S.B. (2001). The changing purpose of Prader-Willi syndrome clinical diagnostic criteria and proposed revised criteria. Pediatrics *108*, E92.

Guo, S., Rena, G., Cichy, S., He, X., Cohen, P., and Unterman, T. (1999). Phosphorylation of serine 256 by protein kinase B disrupts transactivation by FKHR and mediates effects of insulin on insulin-like growth factor-binding protein-1 promoter activity through a conserved insulin response sequence. J. Biol. Chem. *274*, 17184-17192.

Harris, M., Aschkenasi, C., Elias, C.F., Chandrankunnel, A., Nillni, E.A., Bjoorbaek, C., Elmquist, J.K., Flier, J.S., and Hollenberg, A.N. (2001). Transcriptional regulation of the thyrotropin-releasing hormone gene by leptin and melanocortin signaling. J. Clin. Invest. *107*, 111-120.

Hasegawa, K., Kawahara, T., Fujiwara, K., Shimpuku, M., Sasaki, T., Kitamura, T., and Yoshikawa, K. (2012). Necdin controls Foxo1 acetylation in hypothalamic arcuate neurons to modulate the thyroid axis. J. Neurosci. *32*, 5562-5572.

Hasegawa, K., and Yoshikawa, K. (2008). Necdin regulates p53 acetylation via Sirtuin1 to modulate DNA damage response in cortical neurons. J. Neurosci. *28,* 8772-8784.

Holm, V.A., Cassidy, S.B., Butler, M.G., Hanchett, J.M., Greenswag, L.R., Whitman, B.Y., and Greenberg, F. (1993). Prader-Willi syndrome: consensus diagnostic criteria. Pediatrics *91,* 398-402.

Huang, H., Regan, K.M., Lou, Z., Chen, J., and Tindall, D.J. (2006). CDK2-dependent phosphorylation of FOXO1 as an apoptotic response to DNA damage. Science *314,* 294-297.

Huang, H., Regan, K.M., Wang, F., Wang, D., Smith, D.I., van Deursen, J.M., and Tindall, D.J. (2005). Skp2 inhibits FOXO1 in tumor suppression through ubiquitin-mediated degradation. Proc. Natl. Acad. Sci. U. S. A. *102,* 1649-1654.

Huang, H., and Tindall, D.J. (2007). Dynamic FoxO transcription factors. J. Cell. Sci. *120,* 2479-2487.

Imai, S., and Guarente, L. (2010). Ten years of NAD-dependent SIR2 family deacetylases: implications for metabolic diseases. Trends Pharmacol. Sci. *31,* 212-220.

Jin, D.K. (2011). Systematic review of the clinical and genetic aspects of Prader-Willi syndrome. Korean J. Pediatr. *54,* 55-63.

Jing, E., Gesta, S., and Kahn, C.R. (2007). SIRT2 regulates adipocyte differentiation through FoxO1 acetylation/deacetylation. Cell. Metab. *6,* 105-114.

Jong, M.T., Carey, A.H., Caldwell, K.A., Lau, M.H., Handel, M.A., Driscoll, D.J., Stewart, C.L., Rinchik, E.M., and Nicholls, R.D. (1999). Imprinting of a RING zinc-finger encoding gene in the mouse chromosome region homologous to the Prader-Willi syndrome genetic region. Hum. Mol. Genet. *8,* 795-803.

Kaestner, K.H., Knochel, W., and Martinez, D.E. (2000). Unified nomenclature for the winged helix/forkhead transcription factors. Genes Dev. *14,* 142-146.

Kamei, Y., Miura, S., Suzuki, M., Kai, Y., Mizukami, J., Taniguchi, T., Mochida, K., Hata, T., Matsuda, J., Aburatani, H., Nishino, I., and Ezaki, O. (2004). Skeletal muscle FOXO1 (FKHR) transgenic mice have less skeletal muscle mass, down-regulated Type I (slow twitch/red muscle) fiber genes, and impaired glycemic control. J. Biol. Chem. *279,* 41114-41123.

Kim, M.S., Pak, Y.K., Jang, P.G., Namkoong, C., Choi, Y.S., Won, J.C., Kim, K.S., Kim, S.W., Kim, H.S., Park, J.Y., Kim, Y.B., and Lee, K.U. (2006). Role of hypothalamic Foxo1 in the regulation of food intake and energy homeostasis. Nat. Neurosci. *9*, 901-906.

King, P.J., Widdowson, P.S., Doods, H.N., and Williams, G. (1999). Regulation of neuropeptide Y release by neuropeptide Y receptor ligands and calcium channel antagonists in hypothalamic slices. J. Neurochem. *73*, 641-646.

Kitamura, T., Feng, Y., Kitamura, Y.I., Chua, S.C.,Jr, Xu, A.W., Barsh, G.S., Rossetti, L., and Accili, D. (2006). Forkhead protein FoxO1 mediates Agrp-dependent effects of leptin on food intake. Nat. Med. *12*, 534-540.

Kitamura, T., Nakae, J., Kitamura, Y., Kido, Y., Biggs, W.H.,3rd, Wright, C.V., White, M.F., Arden, K.C., and Accili, D. (2002). The forkhead transcription factor Foxo1 links insulin signaling to Pdx1 regulation of pancreatic beta cell growth. J. Clin. Invest. *110,* 1839-1847.

Kitamura, Y.I., Kitamura, T., Kruse, J.P., Raum, J.C., Stein, R., Gu, W., and Accili, D. (2005). FoxO1 protects against pancreatic beta cell failure through NeuroD and MafA induction. Cell. Metab. *2,* 153-163.

Kondratov, R.V., Chernov, M.V., Kondratova, A.A., Gorbacheva, V.Y., Gudkov, A.V., and Antoch, M.P. (2003). BMAL1-dependent circadian oscillation of nuclear CLOCK: posttranslational events induced by dimerization of transcriptional activators of the mammalian clock system. Genes Dev. *17,* 1921-1932.

Kousteni, S. (2012). FoxO1, the transcriptional chief of staff of energy metabolism. Bone *50,* 437-443.

Kousteni, S. (2011). FoxO1: a molecule for all seasons. J. Bone Miner. Res. *26,* 912-917.

Kozlov, S.V., Bogenpohl, J.W., Howell, M.P., Wevrick, R., Panda, S., Hogenesch, J.B., Muglia, L.J., Van Gelder, R.N., Herzog, E.D., and Stewart, C.L. (2007). The imprinted gene Magel2 regulates normal circadian output. Nat. Genet. *39,* 1266-1272.

Kume, K., Zylka, M.J., Sriram, S., Shearman, L.P., Weaver, D.R., Jin, X., Maywood, E.S., Hastings, M.H., and Reppert, S.M. (1999). mCRY1 and mCRY2 are essential components of the negative limb of the circadian clock feedback loop. Cell *98,* 193-205.

Kuwako, K., Taniura, H., and Yoshikawa, K. (2004). Necdin-related MAGE proteins differentially interact with the E2F1 transcription factor and the p75 neurotrophin receptor. J. Biol. Chem. *279,* 1703-1712.

Lavi-Itzkovitz, A., Tcherpakov, M., Levy, Z., Itzkovitz, S., Muscatelli, F., and Fainzilber, M. (2012). Functional consequences of necdin nucleocytoplasmic localization. PLoS One *7,* e33786.

Lee, S., Kozlov, S., Hernandez, L., Chamberlain, S.J., Brannan, C.I., Stewart, C.L., and Wevrick, R. (2000). Expression and imprinting of MAGEL2 suggest a role in Prader-willi syndrome and the homologous murine imprinting phenotype. Hum. Mol. Genet. *9,* 1813-1819.

Lee, S., Walker, C.L., Karten, B., Kuny, S.L., Tennese, A.A., O'Neill, M.A., and Wevrick, R. (2005). Essential role for the Prader-Willi syndrome protein necdin in axonal outgrowth. Hum. Mol. Genet. *14,* 627-637.

Lee, S., Walker, C.L., and Wevrick, R. (2003). Prader-Willi syndrome transcripts are expressed in phenotypically significant regions of the developing mouse brain. Gene Expr. Patterns *3,* 599-609.

Lehtinen, M.K., Yuan, Z., Boag, P.R., Yang, Y., Villen, J., Becker, E.B., DiBacco, S., de la Iglesia, N., Gygi, S., Blackwell, T.K., and Bonni, A. (2006). A conserved MST-FOXO signaling pathway mediates oxidative-stress responses and extends life span. Cell *125,* 987-1001.

Li, P., Lee, H., Guo, S., Unterman, T.G., Jenster, G., and Bai, W. (2003). AKT-independent protection of prostate cancer cells from apoptosis mediated through complex formation between the androgen receptor and FKHR. Mol. Cell. Biol. *23,* 104-118.

Manning, B.D., and Cantley, L.C. (2007). AKT/PKB signaling: navigating downstream. Cell *129,* 1261-1274.

Matsuzaki, H., Daitoku, H., Hatta, M., Aoyama, H., Yoshimochi, K., and Fukamizu, A. (2005). Acetylation of Foxo1 alters its DNA-binding ability and sensitivity to phosphorylation. Proc. Natl. Acad. Sci. U. S. A. *102,* 11278-11283.

Matsuzaki, H., Daitoku, H., Hatta, M., Tanaka, K., and Fukamizu, A. (2003). Insulin-induced phosphorylation of FKHR (Foxo1) targets to proteasomal degradation. Proc. Natl. Acad. Sci. U. S. A. *100,* 11285-11290.

McCubrey, J.A., Steelman, L.S., Chappell, W.H., Abrams, S.L., Wong, E.W., Chang, F., Lehmann, B., Terrian, D.M., Milella, M., Tafuri, A., *et al.* (2007). Roles of the Raf/MEK/ERK pathway in cell growth, malignant transformation and drug resistance. Biochim. Biophys. Acta *1773,* 1263-1284.

Mercer, R.E., Chee, M.J., and Colmers, W.F. (2011). The role of NPY in hypothalamic mediated food intake. Front. Neuroendocrinol. *32,* 398-415.

Mercer, R.E., and Wevrick, R. (2009). Loss of Magel2, a candidate gene for features of Prader-Willi syndrome, impairs reproductive function in mice. PLoS One *4,* e4291.

Miller, J.L., Lynn, C.H., Driscoll, D.C., Goldstone, A.P., Gold, J.A., Kimonis, V., Dykens, E., Butler, M.G., Shuster, J.J., and Driscoll, D.J. (2011). Nutritional phases in Prader-Willi syndrome. Am. J. Med. Genet. A. *155A,* 1040-1049.

Minokoshi, Y., Alquier, T., Furukawa, N., Kim, Y.B., Lee, A., Xue, B., Mu, J., Foufelle, F., Ferre, P., Birnbaum, M.J., Stuck, B.J., and Kahn, B.B. (2004). AMP-kinase regulates food intake by responding to hormonal and nutrient signals in the hypothalamus. Nature *428,* 569-574.

Modur, V., Nagarajan, R., Evers, B.M., and Milbrandt, J. (2002). FOXO proteins regulate tumor necrosis factor-related apoptosis inducing ligand expression. Implications for PTEN mutation in prostate cancer. J. Biol. Chem. *277,* 47928-47937.

Morris, D.L., and Rui, L. (2009). Recent advances in understanding leptin signaling and leptin resistance. Am. J. Physiol. Endocrinol. Metab. *297,* E1247-59.

Motta, M.C., Divecha, N., Lemieux, M., Kamel, C., Chen, D., Gu, W., Bultsma, Y., McBurney, M., and Guarente, L. (2004). Mammalian SIRT1 represses forkhead transcription factors. Cell *116,* 551-563.

Nakae, J., Barr, V., and Accili, D. (2000). Differential regulation of gene expression by insulin and IGF-1 receptors correlates with phosphorylation of a single amino acid residue in the forkhead transcription factor FKHR. EMBO J. *19,* 989-996.

Nakae, J., Biggs, W.H.,3rd, Kitamura, T., Cavenee, W.K., Wright, C.V., Arden, K.C., and Accili, D. (2002). Regulation of insulin action and pancreatic beta-cell function by mutated alleles of the gene encoding forkhead transcription factor Foxo1. Nat. Genet. *32,* 245-253.

Nakae, J., Kitamura, T., Kitamura, Y., Biggs, W.H.,3rd, Arden, K.C., and Accili, D. (2003). The forkhead transcription factor Foxo1 regulates adipocyte differentiation. Dev. Cell. *4,* 119-129.

Nakamura, N., Ramaswamy, S., Vazquez, F., Signoretti, S., Loda, M., and Sellers, W.R. (2000). Forkhead transcription factors are critical effectors of cell death and cell cycle arrest downstream of PTEN. Mol. Cell. Biol. *20,* 8969-8982.

Neumann, L.C., Markaki, Y., Mladenov, E., Hoffmann, D., Buiting, K., and Horsthemke, B. (2012). The imprinted NPAP1/C15orf2 gene in the Prader-Willi syndrome region encodes a nuclear pore complex associated protein. Hum. Mol. Genet. *21,* 4038-4048.

Nicholls, R.D., Knoll, J.H., Butler, M.G., Karam, S., and Lalande, M. (1989). Genetic imprinting suggested by maternal heterodisomy in nondeletion Prader-Willi syndrome. Nature *342,* 281-285.

Niswender, K.D., Morton, G.J., Stearns, W.H., Rhodes, C.J., Myers, M.G.,Jr, and Schwartz, M.W. (2001). Intracellular signalling. Key enzyme in leptin-induced anorexia. Nature *413,* 794-795.

Nixon, G.M., and Brouillette, R.T. (2002). Sleep and breathing in Prader-Willi syndrome. Pediatr. Pulmonol. *34,* 209-217.

Ohman Forslund, K., and Nordqvist, K. (2001). The melanoma antigen genes--any clues to their functions in normal tissues? Exp. Cell Res. *265,* 185-194.

Prader, A., Labhart, A., and Willi, H. (1956). Ein syndrome von adipositas, kleinwuchs, kryptorchismus und oligophrenie nach myotonierartigem zustand im neugeborenenalter. Schweiz Med Wochen *86,* 1260-1261.

Puigserver, P., Rhee, J., Donovan, J., Walkey, C.J., Yoon, J.C., Oriente, F., Kitamura, Y., Altomonte, J., Dong, H., Accili, D., and Spiegelman, B.M. (2003). Insulin-regulated hepatic gluconeogenesis through FOXO1-PGC-1alpha interaction. Nature *423,* 550-555.

Qiang, L., Banks, A.S., and Accili, D. (2010). Uncoupling of acetylation from phosphorylation regulates FoxO1 function independent of its subcellular localization. J. Biol. Chem. *285,* 27396-27401.

Qiu, J., Fang, Y., Ronnekleiv, O.K., and Kelly, M.J. (2010). Leptin excites proopiomelanocortin neurons via activation of TRPC channels. J. Neurosci. *30,* 1560-1565.

Rached, M.T., Kode, A., Silva, B.C., Jung, D.Y., Gray, S., Ong, H., Paik, J.H., DePinho, R.A., Kim, J.K., Karsenty, G., and Kousteni, S. (2010). FoxO1 expression in osteoblasts regulates glucose homeostasis through regulation of osteocalcin in mice. J. Clin. Invest. *120,* 357-368.

Rahmouni, K., Sigmund, C.D., Haynes, W.G., and Mark, A.L. (2009). Hypothalamic ERK mediates the anorectic and thermogenic sympathetic effects of leptin. Diabetes *58,* 536-542.

Rena, G., Prescott, A.R., Guo, S., Cohen, P., and Unterman, T.G. (2001). Roles of the forkhead in rhabdomyosarcoma (FKHR) phosphorylation sites in regulating 14-3-3 binding, transactivation and nuclear targetting. Biochem. J. *354,* 605-612.

Rena, G., Woods, Y.L., Prescott, A.R., Peggie, M., Unterman, T.G., Williams, M.R., and Cohen, P. (2002). Two novel phosphorylation sites on FKHR that are critical for its nuclear exclusion. EMBO J. *21,* 2263-2271.

Runte, M., Huttenhofer, A., Gross, S., Kiefmann, M., Horsthemke, B., and Buiting, K. (2001). The IC-SNURF-SNRPN transcript serves as a host for multiple small nucleolar RNA species and as an antisense RNA for UBE3A. Hum. Mol. Genet. *10,* 2687-2700.

Sahoo, T., del Gaudio, D., German, J.R., Shinawi, M., Peters, S.U., Person, R.E., Garnica, A., Cheung, S.W., and Beaudet, A.L. (2008). Prader-Willi phenotype caused by paternal deficiency for the HBII-85 C/D box small nucleolar RNA cluster. Nat. Genet. *40,* 719-721.

Sahu, A. (2003). Leptin signaling in the hypothalamus: emphasis on energy homeostasis and leptin resistance. Front. Neuroendocrinol. *24,* 225-253.

Salehi, A.H., Roux, P.P., Kubu, C.J., Zeindler, C., Bhakar, A., Tannis, L.L., Verdi, J.M., and Barker, P.A. (2000). NRAGE, a novel MAGE protein, interacts with the p75 neurotrophin receptor and facilitates nerve growth factor-dependent apoptosis. Neuron *27,* 279-288.

Saltiel, A.R., and Kahn, C.R. (2001). Insulin signalling and the regulation of glucose and lipid metabolism. Nature *414,* 799-806.

Schule, B., Albalwi, M., Northrop, E., Francis, D.I., Rowell, M., Slater, H.R., Gardner, R.J., and Francke, U. (2005). Molecular breakpoint cloning and gene expression studies of a novel translocation t(4;15)(q27;q11.2) associated with Prader-Willi syndrome. BMC Med. Genet. *6,* 18.

Seoane, J., Le, H.V., Shen, L., Anderson, S.A., and Massague, J. (2004). Integration of Smad and forkhead pathways in the control of neuroepithelial and glioblastoma cell proliferation. Cell *117,* 211-223.

Spanswick, D., Smith, M.A., Mirshamsi, S., Routh, V.H., and Ashford, M.L. (2000). Insulin activates ATP-sensitive K+ channels in hypothalamic neurons of lean, but not obese rats. Nat. Neurosci. *3,* 757-758.

Suzuki, K., Jayasena, C.N., and Bloom, S.R. (2012). Obesity and appetite control. Exp. Diabetes Res. *2012,* 824305.

Tcherpakov, M., Bronfman, F.C., Conticello, S.G., Vaskovsky, A., Levy, Z., Niinobe, M., Yoshikawa, K., Arenas, E., and Fainzilber, M. (2002). The p75 neurotrophin receptor interacts with multiple MAGE proteins. J. Biol. Chem. *277,* 49101-49104.

Tsai, W.C., Bhattacharyya, N., Han, L.Y., Hanover, J.A., and Rechler, M.M. (2003). Insulin inhibition of transcription stimulated by the forkhead protein Foxo1 is not solely due to nuclear exclusion. Endocrinology *144,* 5615-5622.

Tzivion, G., Dobson, M., and Ramakrishnan, G. (2011). FoxO transcription factors; Regulation by AKT and 14-3-3 proteins. Biochim. Biophys. Acta *1813,* 1938-1945.

Valassi, E., Scacchi, M., and Cavagnini, F. (2008). Neuroendocrine control of food intake. Nutr. Metab. Cardiovasc. Dis. *18,* 158-168.

van der Heide, L.P., Hoekman, M.F., and Smidt, M.P. (2004). The ins and outs of FoxO shuttling: mechanisms of FoxO translocation and transcriptional regulation. Biochem. J. *380,* 297-309.

van der Heide, L.P., and Smidt, M.P. (2005). Regulation of FoxO activity by CBP/p300-mediated acetylation. Trends Biochem. Sci. *30,* 81-86.

van der Horst, A., Tertoolen, L.G., de Vries-Smits, L.M., Frye, R.A., Medema, R.H., and Burgering, B.M. (2004). FOXO4 is acetylated upon peroxide stress and deacetylated by the longevity protein hSir2(SIRT1). J. Biol. Chem. *279,* 28873-28879.

van Mil, E.A., Westerterp, K.R., Gerver, W.J., Curfs, L.M., Schrander-Stumpel, C.T., Kester, A.D., and Saris, W.H. (2000). Energy expenditure at rest and during sleep in children with Prader-Willi syndrome is explained by body composition. Am. J. Clin. Nutr. *71,* 752-756.

Villarejo-Balcells, B., Guichard, S., Rigby, P.W., and Carvajal, J.J. (2011). Expression pattern of the FoxO1 gene during mouse embryonic development. Gene Expr. Patterns *11,* 299-308.

Weselake, S., and Wevrick, R. (2012). Co-morbidity of complex genetic disorders and hypersomnias of central origin: lessons from the underlying neurobiology of wake and sleep. Clin. Genet. *82,* 379-387.

Wevrick, R., and Francke, U. (1997). An imprinted mouse transcript homologous to the human imprinted in Prader-Willi syndrome (IPW) gene. Hum. Mol. Genet. *6,* 325-332.

Wigren, M., and Hansen, S. (2005). ADHD symptoms and insistence on sameness in Prader-Willi syndrome. J. Intellect. Disabil. Res. *49,* 449-456.

Williams, C.A., Beaudet, A.L., Clayton-Smith, J., Knoll, J.H., Kyllerman, M., Laan, L.A., Magenis, R.E., Moncla, A., Schinzel, A.A., Summers, J.A., and Wagstaff, J. (2006). Angelman syndrome 2005: updated consensus for diagnostic criteria. Am. J. Med. Genet. A. *140,* 413-418.

Wirth, J., Back, E., Huttenhofer, A., Nothwang, H.G., Lich, C., Gross, S., Menzel, C., Schinzel, A., Kioschis, P., Tommerup, N., *et al.* (2001). A translocation breakpoint cluster disrupts the newly defined 3' end of the SNURF-SNRPN transcription unit on chromosome 15. Hum. Mol. Genet. *10,* 201-210.

Woods, S.C., and D'Alessio, D.A. (2008). Central control of body weight and appetite. J. Clin. Endocrinol. Metab. *93,* S37-50.

Woods, Y.L., Rena, G., Morrice, N., Barthel, A., Becker, W., Guo, S., Unterman, T.G., and Cohen, P. (2001). The kinase DYRK1A phosphorylates the transcription factor FKHR at Ser329 in vitro, a novel in vivo phosphorylation site. Biochem. J. *355,* 597-607.

Yamagata, K., Daitoku, H., Takahashi, Y., Namiki, K., Hisatake, K., Kako, K., Mukai, H., Kasuya, Y., and Fukamizu, A. (2008). Arginine methylation of FOXO transcription factors inhibits their phosphorylation by Akt. Mol. Cell *32,* 221-231.

Yan, L., Lavin, V.A., Moser, L.R., Cui, Q., Kanies, C., and Yang, E. (2008). PP2A regulates the pro-apoptotic activity of FOXO1. J. Biol. Chem. *283,* 7411-7420.

Yang, G., Lim, C.Y., Li, C., Xiao, X., Radda, G.K., Li, C., Cao, X., and Han, W. (2009). FoxO1 inhibits leptin regulation of pro-opiomelanocortin promoter activity by blocking STAT3 interaction with specificity protein 1. J. Biol. Chem. *284,* 3719-3727.

Yang, Y., Hou, H., Haller, E.M., Nicosia, S.V., and Bai, W. (2005). Suppression of FOXO1 activity by FHL2 through SIRT1-mediated deacetylation. EMBO J. *24,* 1021-1032.

Zhang, X., Gan, L., Pan, H., Guo, S., He, X., Olson, S.T., Mesecar, A., Adam, S., and Unterman, T.G. (2002). Phosphorylation of serine 256 suppresses transactivation by FKHR (FOXO1) by multiple mechanisms. Direct and indirect effects on nuclear/cytoplasmic shuttling and DNA binding. J. Biol. Chem. *277,* 45276-45284.

Zhao, A.Z., Huan, J.N., Gupta, S., Pal, R., and Sahu, A. (2002). A phosphatidylinositol 3-kinase phosphodiesterase 3B-cyclic AMP pathway in hypothalamic action of leptin on feeding. Nat. Neurosci. *5*, 727-728.

Zhao, X., Gan, L., Pan, H., Kan, D., Majeski, M., Adam, S.A., and Unterman, T.G. (2004). Multiple elements regulate nuclear/cytoplasmic shuttling of FOXO1: characterization of phosphorylation- and 14-3-3-dependent and -independent mechanisms. Biochem. J. *378*, 839-849.

Zhao, Y., Yang, J., Liao, W., Liu, X., Zhang, H., Wang, S., Wang, D., Feng, J., Yu, L., and Zhu, W.G. (2010). Cytosolic FoxO1 is essential for the induction of autophagy and tumour suppressor activity. Nat. Cell Biol. *12*, 665-675.